INFLUENCE OF VARIOUS ETHYLENE COPOLYMERS ON THE SILANE-WATER CROSSLINKING OF HIGH-DENSITY POLYETHYLENE

SOONTAREE KOSITCHAIYONG

A THESIS SUBMITTED IN PARTIAL FULFILLMENT
OF THE REQUIREMENTS FOR
THE DEGREE OF MASTER OF SCIENCE
(POLYMER SCIENCE AND TECHNOLOGY)
FACULTY OF GRADUATE STUDIES
MAHIDOL UNIVERSITY
2008

COPYRIGHT OF MAHIDOL UNIVERSITY

Copyright by Mahidol University

Thesis
Entitled

INFLUENCE OF VARIOUS ETHYLENE COPOLYMERS ON THE SILANE-WATER CROSSLINKING OF HIGH-DENSITY POLYETHYLENE

Soontaree Kositchaiyong
.....
Miss Soontaree Kositchaiyong
Candidate

K. Sirisinha
.....
Assoc. Prof. Kalyanee Sirisinha,
Ph.D.
Major-Advisor

.....
Assoc. Prof. Chakrit Sirisinha,
Ph.D.
Co-Advisor

T. Nipithakul
.....
Lect. Thirawan Nipithakul,
Doctorat de l'Université de Haute Alsace
Co-Advisor

B. Mahaisavariya
.....
Prof. Banchong Mahaisavariya,
M.D.
Dean
Faculty of Graduate Studies

P. Sunintaboon
.....
Lect. Panya Sunintaboon,
Ph.D.
Chair
Master of Science Programme
in Polymer Science and Technology
Faculty of Science

Copyright by Mahidol University

Thesis
Entitled

INFLUENCE OF VARIOUS ETHYLENE COPOLYMERS ON THE SILANE-WATER CROSSLINKING OF HIGH-DENSITY POLYETHYLENE

was submitted to the Faculty of Graduate Studies, Mahidol University
for the degree of Master of Science (Polymer Science and Technology)
on
March 14, 2008

Soontaree Kositchaiyong
Miss Soontaree Kositchaiyong
Candidate

Pongdhorn Saeoui
Mr. Pongdhorn Sae-Oui ,
Ph.D.
Chair

K. Sirisinha
Assoc. Prof. Kalyanee Sirisinha,
Ph.D.
Member

T. Nipithakul
Lect. Thirawan Nipithakul,
Doctorat de l'Université de Haute Alsace
Member

Assoc. Prof. Chakrit Sirisinha,
Ph.D.
Member

B. Mahaisavariya
Prof. Banchong Mahaisavariya,
M.D.
Dean
Faculty of Graduate Studies
Mahidol University

Prof. Skorn Mongkolsuk,
Ph.D.
Dean
Faculty of Science
Mahidol University

Copyright by Mahidol University

ACKNOWLEDGEMENTS

I would like to thank my advisor, Assoc. Prof. Kalyanee Sirisinha for helping me to maintain focus and direction throughout the research process and for her attention to detail. I am appreciative of her kindness and encouragement, and for valuable guidance in all aspects of research.

Thank are extended to Assoc. Prof. Chakrit Sirisinha, Dr. Thirawan Nipithakul and Dr. Pongdhorn Sae-Oui for providing helpful advice and for many useful discussions throughout the course of this thesis.

I would also like to thank all members of the Polymer Science and Technology Program in the Department of Chemistry, Faculty of Science, Mahidol University and my friends for their help and suggestion during this work and pleasant working atmosphere and many enjoyable moments.

Finally, I am grateful to my parents and my family for their continuous encouragement and support throughout the course of this study.

Soontaree Kositchaiyong

Copyright by Mahidol University

INFLUENCE OF VARIOUS ETHYLENE COPOLYMERS ON THE SILANE-WATER CROSSLINKING OF HIGH-DENSITY POLYETHYLENE

SOONTAREE KOSITCHAIYONG 4737770 SCPO/M

M.Sc. (POLYMER SCIENCE AND TECHNOLOGY)

THESIS ADVISORS: KALYANEE SIRISINHA, Ph.D. (POLYMER TECHNOLOGY), CHAKRIT SIRISINHA, Ph.D. (POLYMER TECHNOLOGY), THIRAWAN NIPITHAKUL, Doctorat de l'Université de Haute Alsace, (POLYMER SCIENCE)

ABSTRACT

The silane-grafting and water-crosslinking of high-density polyethylene (HDPE) and its blends with various ethylene copolymers were investigated. Various ethylene copolymers including ethylene-octene copolymer (EO), ethylene-butene copolymer (EB) and ethylene-vinyl acetate copolymer (EVA) were introduced to the HDPE, in order to facilitate diffusion of water which aids crosslink reaction. The HDPE and its blends were first grafted with vinyl trimethoxysilane (VTMS) by a free-radical reaction initiated by dicumyl peroxide (DCP). The grafted samples were subsequently crosslinked in hot water. The effects of ethylene copolymers on the degree of grafting were characterised using Fourier Transform Infrared Spectroscopy (FTIR) technique. The effects of ethylene copolymers and crosslinking time on crosslinking degree were investigated using solvent extraction, rheological measurement and FTIR analysis. The crystallisation behaviours, thermal and mechanical properties of the crosslinked samples were also investigated.

The results showed that an increase in amount of silane absorption in ethylene copolymers did not help to improve the efficiency of silane grafting in the blend. The presence of bulky acetate group and steric side chain comonomer in ethylene copolymers led to some difficulties in silane reaction. The degree of crosslinking was found to depend on the crosslinking time and structure of copolymers. As the crosslinking time increased, the degree of crosslinking increased. The incorporation of ethylene copolymers increased the degree and rate of crosslinking of HDPE. The hydrophilicity of the copolymers played a major role in silane crosslinking, whereas the amount of crystalline component in the copolymers showed a minor effect. The silane crosslinking occurred mainly in the amorphous region of the sample. The presence of crosslink networks improved the tensile modulus and caused a reduction in elongation and strength at breaks. The crosslinked products exhibited an improvement in the thermal oxidative stability, thermal decomposition activation energy and heat deflection property.

KEY WORDS: HIGH-DENSITY POLYETHYLENE/ ETHYLENE COPOLYMERS SILANE-WATER CROSSLINKING/ PROPERTIES

118 pp.

Copyright by Mahidol University

ผลของเอทธิลีนโคพอลิเมอร์ต่างชนิดที่มีต่อการเชื่อมโยงสายโซ่ของพอลิเอทธิลีนชนิดความหนาแน่นสูงโดยใช้ไซเลนและน้ำ (INFLUENCE OF VARIOUS ETHYLENE COPOLYMERS ON THE SILANE-WATER CROSSLINKING OF HIGH-DENSITY POLYETHYLENE)

สุนทรีย์ โฆษิตชัยยงค์ 4737770 SCPO/M

วท.ม. (วิทยาศาสตร์และเทคโนโลยีพอลิเมอร์)

คณะกรรมการควบคุมวิทยานิพนธ์: กัลยาณี สิริสิงห, Ph.D. (POLYMER TECHNOLOGY), ชาคริต สิริสิงห, Ph.D. (POLYMER TECHNOLOGY), ถิรวรรณ นิพิฏฐกุล, Doctorat de l'Université de Haute Alsace, (POLYMER SCIENCE)

บทคัดย่อ

งานวิจัยนี้เป็นการศึกษาการกราฟท์ และการเชื่อมโยงสายโซ่ของพอลิเอทธิลีนชนิดความหนาแน่นสูงและพอลิเมอร์ผสมของพอลิเอทธิลีนชนิดความหนาแน่นสูงกับเอทธิลีนโคพอลิเมอร์ต่างชนิดโดยใช้ไซเลนและน้ำ ซึ่งเอทธิลีนโคพอลิเมอร์ที่ใช้ในงานวิจัยนี้ประกอบไปด้วยเอทธิลีนออกทีนโคพอลิเมอร์และเอทธิลีนบิวทีนโคพอลิเมอร์รวมทั้งเอทธิลีนไวนิลอะซิเตทโคพอลิเมอร์ โดยเอทธิลีนโคพอลิเมอร์จะถูกผสมกับพอลิเอทธิลีนชนิดความหนาแน่นสูงเพื่อที่จะช่วยเพิ่มการแพร่ของน้ำและการเกิดปฏิกิริยาเชื่อมโยงสายโซ่ให้ดีขึ้น โดยปฏิกิริยาการกราฟท์จะใช้ไวนิลไตรเมธทอกซีไซเลนเป็นมอนอเมอร์ในการทำปฏิกิริยา และใช้ไดคิวมิลเปอร์ออกไซด์เป็นสารก่อปฏิกิริยา และทำให้เกิดการเชื่อมโยงสายโซ่โดยการทำปฏิกิริยากับน้ำร้อน ในงานวิจัยนี้ได้ทำการวิเคราะห์ผลของเอทธิลีนโคพอลิเมอร์ที่มีต่อปริมาณการกราฟท์ด้วยเทคนิคอินฟราเรดสเปกโตรสโคปี และได้ศึกษาผลของเอทธิลีนโคพอลิเมอร์และเวลาในการเชื่อมโยงสายโซ่ที่มีต่อปริมาณการเชื่อมโยงสายโซ่ โดยวัดปริมาณการเชื่อมโยงสายโซ่ที่ได้ด้วยวิธีการสกัดด้วยตัวทำละลาย และวัดการเปลี่ยนไปของสมบัติการไหลภายหลังการเชื่อมโยงสายโซ่ อีกทั้งยังติดตามการเปลี่ยนไปของหมู่ฟังก์ชันด้วยเทคนิคอินฟราเรดสเปกโตรสโคปี จากนั้นทำการศึกษาความเป็นผลึกและสมบัติทางความร้อนรวมถึงสมบัติเชิงกลของพอลิเมอร์ที่มีการเชื่อมโยงสายโซ่

ผลการวิจัยพบว่าการเพิ่มขึ้นของปริมาณการดูดซับไซเลนในเอทธิลีนโคพอลิเมอร์ไม่ได้ช่วยปรับปรุงประสิทธิภาพการกราฟท์ไซเลน ผลของความเกะกะของโคพอลิเมอร์ทำให้การเข้าทำปฏิกิริยาการกราฟท์ด้วยไซเลนเกิดได้ยากขึ้น ส่วนปริมาณการเชื่อมโยงสายโซ่ขึ้นกับเวลาในการเชื่อมโยงสายโซ่และโครงสร้างของเอทธิลีนโคพอลิเมอร์ โดยปริมาณการเชื่อมโยงสายโซ่เพิ่มขึ้นเมื่อใช้เวลาในการทำปฏิกิริยากับน้ำนานขึ้น การเติมเอทธิลีนโคพอลิเมอร์ในพอลิเอทธิลีนชนิดความหนาแน่นสูง มีผลทำให้มีการเพิ่มขึ้นของปริมาณและอัตราการเชื่อมโยงสายโซ่ โดยพบว่าความชอบน้ำของเอทธิลีนโคพอลิเมอร์เป็นปัจจัยหลัก ขณะที่ปริมาณผลึกที่มีในพอลิเมอร์เป็นปัจจัยรอง สำหรับการเชื่อมโยงสายโซ่นั้นเกิดขึ้นในพอลิเมอร์ส่วนที่เป็นอสัณฐาน จากการศึกษาการเชื่อมโยงสายโซ่ของพอลิเมอร์ที่เตรียมขึ้นพบว่าโมดูลัสมีค่าสูงขึ้นแต่มีการยืดออกและความแข็งแรง ณ จุดขาดลดลง นอกจากนี้ผลการวิจัยได้แสดงให้เห็นอย่างชัดเจนว่าพอลิเมอร์ที่ผ่านการเชื่อมโยงสายโซ่แล้วมีเสถียรภาพต่อความร้อนและพลังงานในการสลายตัวเพิ่มขึ้นอีกทั้งมีความคงรูปสูงขึ้น

118 หน้า

Copyright by Mahidol University

CONTENTS

		Page
ACKNOWLEDGEMENTS		iii
ABSTRACT (in English)		iv
ABSTRACT (in Thai)		v
LIST OF TABLES		ix
LIST OF FIGURES		xi
LIST OF ABBREVIATIONS		xiv
CHAPTER		
1	**INTRODUCTION**……..	1
2	**OBJECTIVES**…….....	4
3	**LITERATURE REVIEW**……..	5
	3.1 Polyethylene (PE) and ethylene copolymers ……..…….	5
	3.1.1 High-density polyethylene…….……....	7
	3.1.2 Ethylene copolymers …….....	7
	3.1.3 PE blends: crystallisation and properties……..	9
	3.2 Silane-water crosslinking……...	13
	3.2.1 Silane grafting reaction…….	14
	3.2.2 Silane crosslink reaction ……..	19
	3.2.3 Properties of crosslinked polymer…….	24
4	**MATERIALS AND METHODS**……..	26
	4.1 Materials…….….	26
	4.2 Chemicals……...	28
	4.3 Instruments……...……..	28
	4.4 Preparation of silane-water crosslinked HDPE blends…..	29
	4.4.1 Grafting process…….……	29
	4.4.2 Crosslinking process……..	29

Copyright by Mahidol University

CONTENTS (continued)

		Page
	4.5 Characterisations……...……	30
	4.5.1 Silane absorption determination …….…….	30
	4.5.2 Contact angle measurement……...……..	30
	4.5.3 FTIR analysis…….……...……...	30
	4.5.4 Solvent extraction……...…….	31
	4.5.5 Dynamic rheological testing……...…….	32
	4.5.6 Differential scanning calorimetry……...…….	33
	4.5.7 Thermal gravimetric analysis……..…….	34
	4.5.8 Mechanical testing……...	35
	4.5.9 Heat deflection temperature testing…….	36
5	**RESULTS AND DISCUSSION**…….……..	37
	5.1 Silane-grafted HDPE blends……..……...	37
	5.2 Degree and rate of crosslinking of HDPE blends…….	44
	5.2.1 Solvent extraction results…….	44
	5.2.2 FTIR results……..	50
	5.2.3 Rheology results……...	54
	5.3 Properties of grafted and crosslinked HDPE blends…….	57
	5.3.1 Melting and crystallisation behaviours…….....	57
	5.3.2 Thermal degradation study……...……	63
	5.3.3 Rheological study…….	77
	5.3.4 Mechanical properties……..	87
	5.3.5 Heat deflection temperature…….	95
6	**CONCLUSIONS**……..……..…	98

Copyright by Mahidol University

CONTENTS (continued)

	Page
REFERENCES……	100
APPENDIX……..	108
BIOGRAPHY……..	118

Copyright by Mahidol University

LIST OF TABLES

Table		Page
3.1	Types and uses of the polyethylene…….	6
4.1	Characteristics of polymers used in this study…….	26
4.2	Silane absorption, crystallinity and contact angle of HDPE and various ethylene copolymers ……...	27
4.3	Chemicals used in this study ……..…….	28
4.4	The instruments and models……	28
5.1	IR peak positions and their assignments……..	40
5.2	Effect of ethylene copolymers on the grafting index at 1092 cm^{-1} of HDPE blends……..	41
5.3	Crystallinity, contact angle and silane absorption of HDPE and various ethylene copolymers…….…..	42
5.4	Crosslinking rate and gel content at certain crosslinking time of crosslinked HDPE and its blends…….	49
5.5	Melting temperature (T_m), enthalpy of fusion (ΔH_f), percentage of crystallinity (% χ_c), onset temperature of crystallisation ($T_{c\ onset}$), and crystallisation temperature (T_c) of HDPE, various copolymers and HDPE blends……...….	58
5.6	Melting temperature (T_m), enthalpy of fusion (ΔH_f), percentage of crystallinity (% χ_c), onset temperature of crystallisation ($T_{c\ onset}$), and crystallisation temperature (T_c) of grafted, annealed and crosslinked samples…….	60
5.7	Decomposition temperatures of HDPE and its blends under various ambient gases……..…….	64

Copyright by Mahidol University

LIST OF TABLES (Continued)

Table		Page
5.8	Temperature at 10% weight loss ($T_{10\%}$) and temperature of rapid weight loss (T_d) of individual polymers and HDPE blends under oxygen atmosphere…….....	66
5.9	Gel content and crosslink density values, temperature at 10% weight loss ($T_{10\%}$) and temperature of rapid weight loss (T_d) of HDPE blends and their grafted and crosslinked samples under oxygen atmosphere.…	69
5.10	Decomposition temperature of HDPE blends and their grafted and crosslinked samples…….	72
5.11	Slope and activation energy values of individual polymers and HDPE blends……...	73
5.12	Slope and activation energy values of HDPE blends and their grafted and crosslinked samples……...	76
5.13	Tensile data of HDPE, various copolymers and HDPE blends……...	88
5.14	Tensile data of grafted and crosslinked HDPE and its blends…….	94
5.15	Heat deflection temperatures of HDPE, various copolymers and HDPE blends……..	95
5.16	Heat deflection temperatures of grafted and crosslinked HDPE and its blends……...	97

Copyright by Mahidol University

LIST OF FIGURES

Figure		Page
3.1	Chemical structure of ethylene-vinyl acetate copolymer ……...	7
3.2	Chemical structures of (a) ethylene-butene, (b) ethylene-hexene and (c) ethylene-octene copolymers …….…….	8
3.3	The grafting reaction of silane onto polymer chain……	14
3.4	The silane-water crosslink reaction…….	19
3.5	Effect of silane concentration on the gel content of silane crosslinked LLDPE…….	20
3.6	The crosslinking rates as a function of the content of crystalline component in crosslinked EO/LDPE blends……...	22
4.1	Dimension of the tensile specimen used in this study…….	35
5.1	FTIR spectra of unmodified and grafted HDPE……..……....	38
5.2	FTIR spectra of unmodified and grafted HDPE/EO76 blend…….	38
5.3	FTIR spectra of unmodified and grafted HDPE/EO109 blend……....	39
5.4	FTIR spectra of unmodified and grafted HDPE/EB blend……..	39
5.5	FTIR spectra of unmodified and grafted HDPE/EVA blend……..	40
5.6	Effect of immersing time on the gel content of crosslinked HDPE and its blends……...…….....	45
5.7	Effect of immersing time on the swollen factor of crosslinked HDPE and its blends……	46
5.8	Effect of immersing time on the solvent uptake factor of crosslinked HDPE and its blends……	47
5.9	Effect of immersing time on the gel content and calculated crosslinking rate of crosslinked HDPE and its blends……	48
5.10	FTIR spectra of silane-grafted and crosslinked HDPE……...…	50
5.11	FTIR spectra of silane-grafted and crosslinked HDPE/EO76 blend..	51
5.12	FTIR spectra of silane-grafted and crosslinked HDPE/EO109 blend	51
5.13	FTIR spectra of silane-grafted and crosslinked HDPE/EB blend…..	52

Copyright by Mahidol University

LIST OF FIGURES (Continued)

Figure		Page
5.14	FTIR spectra of silane-grafted and crosslinked HDPE/EVA blend...	52
5.15	Effect of immersing time on the absorption index at 1092 cm^{-1} of crosslinked HDPE and its blends……	53
5.16	Complex modulus values as a function of immersing time of various crosslinked samples……	55
5.17	Crosslink density values as a function of immersing time of various crosslinked samples……	56
5.18	DSC heating thermograms of HDPE and its blends…….……..	58
5.19	DSC cooling thermograms of HDPE and its blends……...	59
5.20	DSC heating thermograms of grafted HDPE and its blends……..….	61
5.21	DSC heating thermograms of annealed HDPE and its blends……	62
5.22	DSC heating thermograms of crosslinked HDPE and its blends……	62
5.23	TGA thermograms of pure HDPE under various ambient gases……	64
5.24	TGA thermograms of HDPE and its blends under oxygen atmosphere……..	66
5.25	TGA thermograms of pure, grafted and crosslinked HDPE under oxygen atmosphere…….	68
5.26	DTG thermograms of (a) HDPE, (b) grafted HDPE and (c) crosslinked HDPE at various heating rates…….	71
5.27	Example of a plot of $-\ln(\beta/T_d^2)$ versus $1/T_d \times 10^{-3}$ for pure HDPE…	74
5.28	Activation energy values of various HDPE and its blends…….	75
5.29	Amplitude sweep of HDPE and its blends (LVE measured at a frequency of 1 $rad.s^{-1}$)……...…….…….	78
5.30	Amplitude sweep of HDPE and its blends (LVE measured at a frequency of 200 $rad.s^{-1}$)……...……..	78
5.31	Angular frequency sweep of HDPE and its blends…….	79
5.32	Angular frequency sweep of HDPE and various copolymers……	80
5.33	Storage and loss modulus of HDPE and its blends…….	81

Copyright by Mahidol University

LIST OF FIGURES (Continued)

Figure		Page
5.34	Storage and loss modulus of grafted HDPE and its blends……	82
5.35	Storage and loss modulus of crosslinked HDPE and its blends…….	83
5.36	Storage modulus of pure, grafted and crosslinked HDPE……..	84
5.37	Storage modulus of unmodified, grafted and crosslinked HDPE/EO76 blend……..	85
5.38	Storage modulus of unmodified, grafted and crosslinked HDPE/EO109 blend……	85
5.39	Storage modulus of unmodified, grafted and crosslinked HDPE/EB blend……	86
5.40	Storage modulus of unmodified, grafted and crosslinked HDPE/EVA blend……...	86
5.41	Experimental and theoretical tensile strength at break values of HDPE blends……...	89
5.42	Experimental and theoretical elongation at break values of HDPE blends……..	89
5.43	Experimental and theoretical modulus values of HDPE blends…….	90
5.44	Tensile strength at break of various HDPE and its blends…….	92
5.45	Elongation at break of various HDPE and its blends……..	92
5.46	Modulus of various HDPE and its blends……...	93
5.47	Yield stress of various HDPE and its blends……..	93
5.48	Heat deflection temperatures of various HDPE and its blends……...	97

Copyright by Mahidol University

LIST OF ABBREVIATIONS

ASTM	American Society for Testing and Materials
DBTDL	Di-n-Butyltin-Dilaurate
DCP	Dicumyl Peroxide
DSC	Differential Scanning Calorimetry
DTG	Derivative Thermal Gravimetric Analysis
E_a	Activation energy
EB	Ethylene-Butene Copolymer
EO	Ethylene-Octene Copolymer
EVA	Ethylene-Vinyl Acetate Copolymer
FTIR	Fourier Transform Infrared Spectroscopy
HDPE	High-Density Polyethylene
HDT	Heat Deflection Temperature
LDPE	Low-Density Polyethylene
LLDPE	Linear Low-Density Polyethylene
MPa	Mega Pascal
kPa	kilo Pascal
PE	Polyethylene
T_m	Melting Temperature
TGA	Thermal Gravimetric Analysis
VTMS	Vinyl Trimethoxysilane

Copyright by Mahidol University

CHAPTER 1
INTRODUCTION

Properties of polymers, particularly the high temperature properties, can be modified by crosslinking of the polymer chains. The creation of direct links or bonds between the carbon backbones of individual polymer chains forms the crosslinked polymer structure. The result of this linkage is to restrict movement of the polymer chains relative to each other, so that when heat or other forms of energy are applied, the basic network structure cannot deform and the excellent properties are retained at higher temperature. Crosslinking also increases impact strength, dimensional stability, tensile strength, thermal properties, chemical resistance, and it improves electrical properties, aging, and solvent resistance of polymer [1-2].

There are a number of ways which can be used for crosslinking such as radiation crosslinking [3-7], peroxide crosslinking [8-12], and silane-water crosslinking [13-41]. In radiation crosslinking, radiation of accelerated electrons (β-radiation) or electromagnetic wave (γ-radiation) abstracts hydrogen from the hydrocarbon chain and produces free radicals; and, by combination of these alkyl radicals, carbon-carbon crosslinks are formed. Non uniform crosslink distribution, thickness restrictions (needed for thick insulation for high voltages), and high cost are disadvantages of this method. In peroxide crosslinking, radicals made of decomposition of peroxides abstract hydrogen from the polymer chain and, like the radiation method, carbon-carbon bonds are formed between polymer chains. Disadvantages of this method are high capital investment for the equipment, high-energy consumption, low outputs, long product changeover times, and limitations on part thickness and part design.

One method which is of interest and becomes increasingly used in the industry is silane crosslinking. Silane crosslinking takes place in two stages. First, a small amount of silane is grafted onto the polymer chains as organic peroxide is applied. In this step, vinyl trimethoxysilane (VTMS) is commonly used. The grafted polymers are subsequently crosslinked in the presence of water or humidity. Compared to other

Copyright by Mahidol University

crosslink methods, each Si atom of silane has three reactive groups so up to six polymer chains may be joined to each crosslink which enhances the mechanical properties of the silane crosslinked products. (Two macromolecules join in other crosslinking methods). The use of silanes results in a more flexible and more economical process for crosslinking. Silane crosslinked polymers are linked through a siloxane bond instead of the carbon-carbon bond created via radiation or peroxide crosslinking. Siloxane bridges are less rigid than carbon-carbon bonds and give flexibility to the crosslinked polymer. Silane technology demonstrates outstanding process flexibility due to its ability to occur the crosslinking at the desired time and its ability to adjust easily the reactivity of the system. An improvement in thermal stability of the silane-crosslinked materials was revealed by Shieh et al. [13], Sirisinha and Kawko [14]. The crosslinked materials also showed strong potential to be used for thermal energy storage applications. The degree of crosslinking was vital importance in determining how well the properties were maintained at elevated temperature. The degree and rate of silane crosslinking depend on several factors. One of which is the amount of crystalline component in the material. The results of previous works have shown that the diffusion of water is faster in the amorphous phase than in crystalline phase [15-18] and silane crosslink occurred mainly in the amorphous phase and leaved the crystalline region unchanged or changed very slightly [19-20].

High-density polyethylene (HDPE) is one of the widely used thermoplastic. It has a low degree of branching and thus stronger intermolecular forces and tensile strength. HDPE has the highest service temperature among polyethylene class. Therefore, HDPE has a wide variety of applications, including heat transfer piping systems, water pipes for domestic water supply, tapes, films, bottles and plastic bags [42-43]. It is our interest to prepare a silane-crosslinked HDPE. However, due to its high level of crystallinity, its silane absorption and water diffusion is very low. To achieve a high degree of grafting, a high silane loading may be required. However, there are two main problems associated with this aspect. (i) The cost of vinyl silane monomer to be used for producing a high degree of crosslinking would be higher. (ii) There is a difficulty in adequately combining whole amount of silane with the base polymer. If the silane is injected as a liquid stream into a conventional extruder and mixed with a

Copyright by Mahidol University

polymer, small gels may be formed because of localised, premature crosslinking in areas of high silane concentration resulting from inadequate mixing.

In this study, a second polymer which has lower crystallinity than HDPE was introduced to the base HDPE polymer to increase silane absorption and diffusion of water which would aid the silane grafting and crosslink reaction. Three types of ethylene copolymers differing in their chain structure and polarity were investigated for their abilities in assisting the silane crosslinking process. These include ethylene-octene copolymer (EO), ethylene-butene copolymer (EB) and ethylene-vinyl acetate copolymer (EVA). The silane-grafted and silane-crosslinked HDPE and its blends with various copolymers were prepared. The effects of ethylene copolymers on the degree of grafting and crosslinking of HDPE were investigated. The measurement of rheological behaviours of crosslinked products was used to determine their crosslink density. The structure, mechanical properties, crystallisation behaviours, thermal stability and thermal degradation kinetics of the silane-crosslinked products were also studied.

Copyright by Mahidol University

CHAPTER 2
OBJECTIVES

In this study, high-density polyethylene (HDPE) and its blends with various ethylene copolymers grafted with silane and crosslinked with water were investigated. The ethylene copolymers were used to improve the efficiency of silane grafting and crosslink reaction of HDPE. The aim of the present work was to study the effects of chemical structure and polarity of the copolymers on the silane grafting and water crosslinking of HDPE. Their effects on properties of crosslinked products were also focused on. Three types of copolymers were used for this purpose. These include ethylene-octene copolymer (EO), ethylene-butene copolymer (EB) and ethylene-vinyl acetate copolymer (EVA).

The thesis is divided into two main parts.

Part I: Melt free-radical grafting of vinyl trimethoxysilane (VTMS) onto HDPE and its blends with various ethylene copolymers was reported. The effects of ethylene copolymers on the degree of grafting were analysed. The silane-grafted polymers were also investigated for their mechanical, rheological and thermal properties.

Part II: Silane-crosslinked HDPE and its blends were described. The effects of different ethylene copolymers on crosslinking degree were focused on. Changes in the crosslink structure were investigated using Fourier Transform Infrared Spectroscopy (FTIR) analysis, solvent extraction and rheological measurement. The crystallisation behaviours, thermal and mechanical properties of the silane-crosslinked products were discussed.

Copyright by Mahidol University

CHAPTER 3
LITERATURE REVIEW

3.1 Polyethylene (PE) and ethylene copolymers

Polyethylene (PE) is one of the most widely used thermoplastic materials because it has many good properties, such as high chemical resistance, high impact strength, flexibility, easy processing and low cost.

There are three main kinds of PE, i.e. high-density polyethylene (HDPE), low-density polyethylene (LDPE) and linear low-density polyethylene (LLDPE). These can all be distinguished by their density which is a result of their degree of crystallinity and type and content of branches. The properties of PE are generally directly influenced by a number of structural and morphological factors [44], including: type, amount and distribution of comonomers, degree of branching and crystallinity, average molecular weight and molecular weight distribution. For simplicity and following conventional practices, the overall effect of these influences is broadly quantified by the density of the PE. Typical properties of these three types of PE are shown in Table 3.1. In this study, only HDPE is focused on.

Copyright by Mahidol University

Table 3.1 Types and uses of polyethylene [42]

Polyethylene	Density range ($g.cm^{-3}$)	Comments and applications
HDPE	0.942-0.965	Stronger and stiffer than LDPE, used mainly in blow moulding, low molecular weight HDPE used for general purpose moulding. Uses include pipe, tapes, films, and bottles.
LDPE	0.915-0.935	Tough and flexible polymer mainly used for packaging film, general purpose moulding of domestic products such as bottles and tubes, depending on the molecular weight.
LLDPE	0.917-0.939	Copolymers of ethylene and α-olefins. Structure similar to HDPE but with short-chain branching, stiffer than LDPE but different melt processability. It is used in many film applications where flexibility, toughness and strength are required in a PE film.

Copyright by Mahidol University

3.1.1 High-density polyethylene

HDPE is prepared from ethylene monomer using a coordination catalyst, e.g. Ziegler-Natta type catalysts, at low or moderate pressures and the ethylene molecules are coordinationally polymerised to predominantly linear macromolecules (i.e. non-branched). The absence of branching results in a more closely packed structure with a high degree of crystallinity and high density of 0.942 to 0.965 $g.cm^{-3}$. HDPE has a mostly linear structure and the highest crystallinity among other types of PE, usually in the 60-80% range, depending upon crystallisation conditions, and molecular weight. It is more rigid and stronger than the low density PE types but less flexible as a result of regular packing of polymer chains. It is also less transparent than the low density PE types because it is more crystalline. It can withstand rather higher temperatures and has better physical and chemical properties. Representing the largest portion of the PE applications, HDPE offers excellent impact resistance, light weight, low moisture absorption and high tensile strength. HDPE is frequently used in plastic bags, water pipes, wire and cable insulation, and extrusion coating.

3.1.2 Ethylene copolymers

The molecular structure of a PE can be modified by the addition of one or more dissimilar monomers to the polymer, resulting in copolymers. The most frequently used comonomer in high pressure ethylene copolymerisation is vinyl acetate. The structure of this copolymer is shown in Figure 3.1.

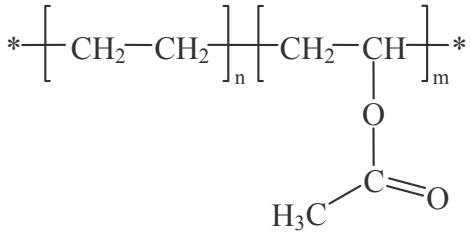

Figure 3.1 Chemical structure of ethylene-vinyl acetate copolymer

Copyright by Mahidol University

Ethylene-vinyl acetate copolymer (EVA) is produced by free-radical polymerisation at high pressures with oxygen or organic peroxide catalysts. EVA, varying in vinyl acetate incorporation from 1 to 60 wt% is commercially available. However, those most commonly used in the wire and cable area have approximately 18 to 28 wt% of vinyl acetate incorporation. As vinyl acetate content increases, density increases and crystallinity decreases; thus, higher vinyl acetate content results in lower stiffness, greater toughness, lower melting point and somewhat higher permeability. The presence of the polar acetate group in the polymer also affects the dielectric constant and dissipation factor, both of which increase linearly with increase of vinyl acetate content.

Ethylene copolymers can also be produced by employing a variety of α-olefin comonomers, e.g. 1-butene, 1-hexene and 1-octene, leading to the structures shown in Figure 3.2.

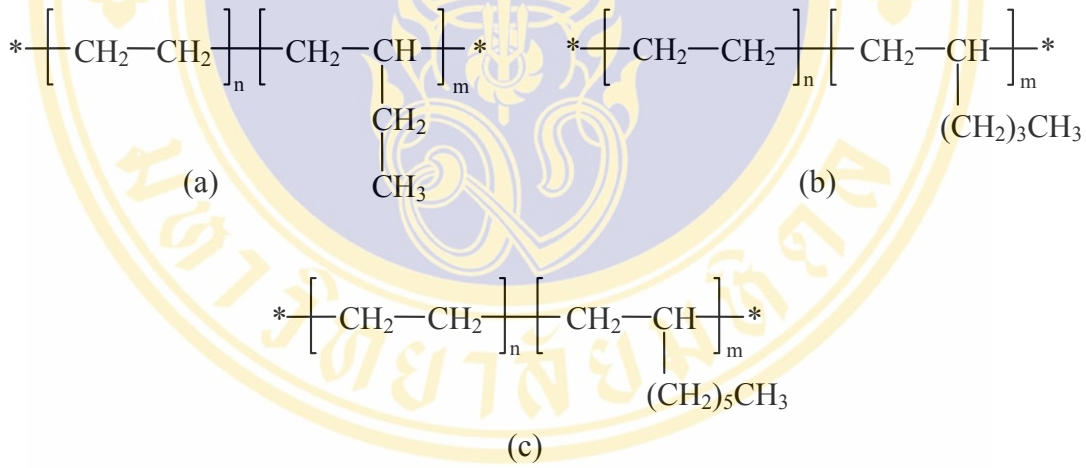

Figure 3.2 Chemical structures of (a) ethylene-butene, (b) ethylene-hexene and (c) ethylene-octene copolymers

Copyright by Mahidol University

Their properties are strongly affected by the degree and the distribution of short chain branching due to the incorporation of α-olefins in the polymer chains [45]. These ethylene copolymers can be synthesised by either Ziegler-Natta or metallocene catalysts, at low pressures and low temperatures, to introduce enough short chain branches into the otherwise linear polymer to reduce the density of the polymer. The crystallinity may range from near zero to that of HDPE depending on the nature and number of branches. The ethyl, butyl and hexyl side chains interfere with the chain folding crystallisation process and, as the number of side chains increases; the material exhibits a lower density. Because of its size, the hexyl side chain disrupts the crystallisation process more effectively than the butyl and ethyl side chain, respectively. Partly as a result of the effect on the crystallisation process, octene and hexene copolymers exhibit better stress crack/stiffness properties than the corresponding butene copolymers. This stress crack relationship is very noticeable in thin-walled containers, for example milk bottles, and is also observed to a lesser extent in wire and cable insulations and jackets. The influence of increasing branch length on the thermal behaviour is to some extent similar to that of increasing comonomer content [46].

3.1.3 PE blends: crystallisation and properties

This section reviews the literature relating to blends of linear HDPE and ethylene copolymers. The factors controlling blend morphology also thermal and mechanical properties of these blends are discussed.

Investigations of the morphology, in both the melt and solid state, of HDPE blends, varying in composition and molecular structure of the components, have been reported. Most of these works focused on the understanding of effect of conditions for phase segregation and miscibility and to improve specific properties relative to one-component systems. Traditionally, different PE types are blended in order to improve processability and properties of the final product. For blends of HDPE with other PE, blend compatibility issues were primarily attributable to differences in types and levels of chain branching [47]. The type and level of branching of the LLDPE component, however, was influential with regard to cocrystallisation [48] and minimum branch

Copyright by Mahidol University

contents for phase segregation have been determined for various HDPE/LLDPE blends [49].

Neutron scattering studies of the melt of blends of HDPE and LDPE conclusively showed melt miscibility of the components over the whole range of concentrations [50]. The studies on blends of HDPE and hydrogenated poly(butadiene) (HPBD), which were ethylene-butene copolymer (EB) pointed out that the changing in interaction parameter with increasing branching content of the EB induces liquid-liquid phase separation at a given co-unit content [51]. The solid state morphology of blends of HDPE and HPBD, with ethyl branch contents ranging from 2 to 5.5% mol of branch points, was previously studied using samples that were rapidly crystallised [52]. By using differential scanning calorimetry (DSC) and solvent extraction techniques, it was found that cocrystallisation of the linear and branch components occurs up to a branch content of approximately 4% mol.

Galante et al. [53] studied the cocrystallisation in blends of linear and branched PE (HPBD) under both isothermal and slow cooling crystallisation conditions. They found that a key factor in governing the extent of cocrystallisation in these blends was the closeness of crystallisation rates of each of the components. The extent of the cocrystallisation diminished with increasing concentration of the linear component in the blend. The copolymer composition and molecular structure also had a strong influence on cocrystallisation. The amount of cocrystallisation was favoured at the lowest isothermal crystallisation temperatures and was maximised under quenching conditions.

A report of Nicholson and coworkers [54] indicated that blends of HDPE and LLDPE could phase separate in the melt when the degree of branching exceeds some critical value, probably in the range of 20-30% mol, depending upon the nature of the branch and the molecular weights of the polymers. With mixtures of LLDPE, the likelihood of cocrystallisation was reflected in the separation of melting points. With mixtures of well-separated melting points, such as 130 °C and 112 °C for HDPE and LLDPE, respectively, separate crystals were found, yielding two separate melting peaks during DSC scans. These results had been found by Hu and coworkers [55] in the system of HDPE/LLDPE blends. When the melting points of the HDPE/LLDPE blends were only a few degrees apart, cocrystallisation might be found, yielding a

Copyright by Mahidol University

single intermediate melting point. It seemed obvious that the presence of branches at the interface, with their exclusion to the near crystal surfaces, would affect the packing density of the amorphous chains near the surface, and thus affected the fraction of chains which fold. This would depend on the number and length of branches. With HDPE/LLDPE blends, the effect would be dependent on the extent of co-crystallisation and crystallisation conditions. This was one way in which the morphology, chain topology, and nature of the interfacial region would be affected by branching and blending [56].

Stein et al. [56] found no evidence of cocrystallisation of HDPE and LDPE in the crystalline phase and observed two separate melting points. Stein et al. [56] also reported that the thermal behaviour was strongly dominated by the crystals in HDPE. In the amorphous phase, the blend was miscible and linearly associated with the characteristics of the constituents. Evidence for designating HDPE/LDPE blends as compatible systems from observations of individual melting points with small intermediate melting points was reported by Stafford [57] and Clampitt [58]. Stafford suggested that small shifts in endotherm temperature for the components might be interpreted as evidence for cocrystallisation. This was contradicted to the results of Robertson and Paul [59], who suggested that these small shifts could be due to the difficulty in resolving peaks that were so close together. DSC traces from the work of Rueda et al. on HDPE/LDPE blends [60] clearly showed the presence of three endothermic peaks (which could be related to the melting of three different populations of lamellae). The third, intermediate peak was not observed for HDPE fractions higher than 50%. The lower peak could be associated with the LDPE component, the higher peak with the HDPE component, and the intermediate peak with the mixed material. This mixed material, was not however attributed to any genuine cocrystallisation, but to a process whereby the more defective chains from the HDPE component mixed with the less defective ones from the LDPE component.

The effect of comonomer type of LLDPE on melt miscibility and crystallinity of LLDPE/HDPE blends was studied by Hussein [61]. Two different comonomer types used were EB and EO of very similar M_w, MWD and branch content keeping comonomer type as the only primary molecular variable. The rheological data showed no significant effect for branch type on the melt miscibility of LLDPE/HDPE blends.

Copyright by Mahidol University

The total crystallinity of all blends was found to follow linear additivity rule and the HDPE melting peak was found to shift towards that of LLDPE with the increase of the fraction of EB or EO.

The incompatibility of LDPE/HDPE blends determined by thermal analysis was often supported by poor solid-state mechanical properties [62] and tensile properties of LDPE/HDPE blends were less than those predicted by the rule of mixtures [63]. For blends of LDPE and HDPE, the addition of 2% weight dicumyl peroxide (DCP) results in improved blend compatibility and subsequently improves the tensile properties of the blend [64]. The tensile properties of HDPE/LLDPE blends were shown to vary significantly from the rule of mixtures, particularly when the ratio of levels of HDPE to LLDPE approaches 1 to 1 [65]. This is also the case for the flexural and impact properties of HDPE/LLDPE blends and is attributed to the composition of the amorphous phase of the blend [66].

Sarkhel et al. [67] studied the mechanical properties of binary blend of LDPE and HDPE. The results showed that impact strength of the blends increased with increasing LDPE concentration, whereas tensile strength showed the opposite trends. A study of Hussein [61] on the mechanical properties of LLDPE/HDPE blends was investigated. The mechanical properties were found to change on the addition of LLDPE to HDPE. Values of moduli for the EB/HDPE blends followed the additivity rule. No significant effect of comonomer type was observed in strength at yield for both blends. Similarly, very weak effect of comonomer type was seen on the large stain properties such as elongation at break. However, blends of EB and EO with HDPE showed incompatibility and poor ultimate tensile properties for the HDPE rich blends.

Copyright by Mahidol University

3.2 Silane-water crosslinking

Crosslinking is a broadly used method for the modification of polymer properties. This process involves the formation of three dimensional structures. It extends the range of use by raising the upper temperature limit of application and improves some of the properties of polymer such as dimensional stability, mechanical properties (impact and tensile strength), increased resistance to thermal deformation and better resistance to solvents. Due to the above properties, crosslinked polymer can be used in the production of heat shrinkable articles, central heating tubes, cable insulation [68]. There are three main crosslinking methods, i.e. radiation crosslinking [3-7], peroxide crosslinking [8-12] and silane-water crosslinking [13-41].

In radiation crosslinking, the free radical formed on the polymer backbone is the result of electron beam irradiation and thereby promotes subsequent crosslinking. The primary H radical is generated by a radiation process and abstracts a hydrogen atom from polymer chains. The polymer radicals are formed and these radicals can combine to produce a crosslinked polymer [3]. Advantages of this method are higher resistance to heat and chemicals, better mechanical properties, and high productivity. However, it has some disadvantages including high investment cost, decreasing in initiation crosslinking efficiency with thickness and impossible to crosslink thick sections sufficiently and deterioration of the base polymers.

In peroxide crosslinking, peroxides provide a source of free radicals when heated above their decomposition temperatures. These free radicals are capable of extracting a hydrogen from the polymer backbone, thus transferring the free radicals site to the polymer. With this accomplish, two polymer chains can crosslink together. This method is simple and rapid crosslinking at high temperatures. However, it has some disadvantages such as crosslinking reactions to oxygen, the risk of precuring and high production cost.

The silane-water crosslinking of polymer has been the subject of considerable research in the industry because of its various advantages, such as easy processing, low cost and capital investment, and favorable properties in the processed materials. The most common silane used in the manufacture of silane crosslinkable polymer is vinyl trimethoxysilane (VTMS). This silane has conventionally been introduced into

Copyright by Mahidol University

polymer by melt grafting using a peroxide as initiator. In producing the silane-grafted polymer, a peroxide is mixed with the silane and polymer and all these components are compounded in a melt-mixer chamber. The silane-grafted polymer is then crosslinked by water.

3.2.1 Silane grafting reaction

The silane grafting is a thermochemical reaction in which the peroxide first decomposes at an elevated temperature; this results in the formation of oxy radicals. These oxy radicals have the potential to abstract hydrogen from the polymer molecule and can attack the vinyl group of a molecule and convert it into free radicals. These free radicals either combine with one another or attack another molecule in a similar fashion to propagate the free-radical reaction. This process results in the grafting of vinyl silane onto polymer chains. The grafting reaction mechanisms are shown in Figure 3.3.

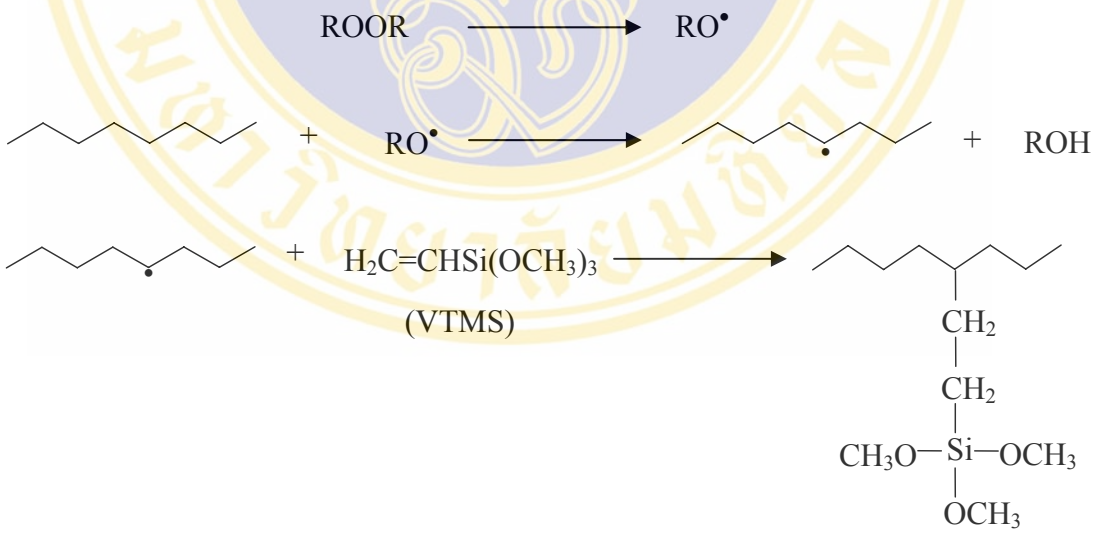

Figure 3.3 The grafting reaction of silane onto polymer chain

Copyright by Mahidol University

There are many factors that influence the extent of the silane grafting reaction. These factors include silane monomer type and concentration, initiator type and concentration, reaction temperature and time, structure of polymer and the incorporation of additives into the system.

(i) Silane monomer type and concentration

The vast majority of the publications were concerned with the influences of silane monomer types and concentrations on silane grafting reaction. Huang et al. [21] studied silane grafting reaction of polypropylene (PP). They found a much greater grafting of methacryloylpropyltrimethoxysilane (VMMS) than of VTMS and vinyl triethoxysilane (VTES), which is probably the result of large steric hindrance in the case of VTMS and VTES since the reactive sites are close to the bulky alkoxysilane groups. Furthermore, the conjugated structure in VMMS could improve grafting efficiency by stabilising the macroradicals of VMMS-grafted PP. Jiao et al. [22] reported the silane grafting reaction of EO. They found that the extent of silane grafting reaction increased as the amount of VTMS and VTES increased. Shieh et al. [17] investigated the silane grafting of LDPE in which VTMS as silane monomer and DCP as initiator were used. The order of the grafting extent is consistent with that of the amount of silane used; that is, the grafting extent for the sample grafting with 5% silane is the highest and the sample grafting with 1% silane is the least. Nachtigall et al. [23] reported that an increase in VTES concentration resulted in an increasing in the silane grafting degree of PP for constant DCP levels. The degree of functionalisation showed maximum with 0.5-0.75% DCP, for each 5 and 10% VTES. The VTES was proved to be a very reactive compound because even in the absence of peroxide or with a small concentration, the initiator grafting was accomplished.

Copyright by Mahidol University

(ii) Initiator type and concentration

The efficiency of the silane grafting reaction also depends on the type and amount of peroxides. Huang et al. [21] investigated the effect of benzoyl peroxide (BPO) and DCP initiator on silane grafting of PP. No degradation of PP during grafting was observed when BPO was used as an initiator, and the melt flow rates of grafted PP decreased with increasing BPO concentration. In contrast, the use of DCP as an initiator resulted in severe degradation of PP, and the melt flow rates of grafted PP increased gradually with increasing DCP concentration.

In the study of Shieh et al. [24], the effects of amount of peroxide on the grafting reaction of LDPE were investigated. VTMS with 7% was used along with a varied amount of DCP in the range of 0.025-0.3%, to produce the grafting reactions of LDPE. They observed that the extent of the silane grafting reactions increased with an increase of the amount of peroxide in the range of 0-0.1% in which 0.1% of peroxide could lead to a complete grafting reaction. Wang et al. [25] reported that the extent of grafting of LLDPE increased as DCP concentration increased. The more the DCP concentration, the more the VTES grafted on LLDPE. Meksawat [26] studied the effect of DCP concentration (0, 0.05, and 0.1%) on the silane grafting raction of EO. The results suggested that the silane grafting index increased when amount of DCP concentration increased up to 0.1%.

(iii) Reaction temperature and time

The reaction temperature and time were also shown to be important factors controlling the silane grafting reaction. Liu et al. [27] studied the influences of processing temperature in the range of 170-220 °C on silane grafting of PP. They found that the degree of grafting went through a maximum at a processing temperature close to 180 °C. This should be the combined effects of increased temperature itself and increased degradation of PP at high processing temperatures. Therefore, processing temperatures between 170 and 180 °C were the optimum choices considering both degree of grafting and degradation of PP. The effects of reaction temperature and time on silane grafting of EO were observed by Jiao et al. [22]. The

Copyright by Mahidol University

amount of silane-grafted increased significantly with an increase in the reaction temperatures. It is believed that the higher the reaction temperature, the more the radicals produced from the decomposition of DCP leading to an increase of silane grafting yields. The degree of grafting increased as the reaction time increased from 3 to 11 min. The suitable reaction time of the silane grafting of EO at 170 °C is about 8 min. The grafting reaction time at fixed temperatures relates to the half life-time (HLT) of a peroxide used, and the reaction time is usually 5-10 times of HLT of peroxide. For examples, the HLT of DCP at 170 °C is about 1 min. It is also reported in the study of Sen et al. [28] that the extent of grafting increased with increasing the reaction temperature and time.

(iv) Structure of polymer

The polymer structure is one of the parameters that affect the silane grafting reaction. Comparisons of the silane grafting degree of EO, LDPE, and their blends were investigated by Chimdist [19]. The degree of grafting in LDPE and EO was found to be differed due to the structure difference. Compared the two polymers, LDPE has a long chain branch structure which has the number of branch in the range of 20-30 methyl groups per 1000 carbons [69]. In the case of EO, which is one of the LLDPE groups, it usually has the number of short-chain branching in the range of 20-50 methyl groups per 1000 carbons [70].

From the literature [70], HDPE has the number of chain branching in the range of 2–7 per 1000 carbon atoms on the polymer main chain and consists of the more vinyl residue on the polymer chain, although this material has less chain branching than LDPE and LLDPE. As a result, HDPE has the most allyl hydrogens among the three materials, whereas LLDPE has more hydrogens attached to tertiary carbons than LDPE has. Homolytic bond dissociation energies [71] for hydrogens attached to primary, secondary, tertiary, and allyl carbons were 410, 397, 385, and 368 $kJ.mol^{-1}$, respectively. Thus, the least energy needed for a free radical to abstract hydrogen is from an allyl carbon among the four kinds of carbons. In the silane-grafting reaction, therefore, the free radicals generated from DCP mostly should attack and abstract the hydrogens at allyl, tertiary and secondary carbons rather than primary carbons.

Copyright by Mahidol University

Rojas et al. [72] studied the grafting reaction of diethyl maleate (DEM) onto PE. The results obtained from NMR and FTIR analyses showed that DEM insertion onto PE chains preferentially occurs in secondary carbons of the main chain regardless of the branch type and content of the copolymer (up to 1-hexene). The reason for this behaviour was reported to be related to steric effects produced by the size of the DEM molecules. It seemed that DEM not only avoids the tertiary carbons where the branches are located but also, in PE copolymers with less than 4 mol % branch content, it prefers to insert in the secondary carbons that are a few carbon atoms away from the branch point. A statistical factor is also involved since there is an excess of secondary carbons as compared to tertiary ones per PE chain that would explain why the peroxide attacks secondary carbons preferentially instead of more reactive tertiary ones. In contrast, Shieh et al. [24] quantitatively compared the extents of grafting reactions of three polyolefins with 17.5 phr of silane, and found the grafting in the order of LLDPE>LDPE>HDPE. The results were explained by the presence of more hydrogens attached to tertiary carbons of LLDPE than LDPE.

(v) The incorporation of additives

A number of reports reviewed that the incorporation of additives could improve the grafting reaction of polymer. Parent et al. [29] studied the functionalisation of EVA with VTES carried out by a free-radical melt-grafting in the presence of added comonomers. Silane graft yields were determined by proton NMR spectroscopy. Comonomers evaluated were maleic anhydride (MA), 1-vinyl-2-pyrrolidone (VP), and 1-dodecene (DD). Of the additives studied, MA suppressed both silane grafting and peroxide-initiated crosslinking, whereas VP and DD suppressed crosslinking more extensively than VTES grafting; optimum performance was found at a comonomer: vinylsilane mole ratio of 0.2.

Liu et al. [27] studied the effect of additive types (styrene and ethylene glycol dimethacrylate) on silane grafting reaction of PP. They observed that introduction of styrene into the grafting system markedly improved the degree of grafting and reduced the degradation of PP during grafting. Ethylene glycol dimethacrylate showed a better

Copyright by Mahidol University

performance in reducing the degradation of PP during grafting, but it was not as effective in improving the degree of grafting.

3.2.2 Silane crosslink reaction

The crosslink reaction of the silane-grafted polymer is demonstrated to be through hydrolysis of the methoxy groups with water followed by condensation of the formed silanol groups and subsequently condensation to form siloxane bonds. The mechanisms of water crosslink reaction of polymer are shown in Figure 3.4.

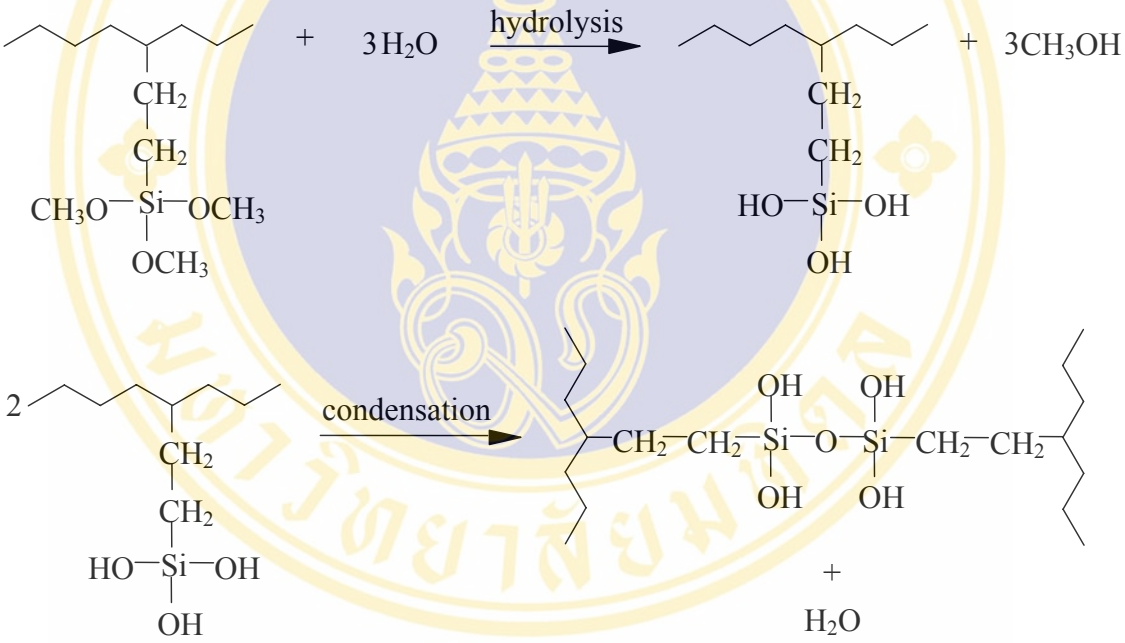

Figure 3.4 The silane-water crosslink reaction

Copyright by Mahidol University

The parameters affecting the silane crosslink reaction including the degree of silane grafting, crosslinking temperature and time, morphology (amount of crystalline component in the material), thickness of sample and the presence of catalyst in the systems.

(i) Degree of silane grafting

One of the main factors for the silane crosslink reaction is the degree of silane grafting. Celina and George [30] studies the silane crosslinking of PE in which VTES and DCP were used. They found an increase in the crosslinking degree with increasing silane concentration. In the study of Wang et al. [25], the effect of VTES concentration on the degree of crosslinking (gel content) of the silane crosslinked LLDPE was investigated as illustrated in Figure 3.5. They observed that the gel content increases gradually with the increase in the VTES concentration. When the VTES concentration is more than 3%, the gel almost levels off.

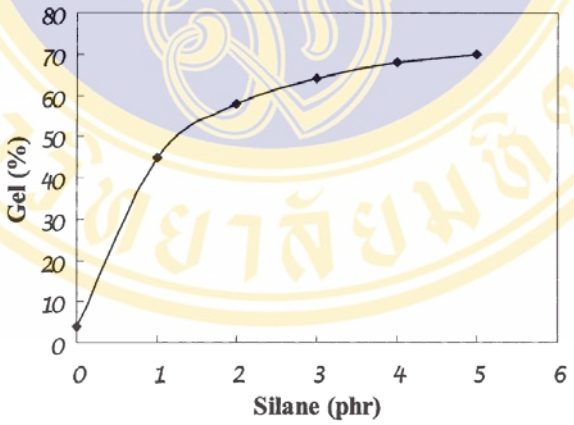

Figure 3.5 Effect of silane concentration on the gel content of silane crosslinked LLDPE [25]

Copyright by Mahidol University

(ii) Crosslinking temperature and time

There are many reports concerning the effect of crosslinking temperature and time on the degree of crosslinking [16, 28, 31-32, 73]. The degree of crosslinking was found to increase with increasing time. More crosslinks were believed to form in the crosslinked network structures after prolonged crosslinking time. The degree of crosslinking of the silane-crosslinked materials conducted for a certain crosslinking time increased with increasing temperatures. This was demonstrated that the diffusion rate of water and the subsequent hydrolysis and condensation rates of the silyl trimethoxy moiety increased with increasing temperatures. The crosslinking rates are found to be linearly related to the temperatures which could be described by the Arrhenius equation [17] that follows:

$$r = A \exp(-E/RT) \quad (3.1)$$

where r = the crosslinking rate ($\%.hr^{-1}$)
A = a constant
T = an absolute temperature
R = the gas constant
E = the overall activation energy for the crosslinking

From this equation, it can be seen that the crosslinking rate increased with an increase in crosslinking temperature. However, the crosslinking of silane grafted polymer is processed after shaping the product; therefore, in order to prevent deforming of the final product the temperature used for the crosslinking process is limited to be below the melting temperature of that polymer.

Copyright by Mahidol University

(iii) Morphology and thickness of sample

The diffusion of water had been previously reported to be one of the parameters determining the rate of crosslinking, and to be dependent on both the morphology (content of crystalline component) and thickness of the sample. Many studies [15, 17-18, 33] focused on the influence of morphology of sample on silane crosslink reaction of PE system. The polymers with lower crystallinity showed higher diffusion rate of water than the ones with higher crystallinity and resulted in a higher crosslinking speed. The crosslinking rates are inversely proportional to the contents of crystalline component of the samples as shown in Figure 3.6. This is because the diffusion of water decreases with increasing content of the crystalline component in the sample. This suggested that the crosslinking reactions occur mainly in the amorphous domain of the sample.

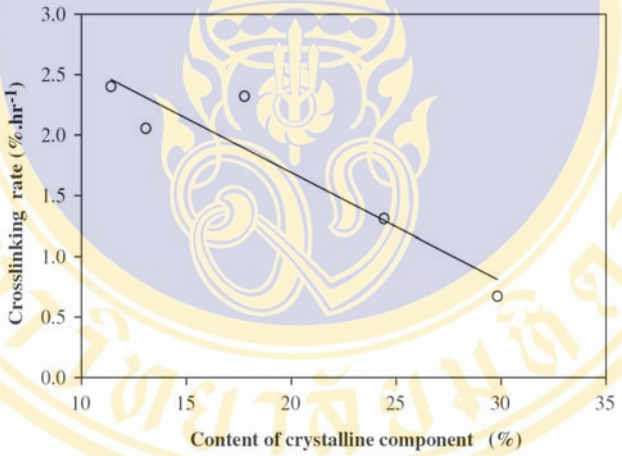

Figure 3.6 The crosslinking rates as a function of the content of crystalline component in crosslinked EO/LDPE blends [18]

Shieh et al. [17] studied the effect of thickness of sample on silane crosslinking process of LDPE. The two different thicknesses of samples after crosslinking for 38 hrs were investigated. They found that the degree of crosslinking and crosslinking rate for the thinner sample was slightly less dependent on the content of crystalline component than that for the thicker one. The overall activation energy was apparently dependent on the thickness of sample. The crosslinking reaction of the thinner sample has a smaller overall activation energy, and is thus less temperature dependent than that of the thicker one.

Copyright by Mahidol University

(iv) The presence of catalyst

It was reported earlier that the crosslinking rate of silane crosslink reaction could be increased markedly by the use of some catalysts, e.g. di-n-butyltin-dilaurate (DBTDL), dibutyltin-diacetate, and dibutyltin-dioctoate [28, 31-32, 34].

Sen et al. [28] studied the moisture crosslinking of the silane-grafted PE and ethylene propylene rubber in the presence of a catalyst. The effects of the structures of three catalysts including stannous-octoate, DBTDL, and dialkyltin-mercaptide and their catalyst concentrations were observed. They found that the gel content increased with an increase in the concentration of the catalysts. At a low concentration, the order of their efficiency was stannous-octoate<DBTDL<dialkyltin-mercaptide. Although at a high concentration, all three catalysts resulted in the same degree of crosslinking. These tin compounds catalysed the silanol condensation reaction by their Lewis acid behaviours. Probably due to stronger Lewis acid character of the mercaptide over carboxylates, dialkyltin-mercaptide was found to be the most effective catalyst. Similarly, between the two tin carboxylates, DBTDL showed more pronounced activity than stannous-octoate, due to its stronger lewis acid behaviour.

In the case of silane-water crosslinked HDPE, the results of Narkis et al. [31] revealed that in the case of uncatalysed system, 70% gel was obtained within 400 hrs of crosslinking time. In the presence of DBTDL catalyst, the crosslink reaction tendency was very high. The polymer was practically fully crosslinked with 80% gel in about 10 hrs under the same condition. A similar result was reported by Hjertberg et al. [32] on the silane crosslinking of ethylene-vinyltrimethoxysilane (EVS) copolymers. The addition of DBTDL catalyst increased the reaction rate considerably and a final gel content of 70-75% was obtained.

Palmlof and Hjertberg [34] studied the catalytic effects on the crosslinking behaviour of poly (ethylene-co-vinyltrimethoxysilane). The three different catalysts used were the commonly used DBTDL, stearic acid, and ethylene-acrylic acid (EAA) copolymer. The DBTDL was found to strongly catalyse the first step of the crosslinking reaction, that is, the hydrolysis. Concerning the catalytic activity of the carboxylic acids, the low molecular weight stearic acid has been shown to be a much more effective catalyst than is the polymer-bound carboxylic acid (EAA).

Copyright by Mahidol University

3.2.3 Properties of crosslinked polymer

The silane-water crosslinking technique offers technological advantages and improvements in many useful properties of crosslinked materials.

Kuan et al. [35] studied silane-grafted and water-crosslinked PE in the presence of DBTDL catalyst and the silane monomer used was VTMS. The initiators used were DCP, DHBP, di (2-tert-butylperoxypropyl-(2))-benzene (DIPP). The results showed that after water crosslinking for 4 hrs at 85 °C, the tensile strength increased from 5.5 to 6.7%, compared to the silane-grafted HDPE. From the DSC results, multiple melting behaviours were observed for crosslinked LDPE and LLDPE, which is the result of the phase separation of the two different crystals, the PE crystalline and the newly formed Si-O-Si crystalline. The heat deflection temperature (HDT) of crosslinked HDPE was increased with increasing crosslinking time. After being crosslinked for 6 hrs, the HDT can be increased from 78.1 to 101.2 °C (greater than that of LDPE and LLDPE).

In the study of Shieh et al. [13], silane grafting reactions of LDPE were performed in an extruder, followed by crosslinking with boiled water. DBTDL at the concentration of 0.05%, VTMS at the concentration of 2% and various amounts (0.05, 0.1, and 0.15%) of DCP were used. The thermal properties of both silane-grafted and silane-water crosslinked LDPE were investigated using DSC and TGA. DSC data showed that the silane grafts onto the LDPE molecules were thermally stable in the absence of moisture under 130 °C under which the silane grafted LDPE could be processed or recycled. The silane grafts on the LDPE molecules reduced the T_m of LDPE and gave rise to an endotherm shoulder at about 85 °C. TGA data showed that the decomposition temperature of the silane-grafted LDPE was much higher than that LDPE due to the peroxide-induced crosslink reactions during the silane grafting reactions performed in an extruder. Silane-crosslinked LDPE displayed multiple melting behaviours resulting from phase separation during crosslinking of LDPE with water. The phase separation gave rise to two melting points, including one about 94 °C and the other about 107 °C. Shieh et al. [36] also reported an increase in the degradation temperatures after silane grafting reactions and crosslink reactions. The degradation temperature of the crosslinked LDPE was higher than that of either the

Copyright by Mahidol University

grafted LDPE or the ungrafted LDPE, suggesting that the crosslink reactions of LDPE can raise its upper temperature limit of application.

Beltran et al. [37] studied silane grafting and moisture crosslinking of PP in the presence of DBTDL catalyst. DCP at concentrations of 0.2 and 0.4 wt%, and various amounts (2, 4, 6, 8 and 12%) of VTMS and epoxytrimethoxysilane (ETMS) were used. The results showed that the modulus at tensile testing temperatures increased by 39% at 90 °C and 33% at 130 °C, while the tensile strength raised by ~22 % at both temperatures. The silane-grafted and water-crosslinked samples showed a more stable thermal behaviour than both the silane-grafted samples and the unmodified PP. A combined effect of filler and silane crosslink network on improving high temperature performance of PP composites was reported by Sirisinha and Kawko [14]. They found an increase in the heat distortion temperature of PP from 138 °C to 198 °C in the crosslinked composite. An improvement in thermal stability of a silane-crosslinked PP was believed to be due partly to the relatively higher strength of the siloxane linkages.

In the study of Sirisinha and Meksawat [16] on silane-crosslinked EO systems, it was found that tensile strength and elongation at break decreased, whereas modulus at intermediate and high strains increased with an increase of crosslinking time, due to the presence of denser network. Sirisinha and Meksawat [33] also reported that the silane-crosslinked polymers could retain the elastomeric characteristics of the pure polymer and showed remarkably higher extensibility, better thermal stability, and energy storage capacity, compared to the peroxide-crosslinked samples. The silane crosslinking technique is, therefore, more suitable for producing the crosslinked polymers for some applications that need a flexible and thermally stable material.

Shah et al. [38] studied the crosslinking of PE with vinyl silane. Improvements in properties such as the tensile behaviour and elongation at break and improved thermal dimensional stability could effectively be tailored by an established and important technique known as crosslinking.

Copyright by Mahidol University

CHAPTER 4
MATERIALS AND METHODS

4.1 Materials

High-density polyethylene (HDPE) as a main material was supplied from Bangkok Polyethylene Co. Ltd., Bangkok, Thailand.

Ethylene copolymers used include ethylene-octene copolymers (EO) with octene content of 7.6% mol (EO76), and that with octene content of 10.9% mol (EO109), ethylene-butene copolymer (EB) with butene content of 16.1% mol and ethylene-vinyl acetate copolymer (EVA) with vinyl acetate content of 18.0% wt.

The details of the materials used in this study are shown in Table 4.1.

Table 4.1 Characteristics of polymers used in this study

Properties	**Materials**				
	HDPE	**EO76**	**EO109**	**EB**	**EVA**
Commercial grade	5000S	E8003[1]	E8150[1]	ENR7256[1]	Polene N8038[2]
Density ($g.cm^{-3}$)	0.954	0.885	0.868	0.885	0.941
Melt flow index at 190 °C ($g.10\ min^{-1}$)	0.8	1.0	0.5	2.0	2.3

[1] DuPont Dow Elastomer Co. Ltd., Wilmington, USA

[2] Thai Petrochemical Industry Public Co. Ltd., Bangkok, Thailand

Copyright by Mahidol University

Since one of the objectives of introducing a copolymer to HDPE is to increase the silane absorption, the experiment on the efficiency of silane absorption among various copolymers has been done. The silane absorption was determined by introducing 3 ml of silane into 3 g of polymer pellets. After 24 hrs, the excess silane was removed and the samples were then weighed. The percentage of silane absorption was calculated and the results are shown in Table 4.2. From Table 4.2, it can be seen that all of the ethylene copolymers used in this study can absorb a higher amount of silane than HDPE does. This may be due to the lower crystallinity in the case of EO76, EO109 and EB, and the higher polarity (or lower contact angle) in the case of EVA compared to HDPE.

Table 4.2 Silane absorption, crystallinity and contact angle of HDPE and various ethylene copolymers

Samples	**Silane absorption (%w/w)**	**Crystallinity (%)**	**Contact angle (°)**
HDPE	2.58 ± 0.05	61	87 ± 1
EO76	7.24 ± 0.40	7	87 ± 1
EO109	15.60 ± 0.83	5	88 ± 1
EB	9.32 ± 0.62	7	87 ± 0
EVA	19.64 ± 0.43	10	78 ± 1

Copyright by Mahidol University

4.2 Chemicals

The chemicals used in this study are listed in Table 4.3.

Table 4.3 Chemicals used in this study

Chemicals	Grade	Manufacturer
Dicumyl Peroxide (DCP)	GR	Fluka
Vinyl trimethoxysilane (VTMS)	GR	Fluka
Xylene	GR	BDH
Acetone	Commercial	Fluka

4.3 Instruments

The instruments used in this study are listed in Table 4.4.

Table 4.4 The instruments and models

Instruments	Models
Haake rheomix	Rheocord 90
Two-roll mill	Collin W100T
Compression moulding machine	Carver 3831.4 DIOAOO
Contact angle goniometer	Kruss, G-1
Fourier Transform Infrared Spectrometer	Perkin Elmer system 2000
Parallel plate rheometer	Physica MCR 500
Differential scanning calorimeter	Perkin Elmer DSC 7
Thermal gravimetric analyser	Mettler Toledo, SDTA851^{e}
Tensile tester	Instron universal tester Model 5566
Heat deflection temperature tester	Ceast 6510

Copyright by Mahidol University

4.4 Preparation of silane-water crosslinked HDPE blends

4.4.1 Grafting process

The grafting reaction was carried out in a Haake Rheocord 90 batch mixer equipped with cam blades. The HDPE and its blends with various copolymers in the ratio of 80/20 (wt/wt) were premixed with 5 wt% VTMS and 0.1 wt% DCP in a container. The mixture was kept immediately under nitrogen gas in a sealed container, and then tumbled-mixed for approximately 5 min and allowed to stand overnight. The reaction was carried out for 7 min at 170 °C in the mixer run at 60 rpm. This condition was selected from the results of the previous study [22]. It was proved to give a maximum grafting content with no gel which might be induced by peroxide crosslink reaction. The silane grafted-products were then two-roll milled to form a sheet of approximately 1 mm thick before cooling down to ambient temperature. The total time for the sheet making is approximately 9 min. The sheet samples were then kept in a desiccator to prevent crosslinking of the silane-grafted polymer before testing.

4.4.2 Crosslinking process

The grafted products from a two-roll mill were cut into small pieces and transferred to a preheated compression mould and then hot pressed at 190 °C under a pressure of 15 MPa for 1 min into sheets of 1 mm thick. The sheets were immersed in hot water at 70 °C for various times, allowing for the hydrolysation of alkoxy groups and condensation of silanol groups, thus silane-crosslinked products were obtained.

Copyright by Mahidol University

4.5 Characterisations

4.5.1 Silane absorption determination

The absorption of silane in different types of base polymers used in this study (i.e. HDPE, EO, EB and EVA) was determined. The polymer pellets of about 3 g were added to a beaker containing 3 ml of silane. The beaker was then sealed and kept for 24 hrs to allow a gradual absorption of silane into the polymer. The excess silane was removed before weighting the sample. The percentage of silane absorption (%w/w) was reported, averaging from at least three specimens.

4.5.2 Contact angle measurement

The contact angle measurement was used to determine the surface properties of solids using the sessile drop method. The film surfaces of test materials were inserted into a Kruss, G-1 contact angle goniometer. The syringe on top applies a single drop of distilled water onto the test specimen. The angle between the baseline of the drop and the tangent at the drop boundary was measured.

4.5.3 FTIR analysis

Samples for FTIR measurements were prepared by making films in a hot press at 190 °C. Before the FTIR measurement, the films were washed in an excessive amount of acetone to remove any unreacted silane. The films of ~100 μm thick were then analysed for the grafting of silane after the reaction. The IR spectra were recorded on a Transmission Fourier Transform Infrared Spectrometer (TS-FTIR) at a resolution of 4 cm^{-1} for 16 scans from 4000-600 cm^{-1}. The intensities of the IR peaks at 798, 1092 and 1192 cm^{-1} corresponded to the absorption of methoxysilane groups ($Si\text{-}OCH_3$) were followed. The degree of grafting was reported in terms of grafting index, calculated from the relative intensity of absorption peak of methoxysilane groups at 1092 cm^{-1} to that of the reference peak of methyl groups at 1377 cm^{-1}. FTIR was also used to

Copyright by Mahidol University

investigate changes in chemical structure of crosslinked samples in the progress of crosslink reaction.

4.5.4 Solvent extraction

In this study, gel content, swollen factor and solvent uptake factor were determined using solvent extraction method according to ASTM D2765-95a. The sample of about 0.3 g was wrapped in a stainless steel cage of 120-mesh and extracted with boiling xylene containing 1% antioxidant (Irganox 1010) for 6 hrs. After extraction the samples were recovered from the hot solvent and transferred into a sealable pre-weighed sample vial to determine the weight of the swollen gel and solvent uptake factor in solvent equilibrium. Final drying was carried out in a vacuum oven at 55 °C for 6 hrs until constant weight and the weight of the insoluble gel fraction was obtained. The gel content, swollen factor and solvent uptake factor were calculated using the following equations. At least three extractions were performed for each sample.

$$\text{Gel content (\%)} = \frac{\text{final weight of dried gel}}{\text{initial weight of sample}} \times 100 \quad (4.1)$$

$$\text{Solvent uptake factor} = \frac{\text{weight of swollen gel}}{\text{weight of dried gel}} \quad (4.2)$$

$$\text{Swollen factor} = \frac{\text{weight of swollen gel}}{\text{initial weight of sample}} \quad (4.3)$$

Copyright by Mahidol University

4.5.5 Dynamic rheological testing

Rheological measurements were carried out using a parallel plate rheometer (Physica MCR 500). The samples were cut into circle from a compression-moulded sheet of 1 mm thick. Parallel plates with a diameter of 25 mm were used in an oscillatory shear mode. The strain sweep test was first performed before dynamic testing to ensure that the frequency sweeps were within a linear viscoelastic region. The frequency was fixed at 1 and 200 rad.s^{-1} and the strain of deformation was varied from 0.1 to 100%. The testing temperature was 200 °C. The dynamic frequency sweep mode was then carried out. The limiting strain obtained from the strain sweep test was fixed at a constant value of 10% and the frequency range was varied from 1 to 200 rad.s^{-1}. The resultant storage (G′), loss (G″) and complex (G*) modulus values were recorded. The G* values determined could be related to the crosslink density (ν), following the theory of elasticity [74] as shown in equation 4.4:

$$G^* = \nu RT \quad (4.4)$$

where R = gas law constant (8.3144 J.$mol^{-1}K^{-1}$)

T = temperature (473 K)

Copyright by Mahidol University

4.5.6 Differential scanning calorimetry

The thermal behaviours of samples were studied by a Perkin-Elmer DSC-7. The samples used were cut from a 1 mm thick sheet. The specimens of about 8±1 mg were heated under nitrogen atmosphere from 50 to 170 °C at a scan rate of 20 °C.min^{-1}. The temperature was then maintained at 170 °C for 5 min before cooling to 50 °C at the same rate. The melting and crystallisation temperature and percentage of crystallinity of samples were examined. The crystallinity (χ_c) was calculated by taking the values of heat of fusion (ΔH_f), which is the area of the melting peak, using the equation 4.5.

Percentage crystallinity, $$\%\chi_c = \frac{\Delta H_f}{\Delta H_{f100}} \times 100 \qquad (4.5)$$

where ΔH_f = the enthalpy of fusion of the samples (J.g^{-1})

ΔH_{f100} = the enthalpy of fusion of a perfectly crystalline polyethylene (100% crystallinity polyethylene) which is equal to 290 J.g^{-1} [75]

Copyright by Mahidol University

4.5.7 Thermal gravimetric analysis

The thermogravimetric experiments were performed using a Perkin-Elmer TGA-7 thermal analyser. The samples were heated in the temperature range from 40 to 600 °C using a heating rate of 20 °C.min^{-1}, with a controlled oxygen flow of 60 ml.min^{-1}. Weights of the samples tested were about 8±1 mg. The onset decomposition temperature (T_{onset}) at 10% weight loss and temperature of rapid weight loss (T_d) is evaluated to indicate the thermal stability of material since there is a starting of degradation effect at this temperature and the majority of decomposition of the samples, respectively.

The thermal degradation kinetics of the samples was also studied, using a nitrogen gas purge rate of 60 ml.min^{-1}. The heating rates were varied at 20, 40, 60, 80 and 100 °C.min^{-1}. The decomposition temperatures were determined from the differential thermogravimetry (DTG) curves at various heating rates. The thermally decomposing activation energy (E_d) was determined from the plot of $-\ln(\beta/T_d^2)$ against $1/T_d$ according to the Kissinger equation [76] (Equation 4.6). The slope of the plot is E_d/R. From this value, the thermal decomposing activation energies were estimated.

$$-\ln\left(\frac{\beta}{T_d^2}\right) = \frac{E_d}{RT_d} - \ln\left(\frac{AR}{E_d}\right) \qquad (4.6)$$

where β = heating rates (^{o}C.min^{-1})

T_d = maximum decomposing temperature (K)

E_d = thermal decomposing activation energy (kJ.mol^{-1})

A = pre-exponential factor

R = gas constant (8.314×10^{-3} kJ.mol^{-1})

Copyright by Mahidol University

4.5.8 Mechanical testing

An Instron 5566 tensile tester with a 1 kN load cell was used with a testing speed of 50 mm.min^{-1} according to ASTM D638-03. At least five specimens were stamped cut from a 1 mm thick compression-mold sheet into dumbbell shape with the dimension as shown in Figure 4.1.

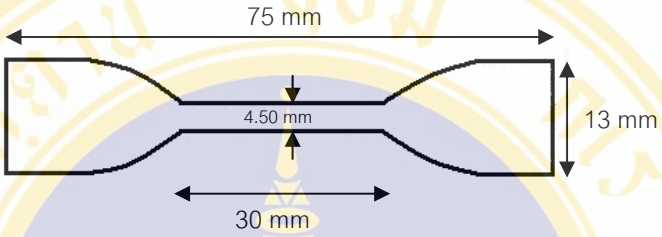

Figure 4.1 Dimension of the tensile specimen used in this study

Tensile properties were determined as follow.

$$\text{Tensile stress,} \qquad \sigma = \frac{F}{A} \tag{4.7}$$

where σ = the tensile stress (MPa)

F = the force (N)

A = the initial cross-section area of the test specimen (mm^2)

$$\text{Percentage of elongation,} \qquad \%\varepsilon = \frac{(L - L_0)}{L_0} \times 100 \tag{4.8}$$

where ε = the tensile strain or elongation

L = the distance between the gauge marks at break (mm)

L_o = the original gauge length (mm)

In this study, the Young's modulus was determined from the initial slope of stress-strain curve.

$$\text{Young's Modulus,} \qquad M = \sigma / \varepsilon \tag{4.9}$$

Copyright by Mahidol University

4.5.9 Heat deflection temperature testing

The heat deflection temperature test was carried out using Ceast 6510 HDT tester. The dimensions of test bars and the test procedure were followed the ASTM D648. The rectangular bars of 3 mm thick were cut from a compression-moulded sheet. A bar of rectangular cross section was tested in the edgewise position as a simple beam with a load applied at its center to give maximum fiber stress of 0.455 MPa. The specimen was immersed under load in a heat-transfer medium (silicone oil), using a heating rate of 2 °C.min^{-1}. The temperature of the medium was measured when the test bar was deflected 0.25 mm. This temperature was recorded as the deflection temperature under flexural load of the test specimen.

Copyright by Mahidol University

CHAPTER 5
RESULTS AND DISCUSSION

This chapter demonstrates the results of the analyses of silane grafting and water-crosslinking of HDPE and its blends with various types of ethylene copolymers. FTIR technique, solvent extraction and rheological measurement were used for the characterisation of structure of the prepared blends. The effects of different copolymers on the crosslinking process and properties of crosslinked products are discussed.

5.1 Silane-grafted HDPE blends

FTIR analysis was used here to analyse the silane-grafted polymers. Effects of various ethylene copolymers on the degree of grafting were compared. Figures 5.1-5.5 show FTIR spectra of HDPE, HDPE/EO76, HDPE/EO109, HDPE/EB and HDPE/EVA, respectively, both before and after grafting reaction with 5% VTMS and 0.1% DCP. The peak positions and their respective assignments are given in Table 5.1. As can be seen in Figures 5.1-5.5, all five unmodified polymers display the IR characteristic peaks at 722, 1377 and 1465 cm^{-1} which assign to the CH_2 rocking, and CH bending vibrations of methyl and methylene groups, respectively [18, 36]. In the case of HDPE/EVA blend (Figure 5.5), the IR spectra shows an absorption peak at 1740 cm^{-1} which is due to carbonyl stretching (>C=O); at 1250 cm^{-1} due to C-O stretching; at 1023 cm^{-1} due to =C-O-C stretching of the ester groups; and at 956 cm^{-1} due to CH deformation of the acetate group [77].

After the silane grafting reaction, the additional peaks at 798, 1092 and 1192 cm^{-1} appear in all of the curves of silane grafted polymers which correspond to the absorption of methoxysilane ($Si-OCH_3$) groups [18, 36, 39]. Compared to other blend systems, the silane-grafted HDPE/EVA shows relatively smaller peak at 1192 cm^{-1}. This was reported earlier to be attributed to the overlapping of absorption of

Copyright by Mahidol University

methoxysilane groups with that of C-O stretching of the ester at 1250 cm^{-1} of EVA [78].

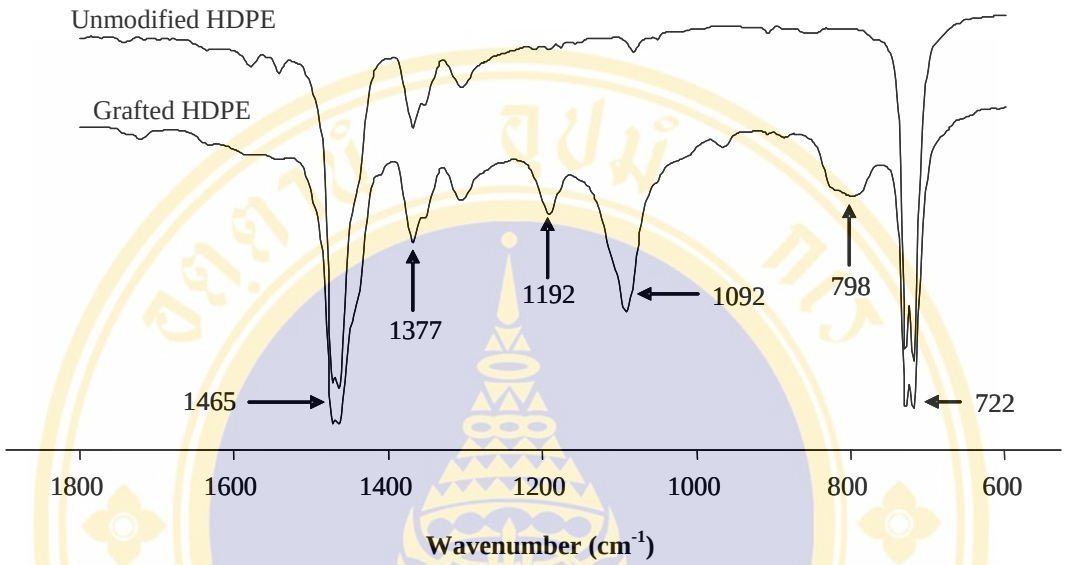

Figure 5.1 FTIR spectra of unmodified and grafted HDPE

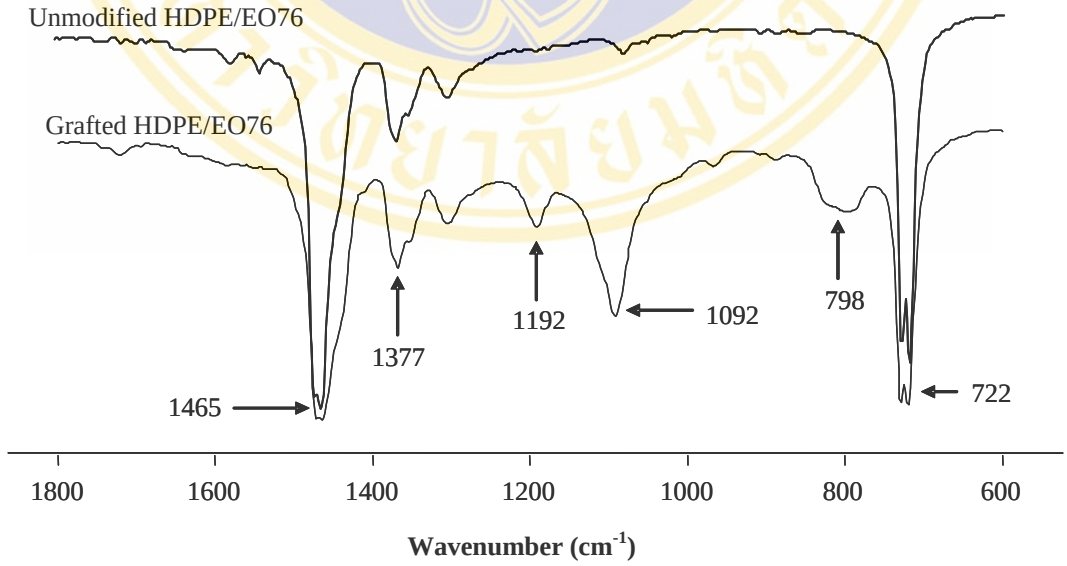

Figure 5.2 FTIR spectra of unmodified and grafted HDPE/EO76 blend

Copyright by Mahidol University

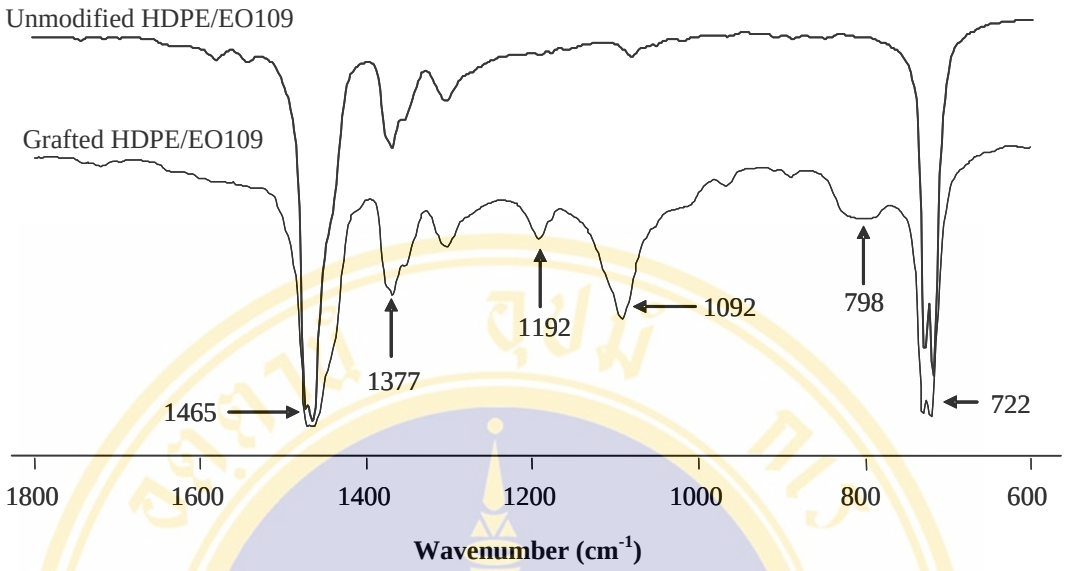

Figure 5.3 FTIR spectra of unmodified and grafted HDPE/EO109 blend

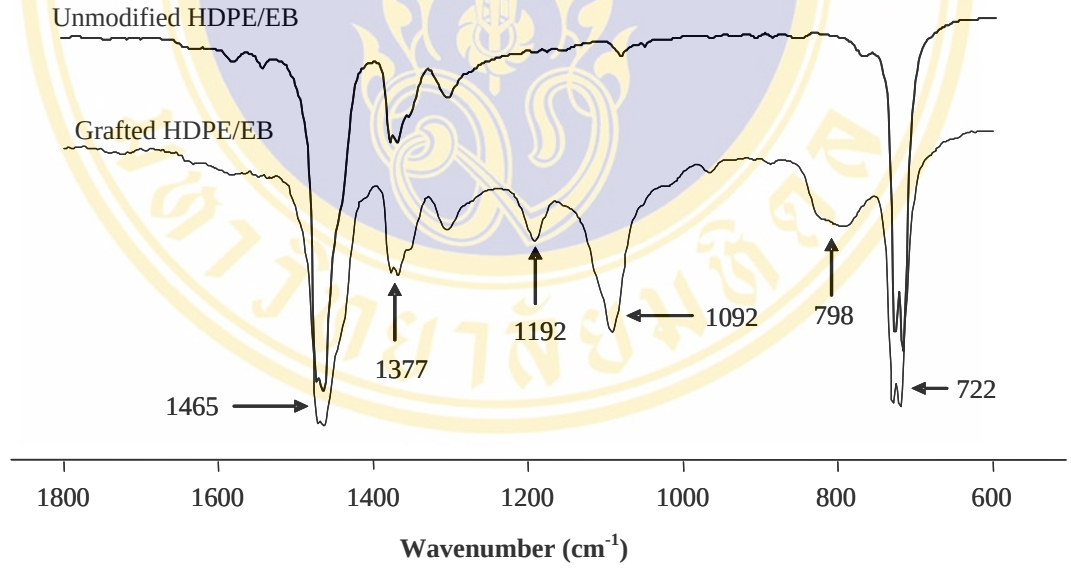

Figure 5.4 FTIR spectra of unmodified and grafted HDPE/EB blend

Copyright by Mahidol University

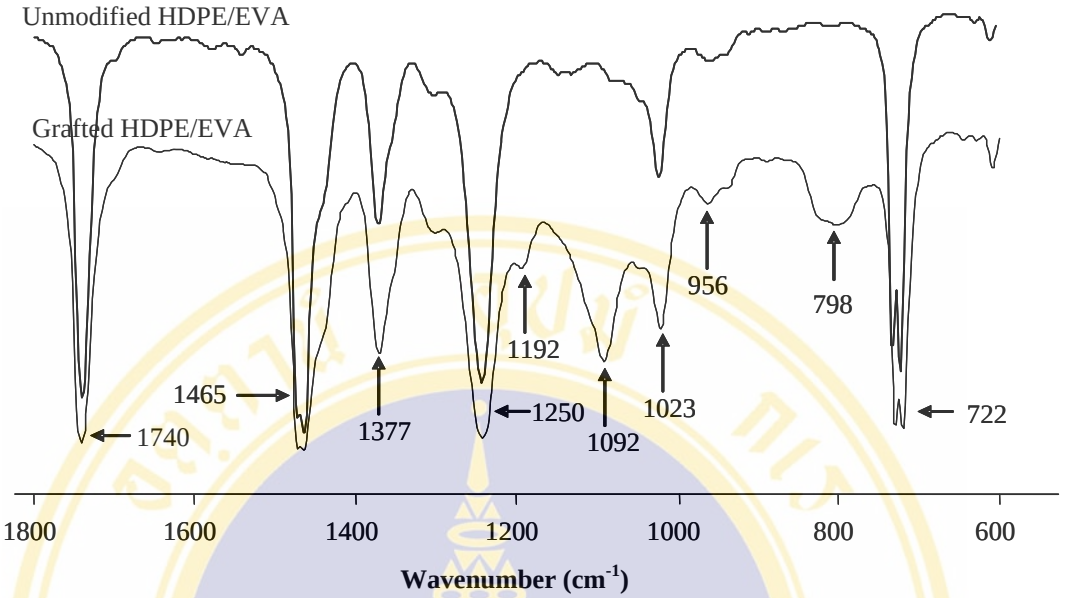

Figure 5.5 FTIR spectra of unmodified and grafted HDPE/EVA blend

Table 5.1 IR peak positions and their assignments [39]

Peak (cm^{-1})	Functional Group
1740	>C=O stretching (ester carbonyl groups)
1465	CH bending vibration (methylene groups)
1377	CH bending vibration (methyl groups)
1250	C-O stretching (ester and acid groups)
1192	Si-O-C (methoxysilane groups)
1092	Si-O-C (methoxysilane groups)
1023	=C-O-C stretching (ester and acid groups)
956	CH deformation (acetate groups)
798	Si-O-C (methoxysilane groups)
722	CH_2 rocking vibration (branch point of PE mainly)

Copyright by Mahidol University

The effect of these ethylene copolymers on the degree of grafting is summarised in Table 5.2. The degree of grafting in terms of grafting index was calculated from the relative intensity of absorption peak at 1092 cm^{-1} to that of the reference peak at 1377 cm^{-1}. The information on crystallinity, polarity and silane absorption of the individual polymers is provided in Table 5.3. Among the four copolymers used, only EVA is a polar polymer which should have high affinity to silane. Table 5.3 reveals the highest percentage of silane absorption in EVA. The silane absorption ability is found to depend strongly on polymer polarity and to a lesser extent on crystallinity. In the case of EB, EO76 and EO109 which are non-polar, EB has the shortest chain branching among the three. EO109 due to its higher amount of comonomer content shows slightly lower crystallinity than EO76.

Table 5.2 Effect of ethylene copolymers on the grafting index at 1092 cm^{-1} of HDPE blends

Samples	Grafting index
HDPE	1.94 ± 0.04
HDPE/EO76	1.58 ± 0.05
HDPE/EO109	1.14 ± 0.02
HDPE/EB	1.74 ± 0.06
HDPE/EVA	0.73 ± 0.04
EO76	1.55 ± 0.05
EO109	0.50 ± 0.02
EB	1.00 ± 0.03
EVA	0.24 ± 0.01

Copyright by Mahidol University

Table 5.3 Crystallinity, contact angle and silane absorption of HDPE and various ethylene copolymers

Samples	Crystallinity (%)	Contact angle (°)	Silane absorption (%w/w)
HDPE	61	87 ± 1	2.58 ± 0.05
EO76	7	87 ± 1	7.24 ± 0.40
EO109	5	88 ± 1	15.60 ± 0.83
EB	7	87 ± 0	9.32 ± 0.62
EVA	10	78 ± 1	19.64 ± 0.43

From Table 5.2, the results indicate the highest grafting degree in HDPE followed by the blends with EB, EO76, EO109 and EVA, respectively. This points out that the increase in amount of silane absorption in EVA does not help improving the efficiency of silane grafting in the blend. The presence of bulky acetate group in EVA might lead to some difficulties in silane reaction. It was reported earlier [79] that the acetate groups in the EVA copolymer were quite bulky in relation to the ethylene groups.

The effects of steric side chain comonomer can be seen also in the blends with EB and EO. Compared to EB and EO, HDPE had less steric effect due to its structure having a very low degree of chain branching. It had a report [70] that the number of chain branching per 1000 carbon atoms on the polymer main chain falls in the range of 2-7 for HDPE and in the range of 20-50 for LLDPE based on the densities of the materials. HDPE has also more allyl hydrogens among LLDPE, whereas LLDPE has more hydrogens attached to tertiary carbons than HDPE has. Homolytic bond dissociation energies for hydrogens attached to primary, secondary, tertiary, and allyl carbons are 410, 397, 385, and 368 $kJ.mol^{-1}$, respectively [71]. The least energy needed for a free radical to abstract hydrogen is from an allyl carbon among the four kinds of carbons. Therefore, the free radicals generated from dicumyl peroxide mostly should attack and abstract the hydrogens at allyl, tertiary and secondary carbons rather than primary carbons. This may be one of the reasons that the silane grafting reaction occurs in HDPE better than that in the ethylene copolymers. In the case of EB and EO,

Copyright by Mahidol University

EB has shorter chain branching or less steric effect than EO. As a result, a higher grafting index is observed in the blends with EB. Similar explanation also goes to the two EO systems. EO76 with an octene content of 7.6% shows higher grafting index than EO109 which has 10.9% octene.

Copyright by Mahidol University

5.2 Degree and rate of crosslinking of HDPE blends

In this work, the silane-grafted HDPE and its blends were immersed in hot water at 70 °C for a certain time to conduct crosslinking reactions. The degree and rate of crosslinking were measured. The gel content, solvent uptake factor and swollen factor were determined by solvent extraction analysis. FTIR analysis and rheological measurement were also used for determining the crosslinking index and crosslink density of various crosslinked samples.

5.2.1 Solvent extraction results

Solvent extraction is generally used in evaluating the crosslinking degree of polymers by determining their gel content, swollen factor and solvent uptake factor after crosslinking reactions. The solvent extraction experiments were performed by extracting the non-crosslinked component from the sample using xylene. The content of crosslinked part or gel was calculated from the weight of dried gel of insoluble fractions after an extraction with xylene with respect to the initial weight of sample. The swollen factor is a relative measured value between the weight of swollen gel after xylene extraction and initial weight of sample. The solvent uptake factor enables the calculation of the ratio of the polymer weight fraction in the swollen gel and weight of dried gel after xylene extraction. Figure 5.6 shows the gel content values of the HDPE and its blends with various copolymers plotted against the immersing time.

Copyright by Mahidol University

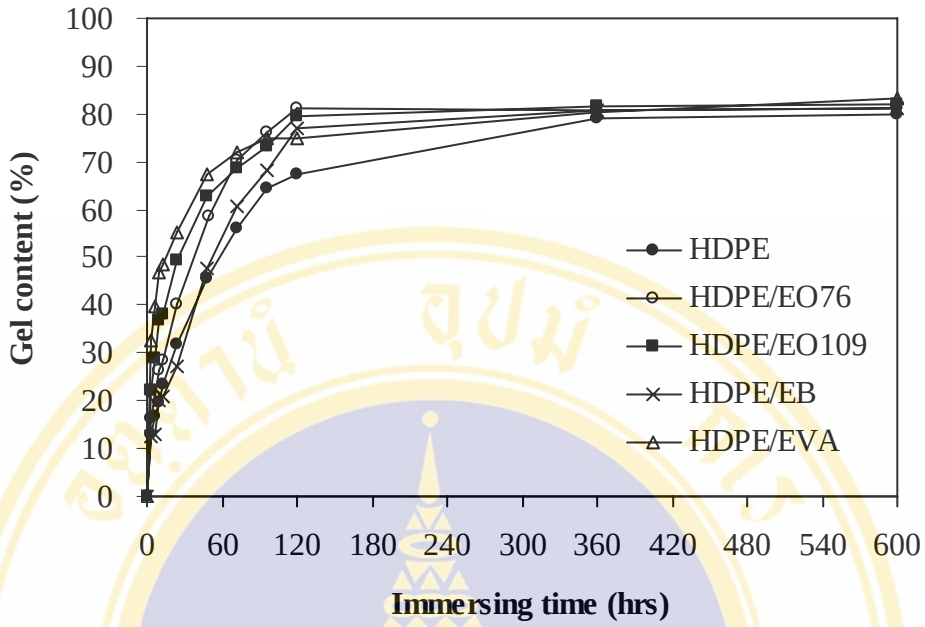

Figure 5.6 Effect of immersing time on the gel content of crosslinked HDPE and its blends

As shown in Figure 5.6, the amount of gel of all samples increases quite rapidly with the increase of crosslinking time in the initial stage ($t \leq 120$ hrs). When the crosslinking time is over 120 hrs, the gel content increases very slowly, and then levels off. It is obvious that the ethylene copolymers containing materials crosslink faster than the pure HDPE, and higher amounts of gel are formed in a shorter period of immersing time. For example, after 48 hrs of crosslinking time, the content of gel are 45.7%, 47.6%, 58.7%, 62.6%, and 67.2% in the case of HDPE, HDPE/EB, HDPE/EO76, HDPE/EO109 and HDPE/EVA, respectively. However, the magnitude of gel content in all blends shows no differences after 360 hrs of crosslinking time. At this stage, the content of gel in all blends reaches a maximum value of ~80%.

Copyright by Mahidol University

In addition to gel content, swollen factor and solvent uptake factor can also be determined from the extraction experiment. The swollen factor and solvent uptake factor results plotted as a function of immersing time are shown in Figures 5.7 and 5.8, respectively.

The results show generally an increase in the swollen factor and a reduction in the solvent uptake factor with increasing immersing time which agree very well with the gel results shown previously. However, the results of swollen factor determined in an initial stage of crosslinking process (t < 120 hrs) show more fluctuation than those obtained from solvent uptake experiment.

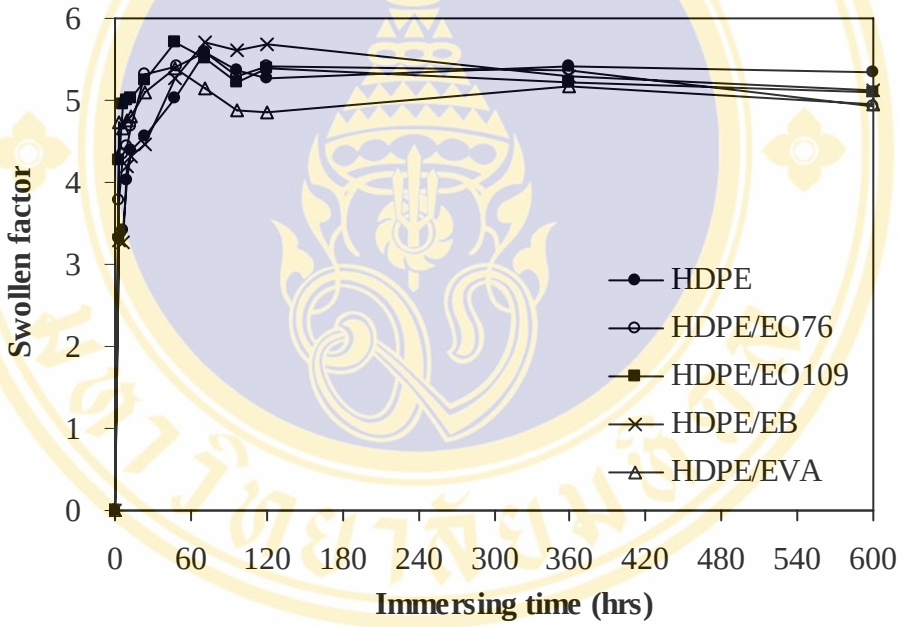

Figure 5.7 Effect of immersing time on the swollen factor of crosslinked HDPE and its blends

Copyright by Mahidol University

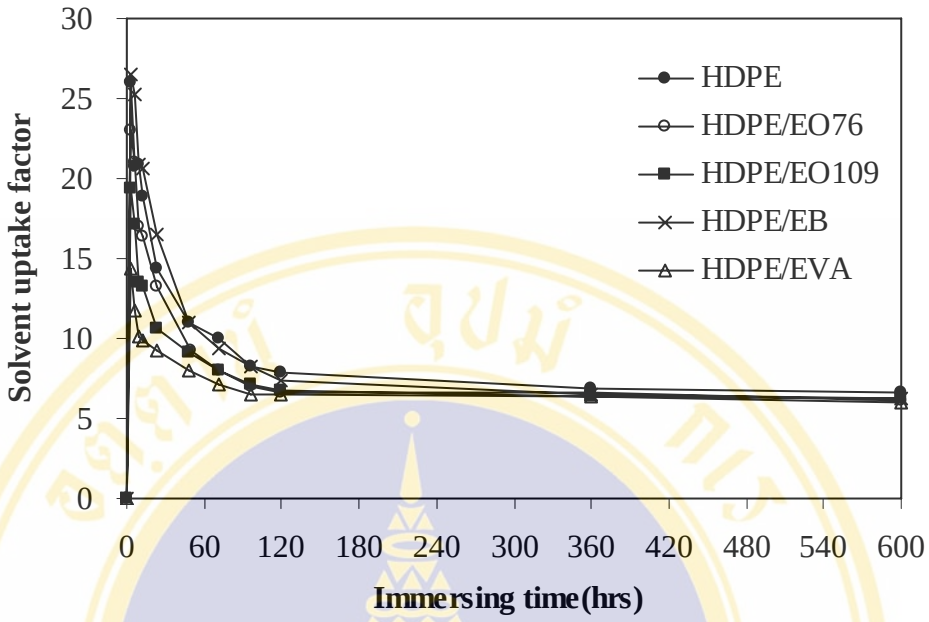

Figure 5.8 Effect of immersing time on the solvent uptake factor of crosslinked HDPE and its blends

Apart from the degree of crosslinking, rate of crosslinking was determined by analysing the slope of the graph in the initial stage (time ranged from 0-12 hrs) as shown in Figure 5.9. Table 5.4 summarises the calculated slope values of crosslinked HDPE and its blends with various copolymers. The incorporation of ethylene copolymers clearly increases the rate of crosslinking. The highest rate is found in the case of HDPE/EVA blends, followed by HDPE/EO109, HDPE/EO76, and HDPE/EB, respectively (Table 5.4). These results point out that the structure and properties of ethylene copolymers play a significant role in crosslinking of HDPE. EVA with its polar groups in the molecules has a strong ability for water diffusion. EO, although, is a hydrophobic material, increases diffusion of water in HDPE due to its low crystalline content.

Copyright by Mahidol University

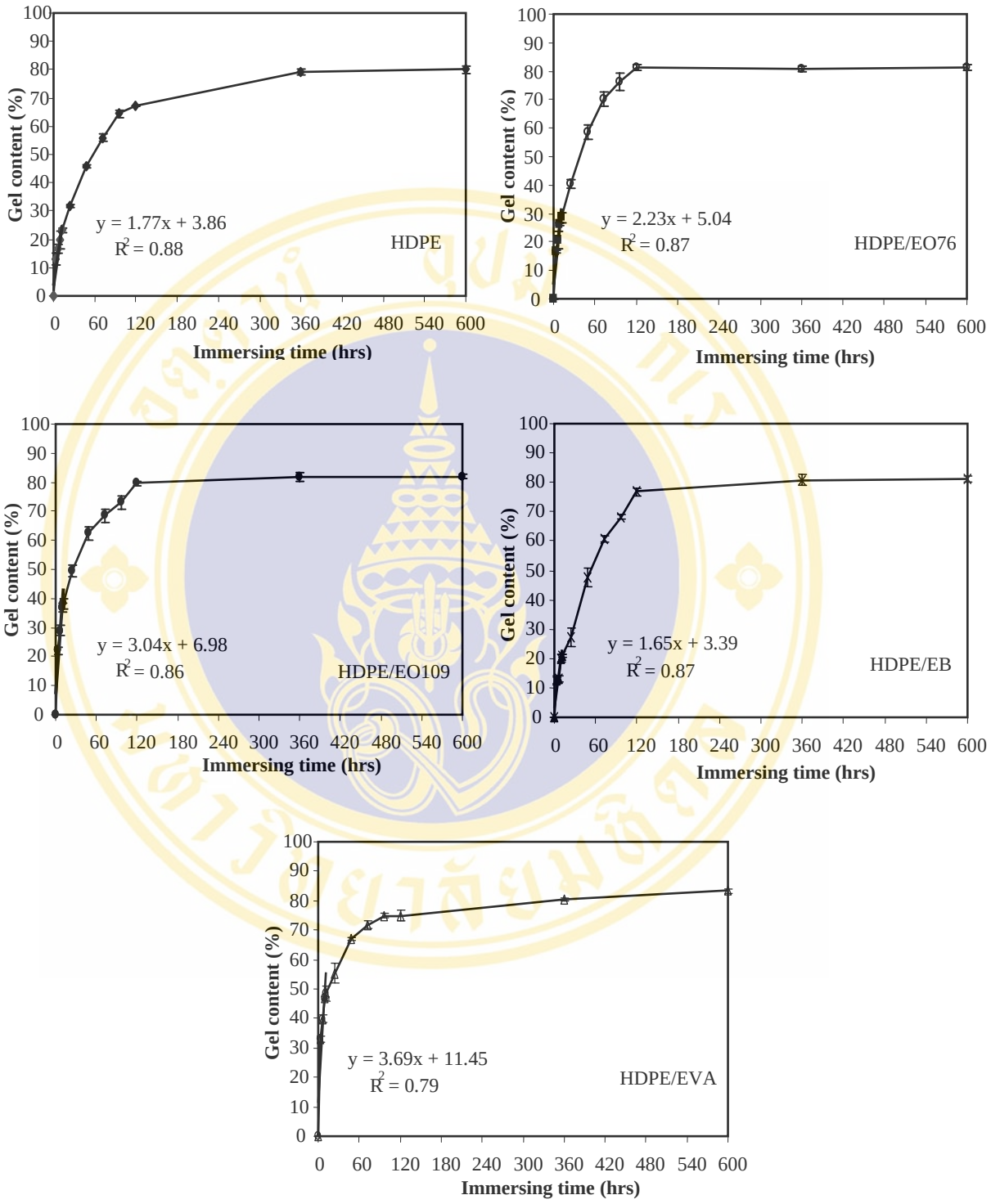

Figure 5.9 Effect of immersing time on the gel content of crosslinked samples

Copyright by Mahidol University

Table 5.4 Crosslinking rate and gel content at certain crosslinking time of crosslinked HDPE and its blends

Samples	Crosslinking rate (%. hr^{-1})	Gel content at 48 hrs (%)	Gel content at 600 hrs (%)
HDPE	1.77	45.69	80.03
HDPE/EO76	2.23	58.65	81.27
HDPE/EO109	3.04	62.55	82.00
HDPE/EB	1.65	47.63	81.22
HDPE/EVA	3.69	67.20	83.35

In a similar work, Sirisinha and Chimdist [18] reported an important role of the content of amorphous and crystalline portion in the EOR/LDPE blends on the rate of crosslinking reaction. Their results showed that the higher the amount of amorphous phase, the higher the rate of water diffusion, and as a consequence, the higher the crosslinking rate. Shieh et al. [17] studied the silane-water crosslinking reactions of LDPE. It was also found that the content of the crystalline in material affected the rate of crosslinking of the sample. The crosslinking rates were inversely proportional to the contents of crystalline component in the samples.

Copyright by Mahidol University

5.2.2 FTIR results

In this section, FTIR was used as an alternative method in evaluating the degree of crosslinking in various samples. FTIR technique is reported earlier to give useful information on the progress of silane-water crosslinking reaction of polymer [18, 20]. The method is non-destructive and less time-consuming. In this study, the crosslink index of various crosslinked samples was calculated from the relative intensity of the absorption peak of methoxysilane groups at 1092 cm^{-1} to that of the reference peak at 1377 cm^{-1}. Since the methoxysilane groups are hydrolysed and condensed to form siloxane linkages during the crosslinking reaction [17, 36], the degree of crosslinking can be followed from a decreasing in methoxysilane groups.

Prior to determining the crosslink index, the evidence of silane crosslinking was investigated. The peaks of ($Si\text{-}OCH_3$) groups of grafted samples are observed at 798, 1092, and 1192 cm^{-1}. The spectrums of the crosslinked HDPE, HDPE/EO76, HDPE/EO109, HDPE/EB and HDPE/EVA clearly show an additional broad band at 1030 cm^{-1}, which can be assigned to the absorption of Si-O-Si as shown in Figures 5.10-5.14.

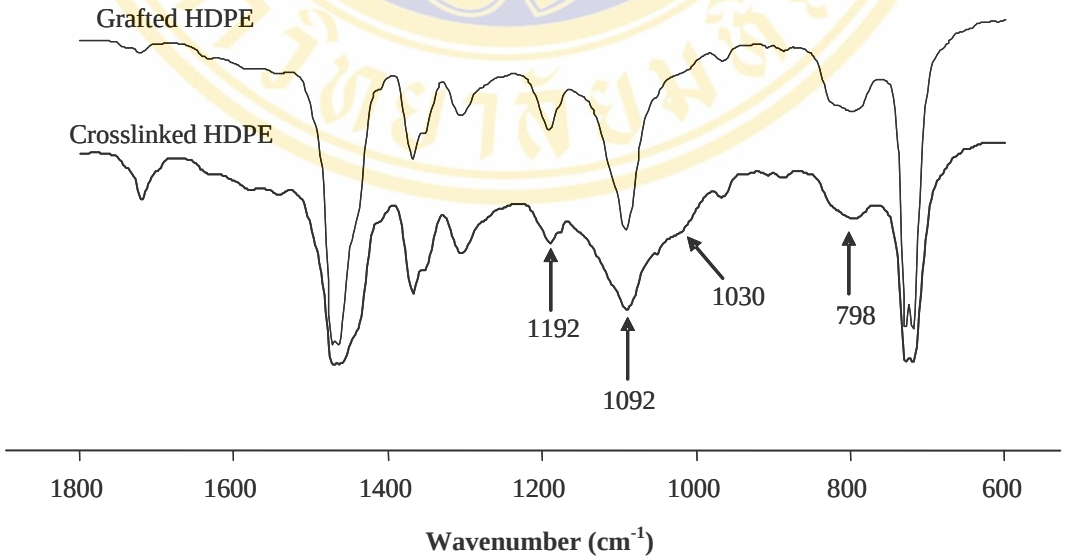

Figure 5.10 FTIR spectra of silane-grafted and crosslinked HDPE

Copyright by Mahidol University

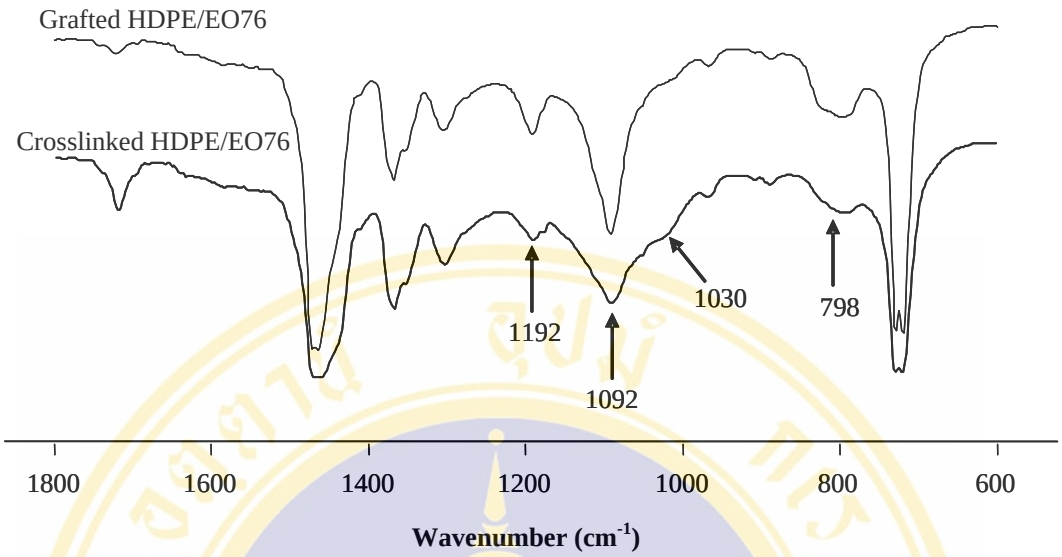

Figure 5.11 FTIR spectra of silane-grafted and crosslinked HDPE/EO76 blend

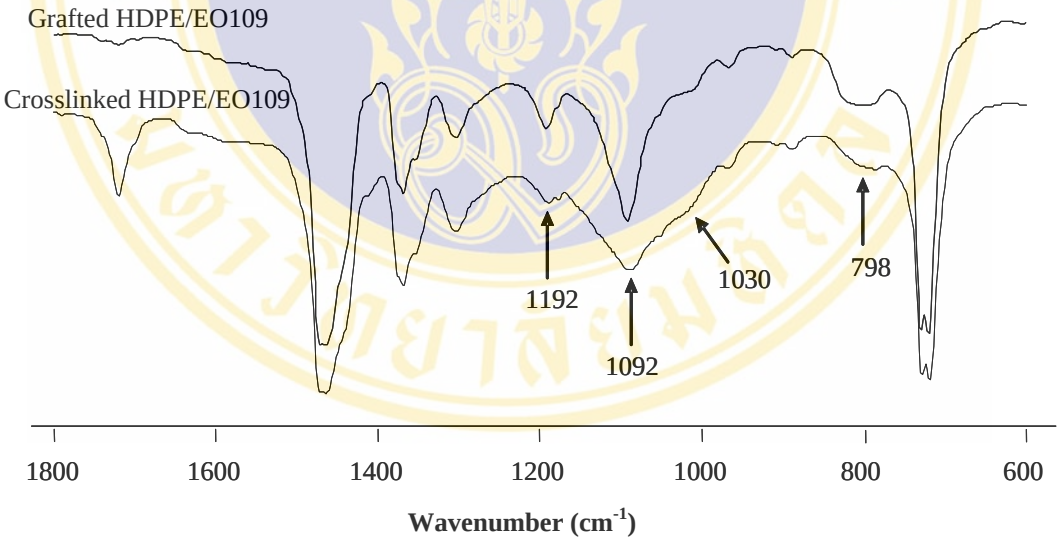

Figure 5.12 FTIR spectra of silane-grafted and crosslinked HDPE/EO109 blend

Copyright by Mahidol University

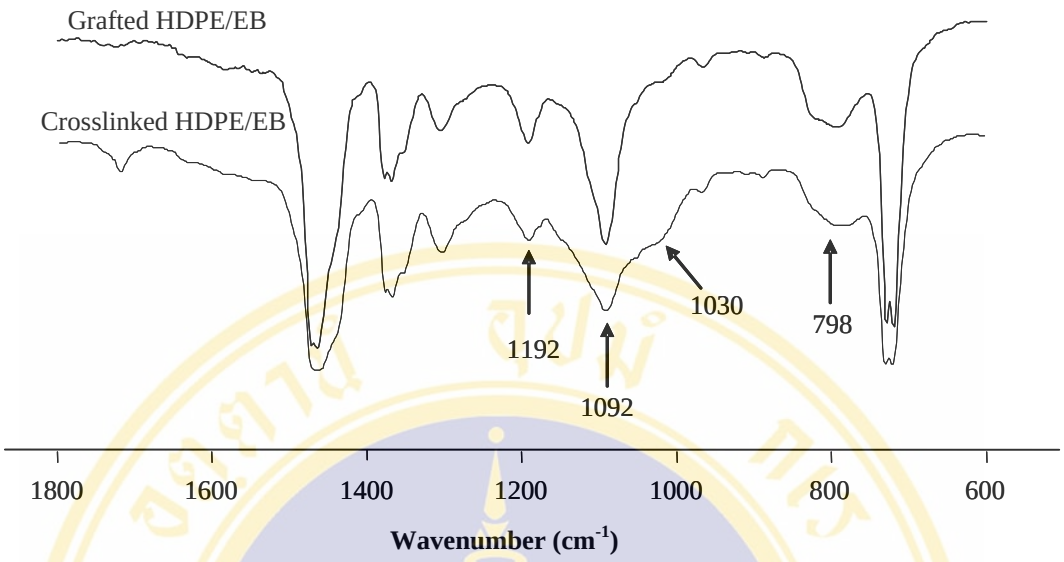

Figure 5.13 FTIR spectra of silane-grafted and crosslinked HDPE/EB blend

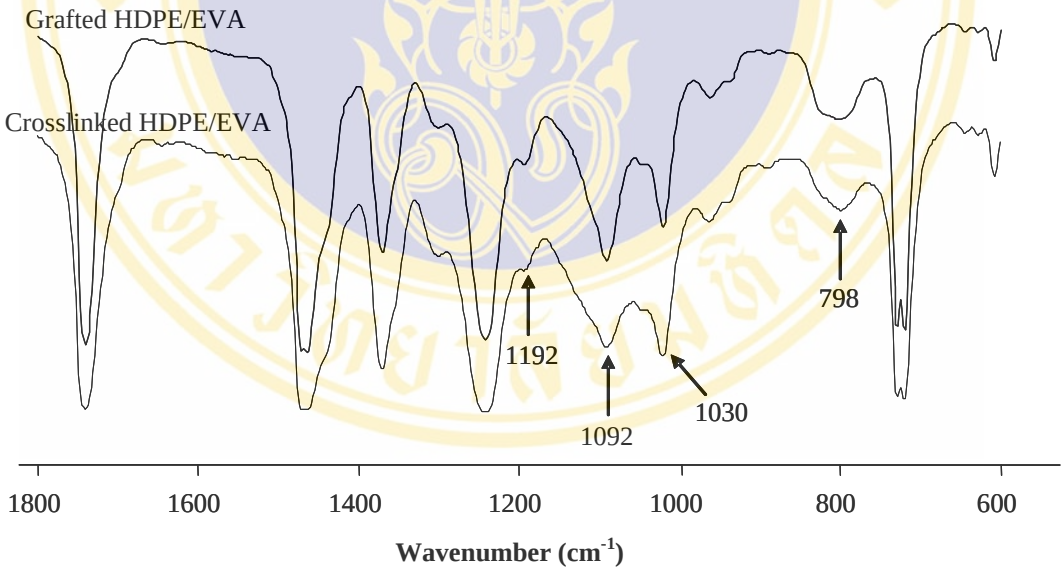

Figure 5.14 FTIR spectra of silane-grafted and crosslinked HDPE/EVA blend

Copyright by Mahidol University

In Figure 5.15, the absorption index at 1092 cm^{-1} is plotted against the immersing time. The absorption index of all crosslinked samples systematically decreases with increasing immersing time. This indicates an increase in Si-O-Si linkages or more crosslink formation. From the results of Figure 5.15, it can be seen that the absorption index at 1092 cm^{-1} of all crosslinked samples clearly decreases in the initial stage of immersing time ($t \leq 120$ hrs), revealing a systematic decrease in the amount of methoxysilane groups in the crosslinked products. Beyond 120 hrs of crosslinking time, the absorption index shows only slight decrease. This finding agrees well with the gel content results.

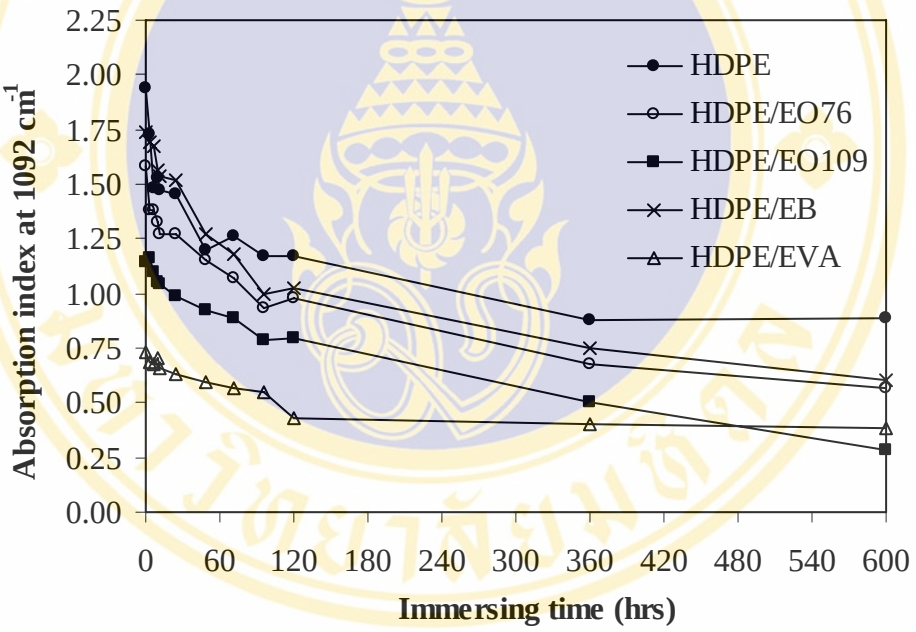

Figure 5.15 Effect of immersing time on the absorption index at 1092 cm^{-1} of crosslinked HDPE and its blends

Copyright by Mahidol University

However, the results of gel content experiment (Figure 5.6) demonstrate that the magnitude of gel obtained after a long crosslinking process ($t \geq 360$ hrs) is not different in all blends. The maximum gel content of 80% is obtained in all samples. From the FTIR results shown in Figure 5.15, the amount of crosslink in all blends seems to be unsimilar. After 360 hrs of immersing time, the highest absorption index at 1092 cm^{-1} is observed in the pure HDPE sample, followed by HDPE/EB, HDPE/EO76, HDPE/109 and HDPE/EVA, respectively. This points out that there must be some differences in the behaviours of crosslink in those materials even though they contain a similar gel content of 80%. To study further on those crosslinked materials, the parallel plate rheometer was used to monitor the density of crosslink in various samples. The rheological results are presented in the next section.

5.2.3 Rheology results

In this study, a parallel plate rheometer was used to monitor the evolution of the crosslinking process. Rheological property as complex modulus (G*) can be correlated to the evolving crosslink density (ν) of the system during crosslinking process. The crosslink density of the crosslinked polymer can be calculated using the theory of elasticity [74], which is expressed by the relation following equation.

$$G^* = \nu RT \tag{5.1}$$

The G* values of various crosslinked materials are illustrated in Figure 5.16. All samples exhibit an increase in the G* values with increasing crosslinking time. At crosslinking time of 0 hrs, HDPE/EO109 shows the highest G* values, followed by HDPE/EO76, HDPE/EB, HDPE and HDPE/EVA, respectively. These reveal the effect of molecular weight and molecular structure of the materials on complex modulus.

Copyright by Mahidol University

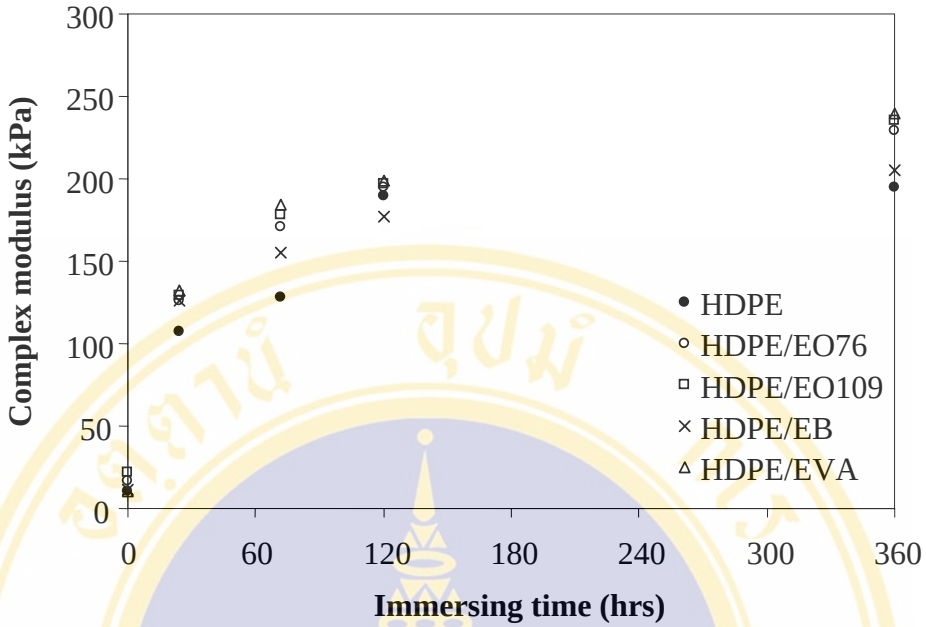

Figure 5.16 Complex modulus values as a function of immersing time of various crosslinked samples

Therefore, the difference in complex modulus values of samples before and after crosslinking for various times was used for the calculation of crosslink density in order to eliminate the effect of other factors (i.e. molecular weight) which might have an influence on the complex modulus values. The calculated crosslink density obtained using equation 5.1 is then plotted against the crosslinking time. The results are shown in Figure 5.17 and the data are summarised in Table A6 of Appendix A.

From Figure 5.17, the crosslink density values of all crosslinked samples increase rapidly with increasing crosslinking time in the initial stage and then gradually increase when crosslinking time is over 120 hrs. It had been reported by Dadbin et al. [74], that the crosslink density of crosslinked LDPE samples increased with an increase in irradiation dose. This indicated that a tighter network structure had occurred in a higher crosslink density. In this work, an increment in crosslink density of crosslinked materials by the addition of ethylene copolymers into HDPE matrix is found. For the samples crosslinked for 72 hrs, the crosslink density values are 0.030, 0.036, 0.039, 0.039 and 0.044 $mol.L^{-1}$ in HDPE, HDPE/EB, HDPE/EO76, HDPE/EO109 and HDPE/EVA blends, respectively. Also, for a long crosslinking time, all crosslinked samples still have different crosslink density. This result agrees

Copyright by Mahidol University

well with the previous FTIR results shown in Figure 5.15, revealing that the samples which have similar gel content could have different crosslink behaviours, i.e. number of crosslinking point within the existing gel. In this study, the highest crosslink density is found in HDPE/EVA blend whereas the lowest is found in HDPE. The hydrophilicity and crystallinity in the blends play strong role in determining the crosslinking of material.

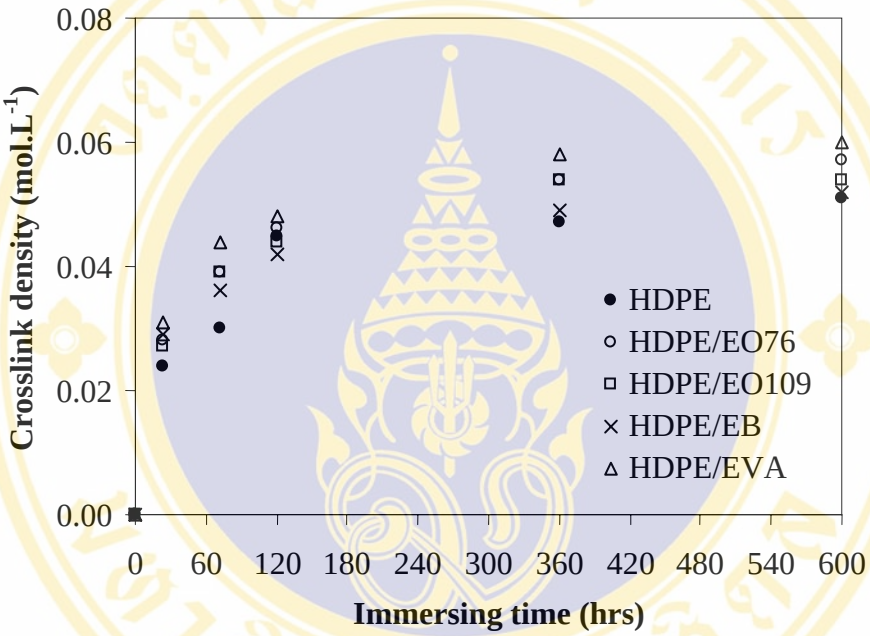

Figure 5.17 Crosslink density values as a function of immersing time of various crosslinked samples

Copyright by Mahidol University

5.3 Properties of grafted and crosslinked HDPE blends

5.3.1 Melting and crystallisation behaviours

In this part, DSC method under non-isothermal conditions was used to investigate the melting and crystallisation behaviours of HDPE blends together with their grafted and crosslinked samples. The data obtained from the DSC heating endotherm was used to determine the melting temperature (T_m), enthalpy of fusion (ΔH_f) and percentage of crystallinity (% χ_c), while the DSC cooling exotherm was used to determine the onset temperature of crystallisation ($T_{c\ onset}$), and crystallisation temperature (T_c).

The DSC melting of HDPE and its blends are shown in Figure 5.18. The DSC results of individual polymers and HDPE blends are summarised in Table 5.5. The endotherm of HDPE shows one melting peak at 133 °C. The melting endotherms slightly shift to lower temperatures when ethylene copolymers were added into HDPE system. Blends of HDPE/EO76, HDPE/EO109 and HDPE/EB show a single peak around 130 °C. While the blends of HDPE/EVA show a major peak of HDPE at 131 °C and a broad shoulder of EVA at the low temperature of 85 °C. The results also show that % χ_c values of HDPE/EO76, HDPE/EO109, HDPE/EB and HDPE/EVA blends are 49, 49, 50, and 49, respectively. To investigate the effect of copolymers on crystallinity of HDPE, the percentage of crystallinity per unit weight of the crystallisable component was calculated and reported as a percentage of normalised crystallinity. Since the weight ratio of HDPE/copolymers used in this study is 80/20 and the % χ_c of 100% HDPE is 61, the percentage of the normalised crystallinity of is 48.8. This result indicates that ethylene copolymers do not affect the crystallisation and crystallinity of HDPE. No cocrystallisation phenomenon is observed in the HDPE blends. This is perhaps due to the different rates of crystallisation between HDPE and ethylene copolymers [53].

Copyright by Mahidol University

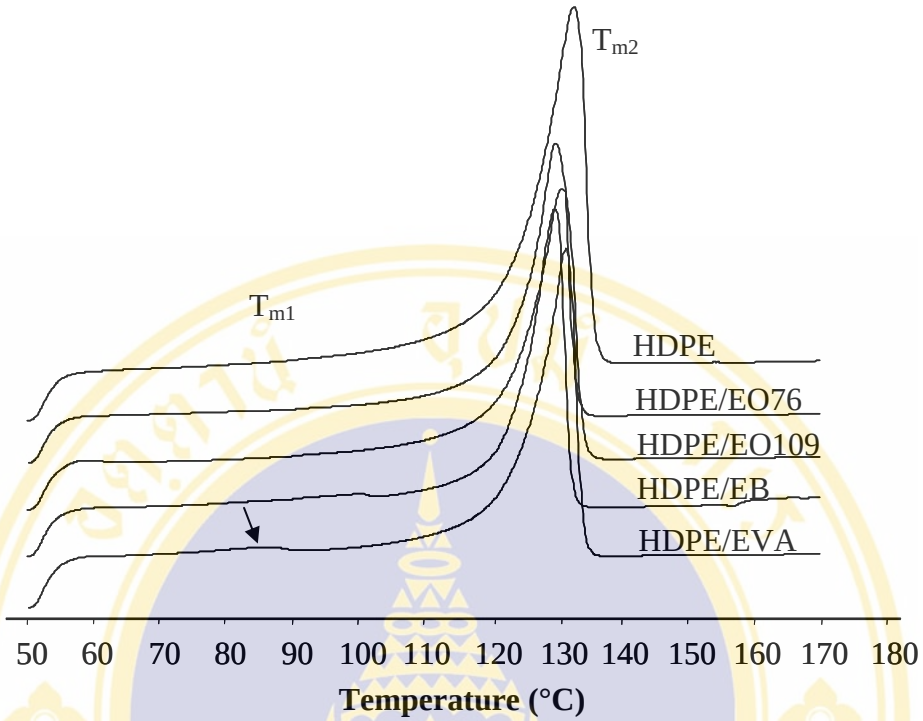

Figure 5.18 DSC heating thermograms of HDPE and its blends

Table 5.5 Melting temperature (T_m), enthalpy of fusion (ΔH_f), percentage of crystallinity (% χ_c), onset temperature of crystallisation ($T_{c\ onset}$), and crystallisation temperature (T_c) of HDPE, various copolymers and HDPE blends

Samples	T_{m1}, T_{m2} (°C)	ΔH_f ($J.g^{-1}$)	% χ_c	$T_{c\ onset}$ (°C)	T_{c1}, T_{c2} (°C)
HDPE	133	176	61	115	111
EO76	81	20	7	65	60
EO109	55	15	5	41	38
EB	82	21	7	61	56
EVA	87	30	10	70	65
HDPE/EO76	130	141	49	114	111
HDPE/EO109	131	142	49	115	112
HDPE/EB	130	146	50	115	112
HDPE/EVA	85, 131	141	49	115	65, 112

Copyright by Mahidol University

The crystallisation behaviours of HDPE and its blends are investigated from the cooling thermograms in Figure 5.19. The $T_{c\ onset}$ and T_c of HDPE and its blends with copolymers are also listed in Table 5.5. The DSC cooling thermogram of HDPE shows a single crystallisation peak at 111 °C. For blends of HDPE/EO76, HDPE/EO109 and HDPE/EB, one crystallisation peak is observed at 111, 112 and 112 °C, respectively. While HDPE/EVA blend displays two crystallisation peaks at 65 and 112 °C. Not only T_c but $T_{c\ onset}$ also does not change after the incorporation of copolymers into HDPE system. This confirms that the ethylene copolymers do not affect the crystallisation behaviours of HDPE.

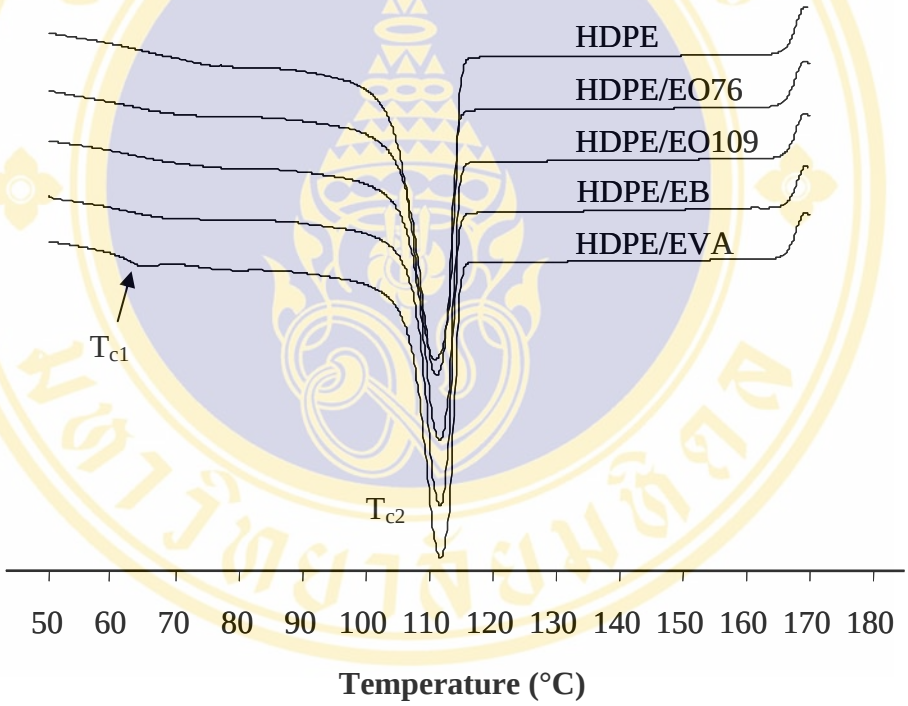

Figure 5.19 DSC cooling thermograms of HDPE and its blends

Copyright by Mahidol University

The DSC results of HDPE and its blends after silane grafting, annealing and water crosslinking process are summarised in Table 5.6. Figure 5.20 shows the DSC heating curves of silane-grafted HDPE and its blends. All samples display only one melting peak at around 130 °C which is slightly lower than the T_m of pure HDPE. The effect of silane grafting can be seen also on its effect to the ΔH_f and % χ_c. The introduction of silane leads to a reduction in the values of ΔH_f and % χ_c. A slight decrease in T_c and $T_{c\ onset}$ is found also in the silane-grafted blends. It was reported [19] earlier that the silane-grafted EO/LDPE blends displayed a slight decrease in T_m, ΔH_f, and % χ_c values, compared to the ungrafted blends.

Table 5.6 Melting temperature (T_m), enthalpy of fusion (ΔH_f), percentage of crystallinity (% χ_c), onset temperature of crystallisation ($T_{c\ onset}$), and crystallisation temperature (T_c) of grafted, annealed and crosslinked samples

System	HDPE/copolymer	T_{m1}, T_{m2} (°C)	ΔH_f ($J.g^{-1}$)	% χ_c	$T_{c\ onset}$ (°C)	T_{c1}, T_{c2} (°C)
Grafted samples	HDPE	132	171	59	117	110
	HDPE/EO76	129	122	42	114	108
	HDPE/EO109	130	129	44	115	110
	HDPE/EB	130	128	44	116	109
	HDPE/EVA	130	129	44	116	110
Annealed samples	HDPE	133	183	63	115	112
	HDPE/EO76	97, 130	150	52	115	111
	HDPE/EO109	132	155	53	115	111
	HDPE/EB	86, 131	155	53	114	112
	HDPE/EVA	85, 132	159	55	115	64, 112
Crosslinked samples	HDPE	132	176	61	117	110
	HDPE/EO76	92, 129	137	47	114	109
	HDPE/EO109	130	136	47	116	109
	HDPE/EB	96, 130	144	50	117	109
	HDPE/EVA	87, 130	145	50	116	109

Copyright by Mahidol University

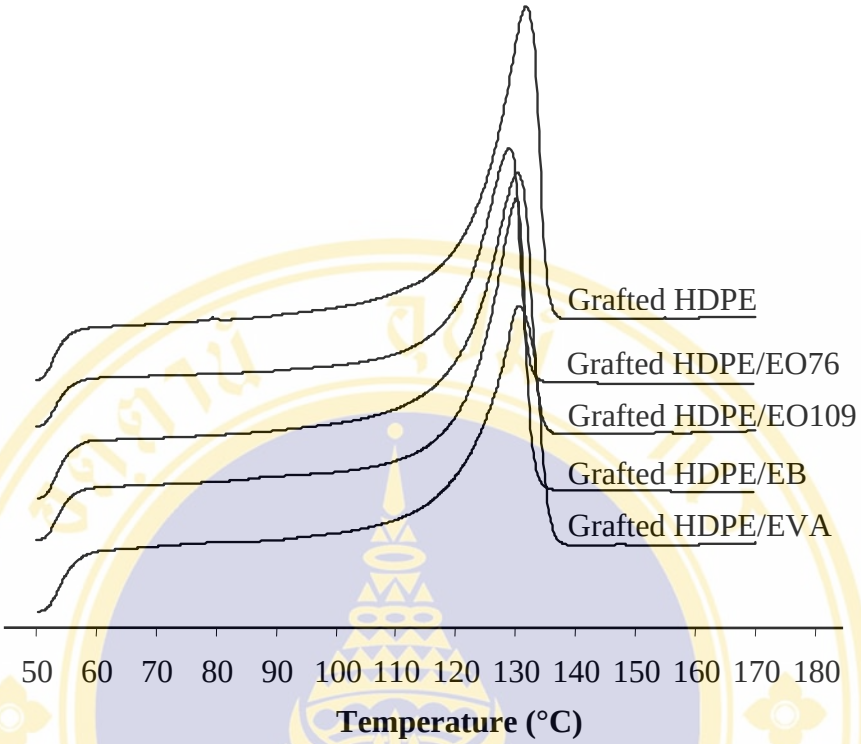

Figure 5.20 DSC heating thermograms of grafted HDPE and its blends

Figures 5.21 and 5.22 show the heating thermograms of annealed and crosslinked HDPE blends, respectively. It can be clearly seen that after annealing and crosslinking the blends of HDPE/EO76, HDPE/EB and HDPE/EVA show two melting peaks, a major sharp peak at ~130 °C is the melting characteristic of HDPE and a small peak at the lower temperature side is a result of the melting of crystalline parts of the copolymers in the blends. In the case of HDPE/EO109, only one melting peak is observed. This might be due to a difficulty in crystallisation of EO109. The similar DSC heating thermograms are observed for the crosslinked systems where the blends containing EO76, EB and EVA show two separate peaks of each component. Compared to the annealed blends, the crosslinked samples show slightly lower values of T_c and % χ_c. This could be due to a difficulty in chain crystallisation brought about by the presence of crosslink network in the systems. However, when compared with the materials crosslinked through other techniques for example peroxide-crosslinked materials, silane-crosslinked materials are able to maintain their crystal structure in the system. This points out the fact that silane crosslinking occurs mainly in the amorphous part [19-20, 30].

Copyright by Mahidol University

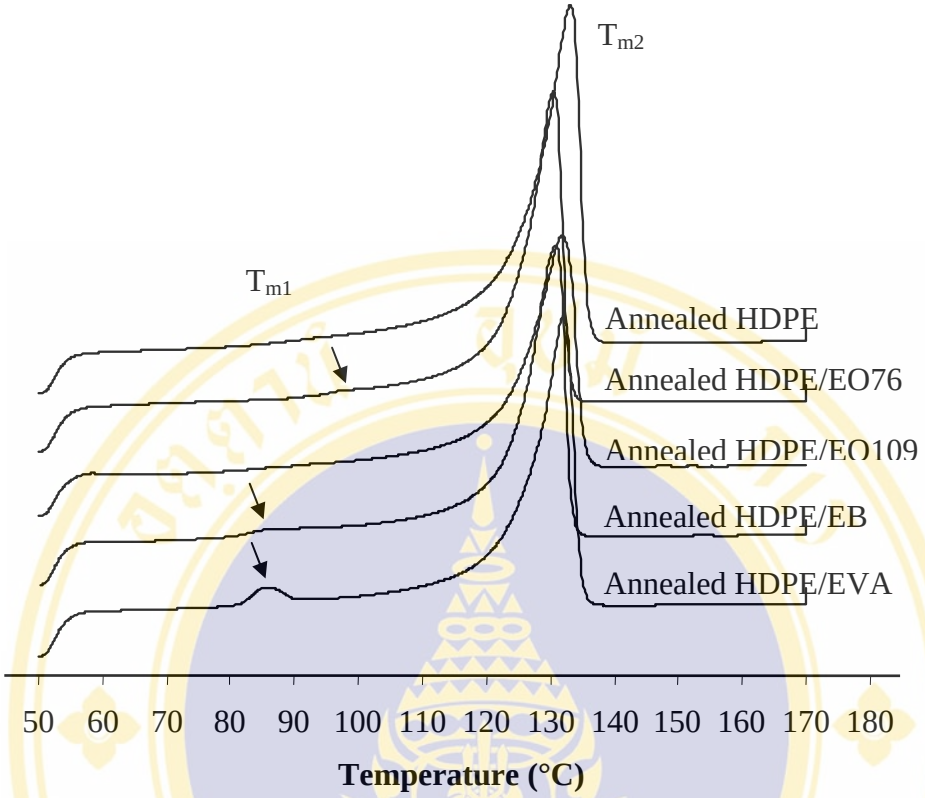

Figure 5.21 DSC heating thermograms of annealed HDPE and its blends

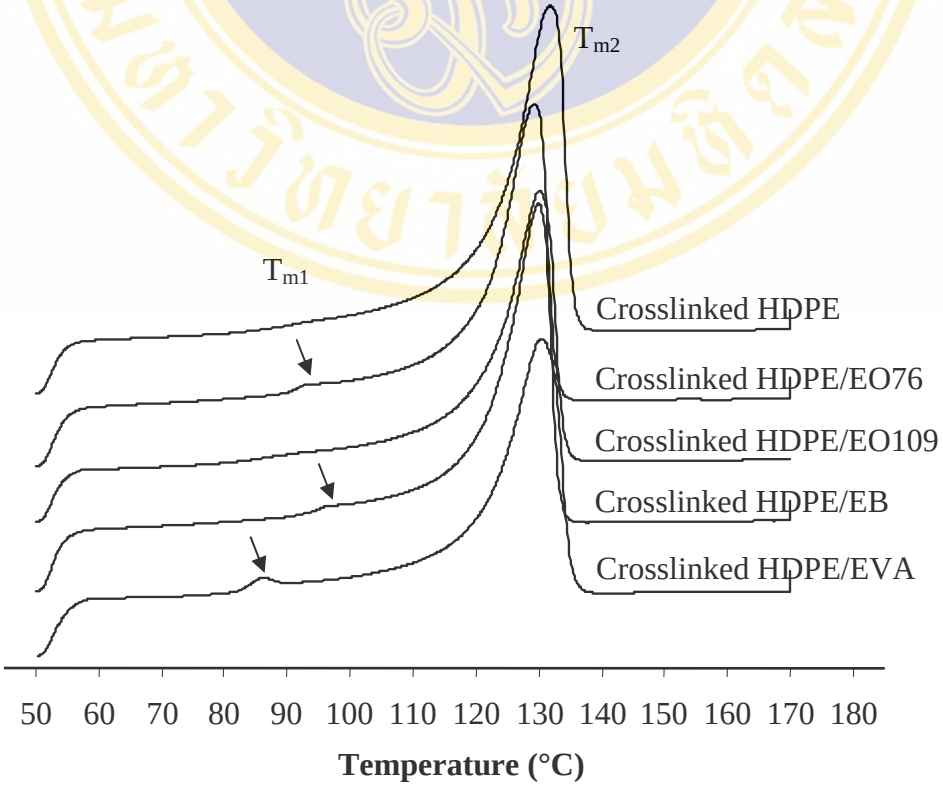

Figure 5.22 DSC heating thermograms of crosslinked HDPE and its blends

Copyright by Mahidol University

5.3.2 Thermal degradation study

The thermal decomposition of polymers was analysed using a thermogravimetric analyser (TGA). In this study, the thermal stability and thermal degradation kinetics of various samples were investigated in terms of the onset decomposition temperatures ($T_{d\ onset}$), maximum decomposition temperatures (T_d) and also activation energy (E_d).

The TGA thermograms of HDPE obtained under various atmospheric conditions at a heating rate of 20 °C.min^{-1} are shown in Figure 5.23. The decomposition temperature results of HDPE and its blends are summarised in Table 5.7. From Figure 5.23, it can be seen that the degradation of HDPE has occurred at a temperature of 494 °C in a nitrogen environment. Whereas in the air and oxygen environment, the degradation temperatures are observed at 469 and 413 °C, respectively. For all of the blend samples, similar results are obtained where the decomposition temperature values run under nitrogen atmosphere are higher than those in air and oxygen atmosphere, respectively. This is owing to the well-known action of oxygen in reducing the stability of polymer bonds when temperature increases. The findings that the degassed or oxygen removed sample showed higher thermal stability was reported elsewhere [80].

Copyright by Mahidol University

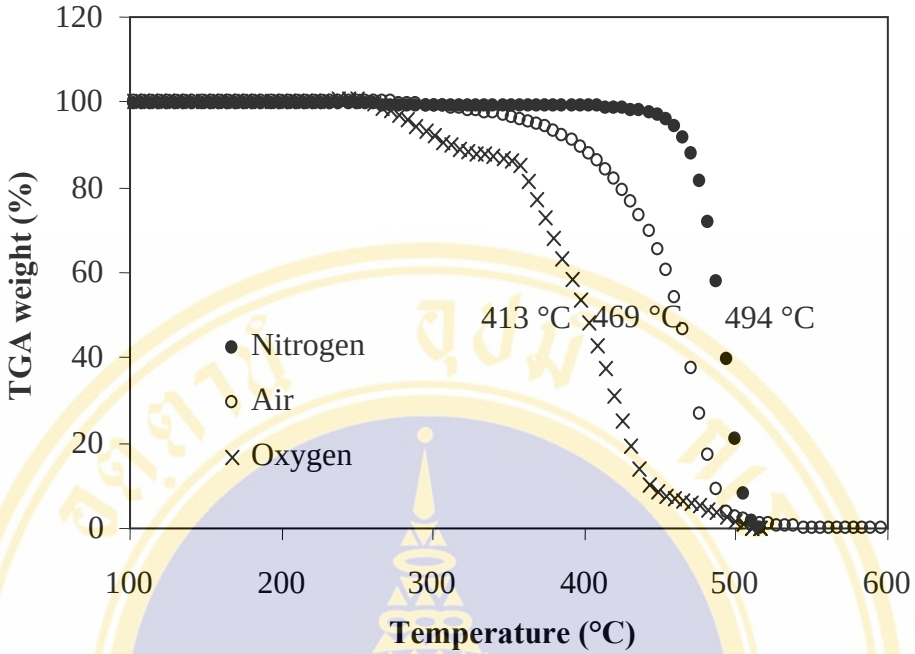

Figure 5.23 TGA thermograms of pure HDPE under various ambient gases

Table 5.7 Decomposition temperatures of HDPE and its blends under various ambient gases

Blend samples	Decomposition temperature (°C)		
	Nitrogen	Air	Oxygen
HDPE	494	469	413
HDPE/EO76	493	470	412
HDPE/EO109	489	469	416
HDPE/EB	492	469	414
HDPE/EVA	491	475	417

Copyright by Mahidol University

In this part, the effect of various ethylene copolymers on the thermal oxidative degradation of HDPE is investigated. The thermal stability of various blend samples under oxygen atmospheric condition is focused on. The TGA thermograms of HDPE and its blends under oxygen atmosphere at a heating rate of 20 °C.min^{-1} are shown in Figure 5.24. The TGA results of individual polymers and their blends are summarised in Table 5.8.

Pure HDPE shows an onset temperature at 320 °C. Similar observation is found also in the case of EO and EB, owing to their similar structures with consist of only carbon-carbon bond. In the case of EVA, a slightly lower onset temperature (313 °C) is seen. This is due to a loss of acetate groups in EVA at that temperature [81]. In the blend series, the addition of copolymers shows a direct effect on the onset temperature of HDPE, i.e. the lowest onset temperature is observed in HDPE/EVA blend. However, no significant difference in the T_d values is observed in all blends. The T_d values in the range of 412-417 °C are resulted.

Copyright by Mahidol University

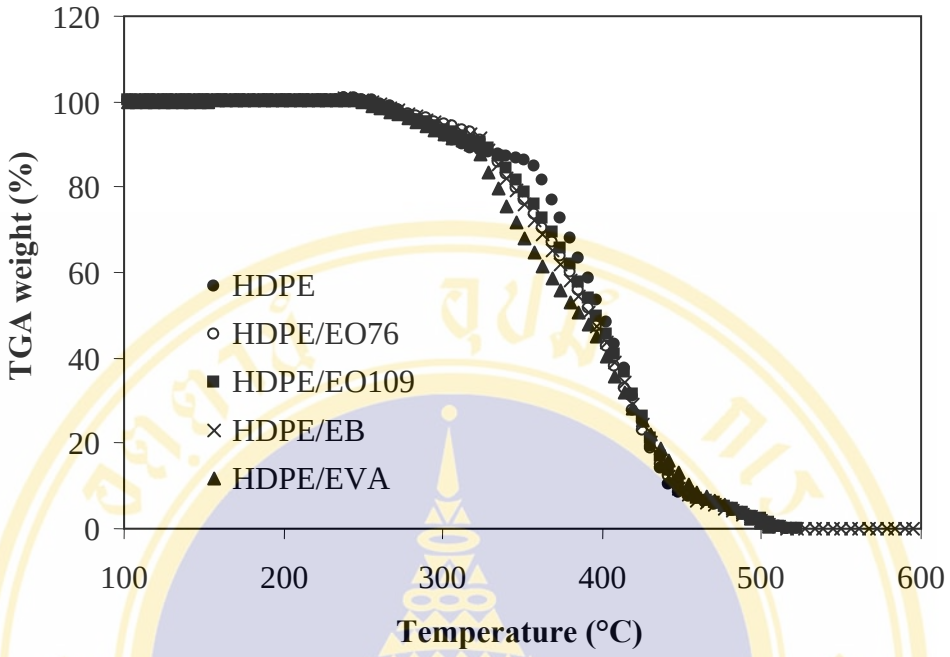

Figure 5.24 TGA thermograms of HDPE and its blends under oxygen atmosphere

Table 5.8 Temperature at 10% weight loss ($T_{10\%}$) and temperature of rapid weight loss (T_d) of individual polymers and HDPE blends under oxygen atmosphere

Samples	$T_{10\%}$ (°C)	T_d (°C)
HDPE	320	413
EO76	322	414
EO109	320	415
EB	321	416
EVA	313	414
HDPE/EO76	319	412
HDPE/EO109	322	416
HDPE/EB	319	414
HDPE/EVA	312	417

Copyright by Mahidol University

To study the effects of the silane grafting and crosslinking on the thermal oxidative stability of HDPE blends, an oxygen atmospheric condition was used. A number of crosslinked samples were selected according to their gel results for example; the samples crosslinked for 120 hrs have approximately 67-75% gel and those crosslinked for 360 and 600 hrs have similar gel content of 80% but show difference in their crosslink density values.

Figure 5.25 shows example of the TGA thermograms of HDPE together with their grafted and crosslinked samples under oxygen atmosphere at a heating rate of 20 °C.min^{-1}. The TGA results are also presented in Table 5.9. Pure HDPE shows $T_{10\%}$ and T_d values at 320 and 413 °C, respectively. After silane grafting reaction, their decomposition values do not change. All grafted HDPE blends also show no difference in the $T_{10\%}$ and T_d values, compared to the ungrafted systems, or it could be said that the silane grafting does not affect the decomposition temperatures of HDPE blends. The thermal oxidative stability of the blends is greatly improved by silane crosslinking. For example, the crosslinking reaction for 600 hrs can raise the $T_{10\%}$ and T_d values of HDPE up to 341 and 449 °C, respectively. All crosslinked HDPE blends also show similar trend. The results suggest that more crosslink network structure could raise the decomposition temperature of the materials. However, the difference in crosslink density among the blend samples used in this part does not show a variation in their decomposition temperature.

Copyright by Mahidol University

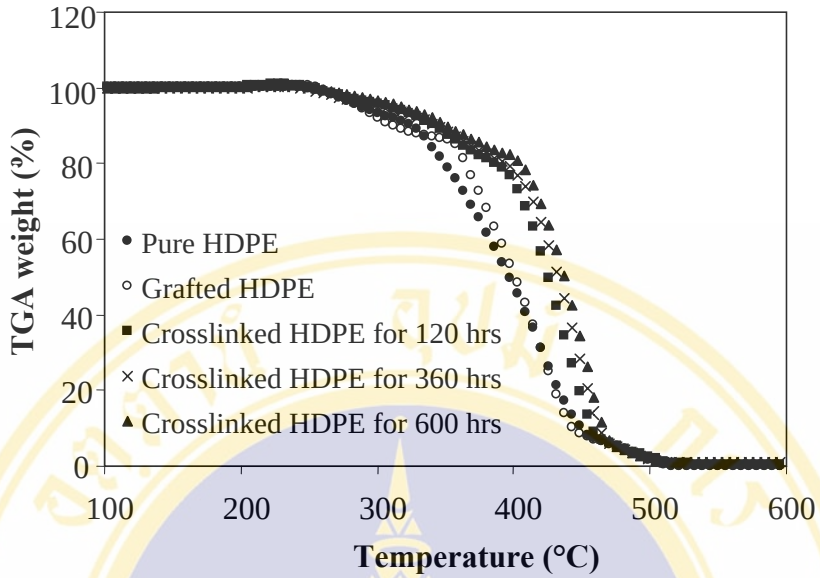

Figure 5.25 TGA thermograms of pure, grafted and crosslinked HDPE under oxygen atmosphere

A similar result was found in the study of Kamphunthong [20] on the thermal properties of silane-crosslinked EO under air atmosphere. The result reported the shift of T_d to higher temperature in the crosslinked samples, with respect to that of the pure EO. The silane-crosslinked sample exhibited better thermal stability than did the pure EO due to higher bond energy of siloxane linkages (444 $kJ.mol^{-1}$), compared to carbon-carbon bonds (348 $kJ.mol^{-1}$) [82].

Copyright by Mahidol University

Table 5.9 Gel content and crosslink density values, temperature at 10% weight loss ($T_{10\%}$) and temperature of rapid weight loss (T_d) of HDPE blends and their grafted and crosslinked samples under oxygen atmosphere

System	Samples	Gel content (%)	Crosslink density ($mol.L^{-1}$)	$T_{10\%}$ (°C)	T_d (°C)
Blend samples	HDPE	0	0	320	413
	HDPE/EO76	0	0	319	412
	HDPE/EO109	0	0	322	416
	HDPE/EB	0	0	319	414
	HDPE/EVA	0	0	312	417
Grafted samples	HDPE	0.02	0.003	322	414
	HDPE/EO76	0.03	0.004	320	414
	HDPE/EO109	0.06	0.006	323	415
	HDPE/EB	0.03	0.003	322	416
	HDPE/EVA	0.07	0.003	313	416
Crosslinked samples (120 hrs)	HDPE	67.16	0.048	339	440
	HDPE/EO76	81.20	0.050	340	441
	HDPE/EO109	79.58	0.050	337	440
	HDPE/EB	76.83	0.045	338	440
	HDPE/EVA	74.79	0.051	329	445
Crosslinked samples (360 hrs)	HDPE	79.10	0.050	338	448
	HDPE/EO76	80.87	0.058	342	441
	HDPE/EO109	81.66	0.060	338	440
	HDPE/EB	80.83	0.052	340	439
	HDPE/EVA	80.33	0.061	330	445
Crosslinked samples (600 hrs)	HDPE	80.03	0.054	341	449
	HDPE/EO76	81.27	0.061	340	446
	HDPE/EO109	82.00	0.060	339	439
	HDPE/EB	81.22	0.055	339	440
	HDPE/EVA	83.35	0.063	329	446

Copyright by Mahidol University

The thermal degradation kinetics are also investigated using TGA method. The Kissinger equation [76] was selected to evaluate the thermal degradation kinetic parameter of HDPE blends and their grafted and crosslinked samples. From Kissinger equation, the activation energy (E_d) of thermal decomposition reaction can be determined from the slope of a plot of logarithm of heating rate (β) versus inverse of temperature ($1/T_d$) at the maximum decomposition temperature under constant heating rate experiments. The details of parameters were reported previously in section 4.5.7.

$$-\ln\left(\frac{\beta}{T_d^2}\right) = \frac{E_d}{RT_d} - \ln\left(\frac{AR}{E_d}\right) \qquad (5.2)$$

The effects of heating rate on decomposition temperature of HDPE and their grafted and crosslinked samples are shown in Figure 5.26. In this part, the samples crosslinked for 360 hrs were selected as representatives of the crosslinked materials with dense network structure, having ~80% gel. The T_d values of various HDPE obtained from the derivative thermogravimetric (DTG) curves are summarised in Table 5.10. As the heating rate increases the decomposition temperature shifts toward the higher values. For examples, in the case of pure HDPE, the T_d values of 494, 497, 501, 505 and 506 °C are observed at the heating rate of 20, 40, 60, 80 and 100 °C. min^{-1}, respectively. This indicates that the effect of heat transfer becomes more apparent at higher heating rate, which leads to a more shift of T_d to higher temperature region [83-85].

Copyright by Mahidol University

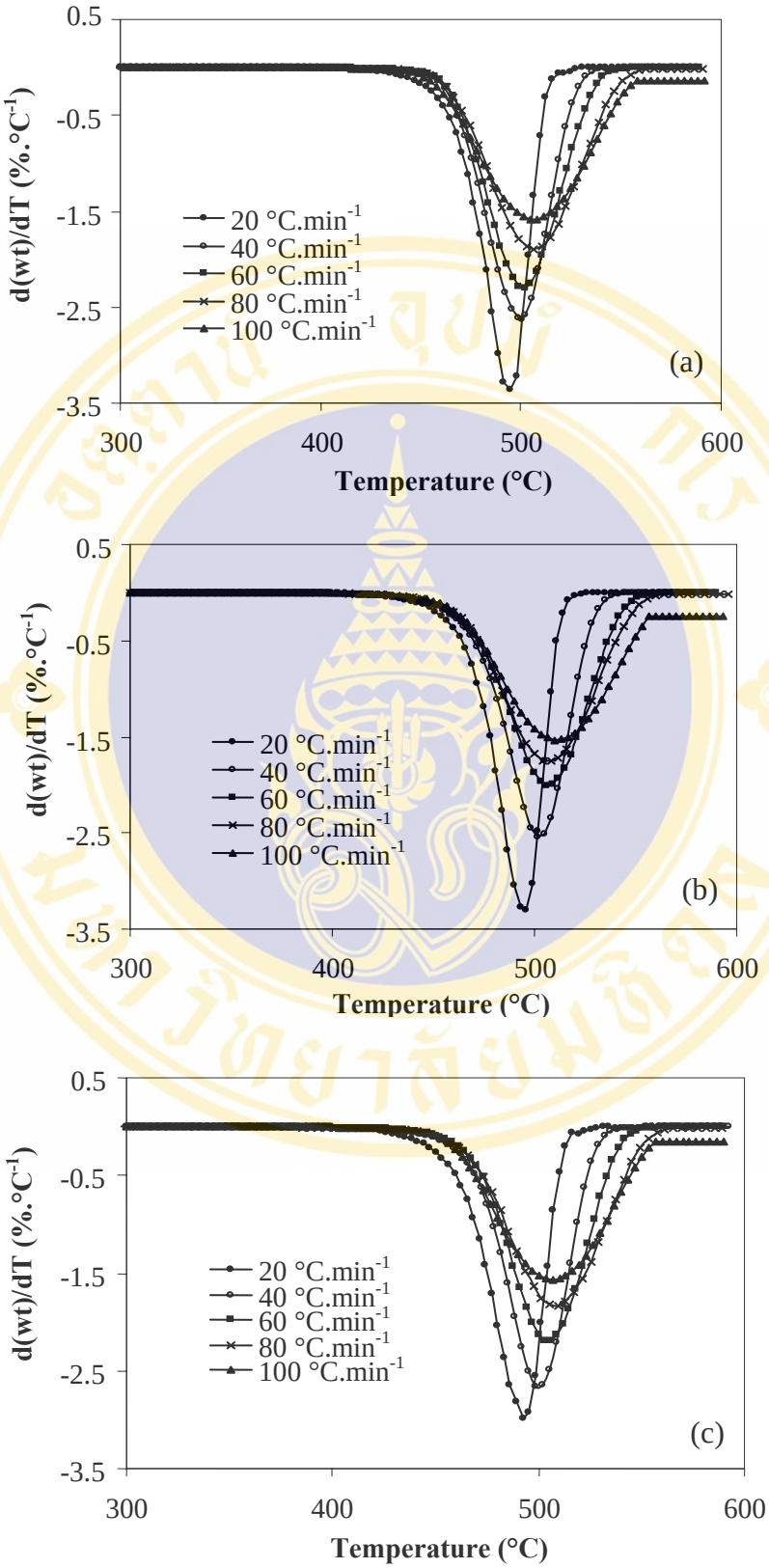

Figure 5.26 DTG thermograms of (a) HDPE, (b) grafted HDPE and (c) crosslinked HDPE at various heating rates

Copyright by Mahidol University

Table 5.10 Decomposition temperature of HDPE blends and their grafted and crosslinked samples

Heating rates ($°C.min^{-1}$)	Decomposition temperature (°C)			
	HDPE/ copolymer	Blend Samples	Grafted samples	Crosslinked samples
20	HDPE	494	492	494
	HDPE/EO76	493	492	494
	HDPE/EO109	489	491	493
	HDPE/EB	492	492	495
	HDPE/EVA	491	491	492
40	HDPE	497	499	501
	HDPE/EO76	497	499	500
	HDPE/EO109	492	492	499
	HDPE/EB	495	500	499
	HDPE/EVA	498	498	499
60	HDPE	501	501	504
	HDPE/EO76	500	502	503
	HDPE/EO109	498	502	503
	HDPE/EB	500	501	504
	HDPE/EVA	500	500	502
80	HDPE	505	504	505
	HDPE/EO76	502	503	505
	HDPE/EO109	499	503	504
	HDPE/EB	501	504	505
	HDPE/EVA	502	502	503
100	HDPE	506	505	506
	HDPE/EO76	505	506	506
	HDPE/EO109	502	501	505
	HDPE/EB	503	505	507
	HDPE/EVA	503	505	504

Copyright by Mahidol University

The decomposition activation energy (E_d) calculated using the Kissinger equation is summarised in Table 5.11 and the plots of logarithm of heating rate and inverse of temperature are included in Appendix Figure B1-4. Figure 5.27 shows an example of such plot. It can be seen that a slope of the straight line of 70.86×10^3 and the calculated E_d values of 589.1 $kJ.mol^{-1}$ are observed in HDPE sample. All HDPE blends show small differences in their slope and E_d values.

Table 5.11 Slope and activation energy values of individual polymers and HDPE blends

Samples	**Slope x 10^3 (E_d/R)**	**E_d ($kJ.mol^{-1}$)**
HDPE	70.86	589.1
EO76	68.76	571.7
EO109	69.60	578.7
EB	69.12	574.7
EVA	69.61	578.7
HDPE/EO76	68.97	573.4
HDPE/EO109	70.51	586.2
HDPE/EB	69.41	577.1
HDPE/EVA	69.69	579.4

Copyright by Mahidol University

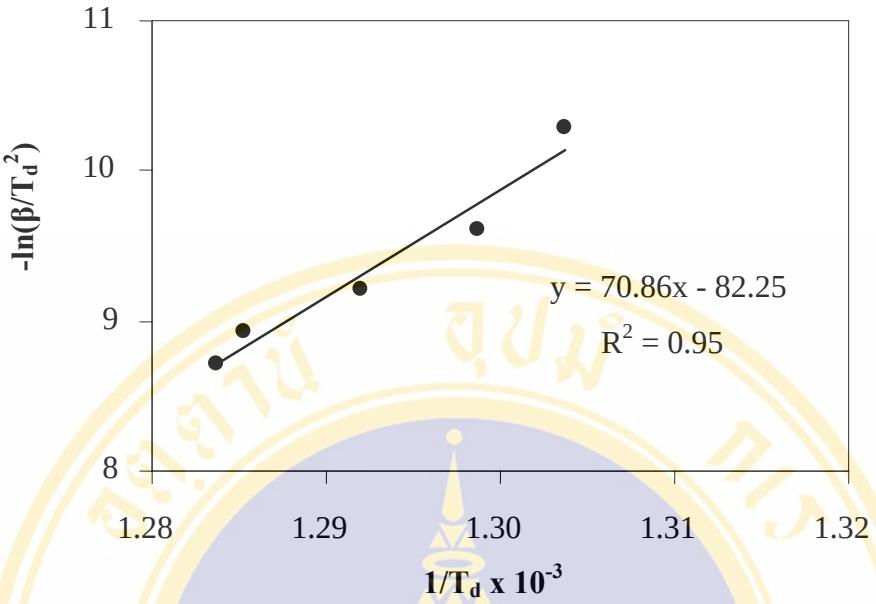

Figure 5.27 Example of a plot of $-\ln(\beta/T_d^2)$ versus $1/T_d \times 10^{-3}$ for pure HDPE

The effects of silane grafting and crosslinking on E_d of various HDPE systems are shown in Figure 5.28 and summarised in Table 5.12. The slope and calculated E_d values of silane-grafted HDPE are 71.08×10^3 and 591.0 $kJ.mol^{-1}$ which is similar to those of unmodified HDPE. All grafted HDPE blends also display similar in E_d values with unmodified HDPE blends. The presence of silane in the systems seems not affect the E_d of the polymer degradation. Crosslinked HDPE shows the slope of the straight line is 75.28×10^3 and the calculated E_d value is 625.9 $kJ.mol^{-1}$. It is clear that the E_d value of HDPE after crosslink reaction is 30 $kJ.mol^{-1}$ higher than that of pure HDPE. The E_d values of all crosslinked HDPE blends are also higher than those of the unmodified polymers. The phenomenon indicates an important role of silane crosslinking in improving the thermal stability of the materials.

Copyright by Mahidol University

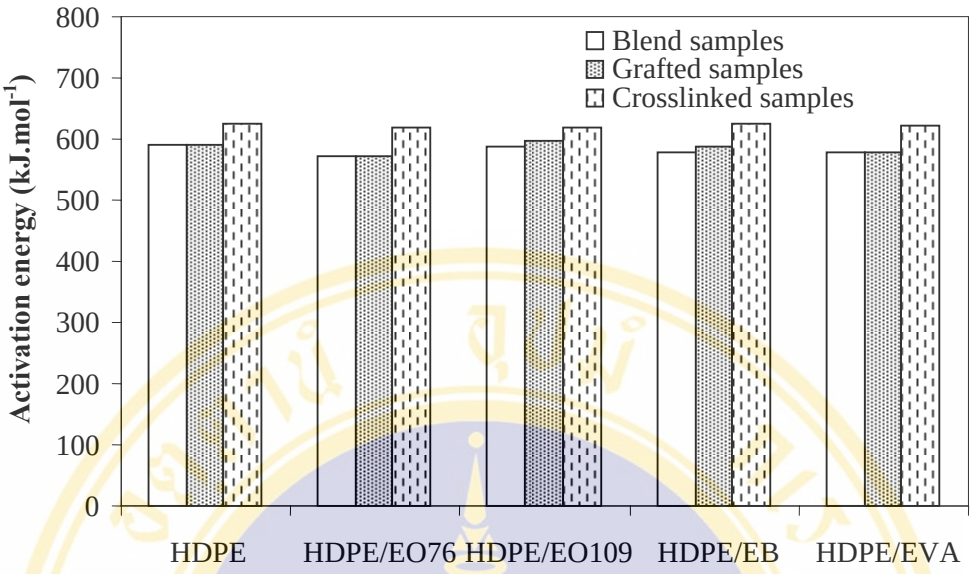

Figure 5.28 Activation energy values of various HDPE and its blends

This similar result was reported by Cho et al. [80] where the crosslinked LDPE had higher thermal decomposition activation energy than pure LDPE. The difference in the values of an uncrosslinked LDPE and its crosslinked samples was about 20 $kJ.mol^{-1}$. This implied that greater thermal stability had been achieved.

Copyright by Mahidol University

Table 5.12 Slope and activation energy values of HDPE blends and their grafted and crosslinked samples

System	HDPE/copolymer	Slope x 10^3 (E_d/R)	E_d (kJ.mol^{-1})
Blend samples	HDPE	70.86	589.1
	HDPE/EO76	68.97	573.4
	HDPE/EO109	70.51	586.2
	HDPE/EB	69.41	577.1
	HDPE/EVA	69.69	579.4
Grafted samples	HDPE	71.08	591.0
	HDPE/EO76	68.94	573.2
	HDPE/EO109	71.67	595.9
	HDPE/EB	70.65	587.4
	HDPE/EVA	69.55	578.2
Crosslinked samples	HDPE	75.28	625.9
	HDPE/EO76	74.33	618.0
	HDPE/EO109	74.54	619.7
	HDPE/EB	75.35	626.5
	HDPE/EVA	74.88	622.6

Copyright by Mahidol University

5.3.3 Rheological study

In this study, the rheological technique was used to monitor the dynamic modulus of materials. The response of the sample yields the shear storage modulus (G′) which indicates the elastic character of the material and the shear loss modulus (G″) which is related to the viscous response of the material.

The dynamic amplitude sweep experiment was first performed to determine the limiting strain (γ) in linear viscoelastic region (LVE). The linear viscoelastic region was measured at a frequency ranged from 1 and 200 $rad.s^{-1}$ and varied strain of deformation from 0.1 to 100%. From dynamic amplitude sweep measurement, G′ of the blend samples was determined and the results are shown in Figures 5.29 and 5.30. It can be seen that all samples exhibit linear viscoelastic region at strains below 20%. Therefore, the dynamic frequency sweep mode is performed in the linear viscoelastic range at a strain amplitude of 10%.

Copyright by Mahidol University

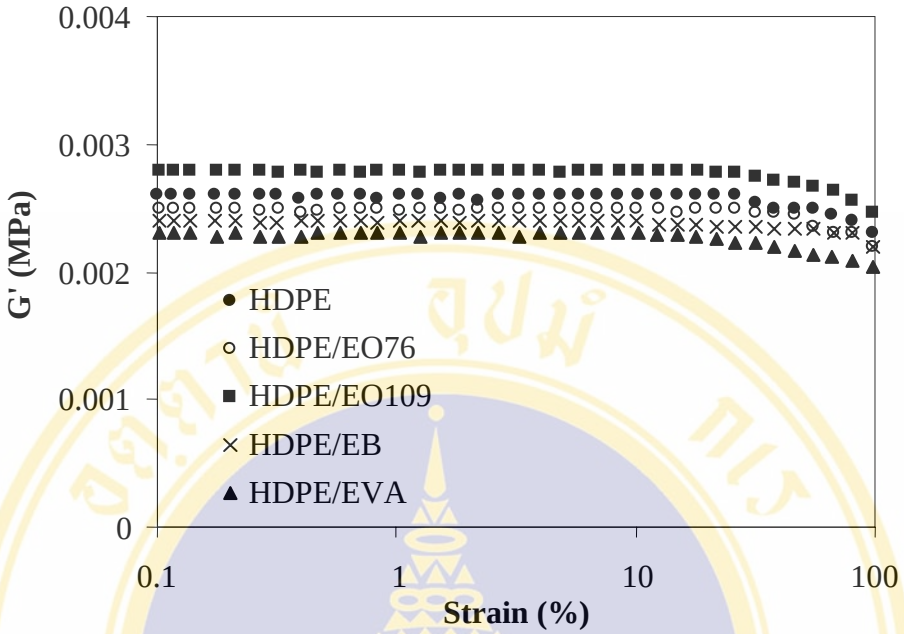

Figure 5.29 Amplitude sweep of HDPE and its blends (LVE measured at a frequency of 1 rad.s^{-1})

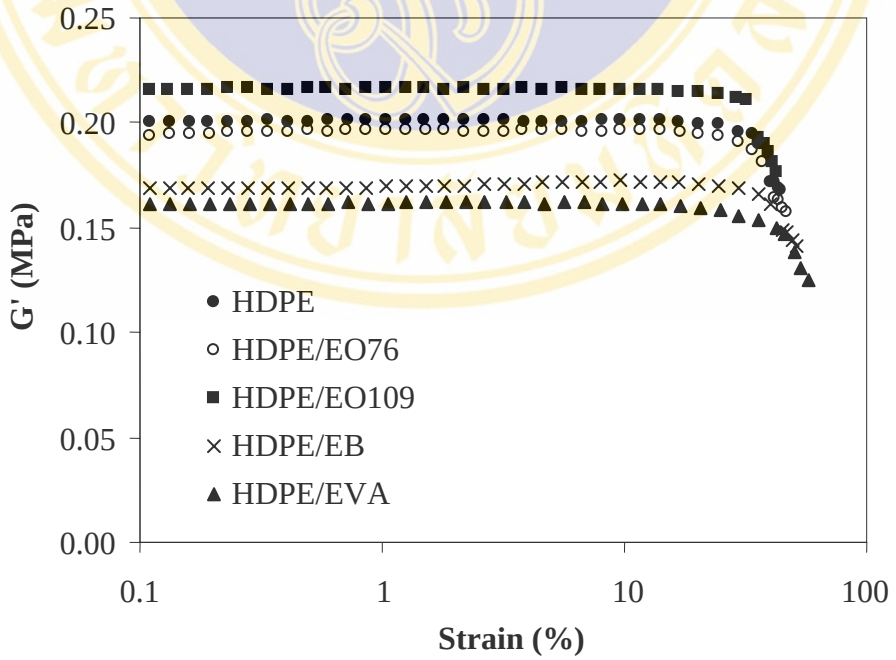

Figure 5.30 Amplitude sweep of HDPE and its blends (LVE measured at a frequency of 200 rad.s^{-1})

Copyright by Mahidol University

The effects of ethylene copolymers on G′ of HDPE are shown in Figure 5.31. It is found that the G′ values of all samples increase with increasing frequency. The G′ of HDPE decreases as the EO76, EB and EVA are incorporated to the HDPE. This is in contrast to that observed in HDPE/EO109 system. The changes in G′ values after the addition of copolymers follow the rule of mixture. The calculated G′ values of all blends are presented also in Figure 5.31. In this study, EO109 has the highest G′ values, followed by HDPE, EO76, EB and EVA, respectively as shown in Figure 5.32. As a consequence, the blend containing EO109 shows the highest G′ whereas the lowest value of G′ is obtained in the HDPE/EVA blend.

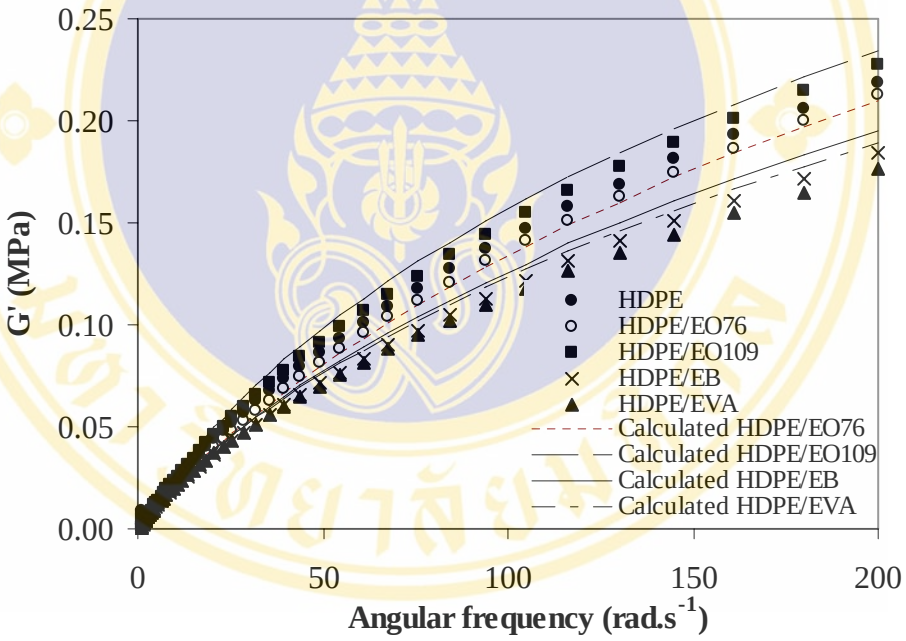

Figure 5.31 Angular frequency sweep of HDPE and its blends

Copyright by Mahidol University

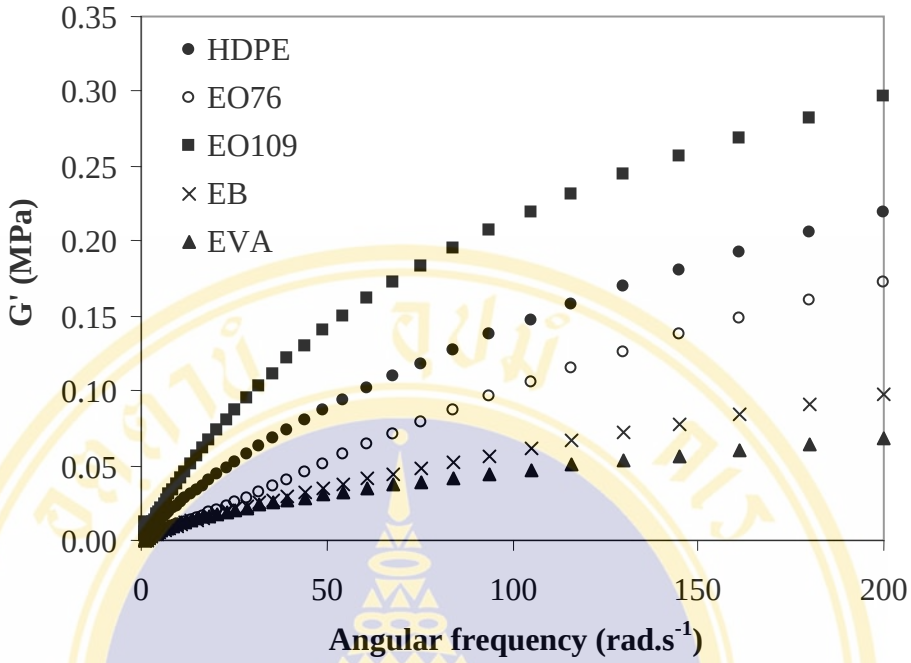

Figure 5.32 Angular frequency sweep of HDPE and various copolymers

Copyright by Mahidol University

Figure 5.33 shows the G′ and G″ of HDPE and its blends as a function of frequency. All HDPE blends show a very strong frequency dependence of G′ and G″. This behavior is a characteristic of uncrosslinked melts. [16]. G″ is larger than G′ at lower frequency range indicating the dominating of viscous over elastic responses. As the higher frequency range, G′ becomes larger than G″ and frequency dependent indicating the dominating of elastic over viscous responses.

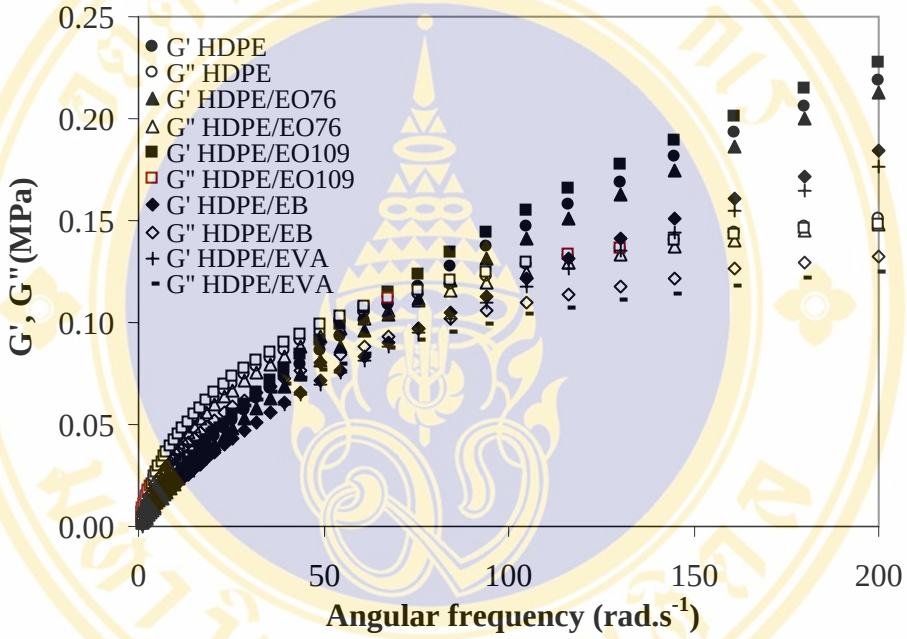

Figure 5.33 Storage and loss modulus of HDPE and its blends

Copyright by Mahidol University

The G′ and G″ of silane-grafted HDPE and its blends are shown in Figure 5.34. For all silane-grafted HDPE blends, it can be observed that G′ is greater than G″ over the entire frequency range. The elastic modulus is dominated more than viscous modulus, indicating that the material has an increment of entangle of polymer chains due to the reacted silane functional groups [20].

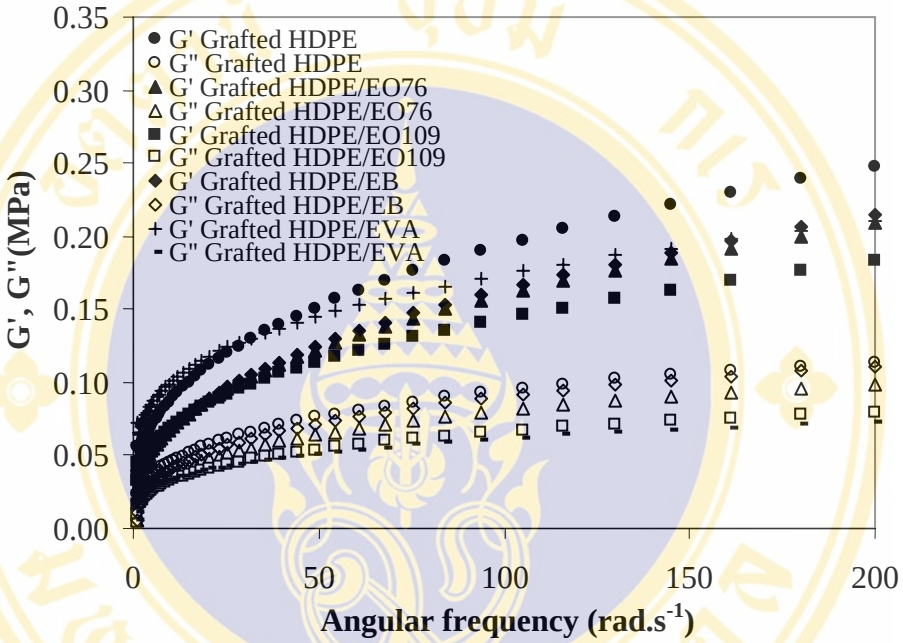

Figure 5.34 Storage and loss modulus of grafted HDPE and its blends

Copyright by Mahidol University

Figure 5.35 shows the G′ and G′′ of silane-crosslinked HDPE and its blends. The samples crosslinked for 360 hrs were selected as representatives of the crosslinked materials having ~80% gel. After crosslinking, G′ values are significantly greater than G′′ values throughout the frequency range and both moduli show a slight dependence on frequency. This observation indicates that the polymer develops a dominant elastic character and simultaneously loses its viscous characteristics which are characteristics of crosslinked systems [86-87].

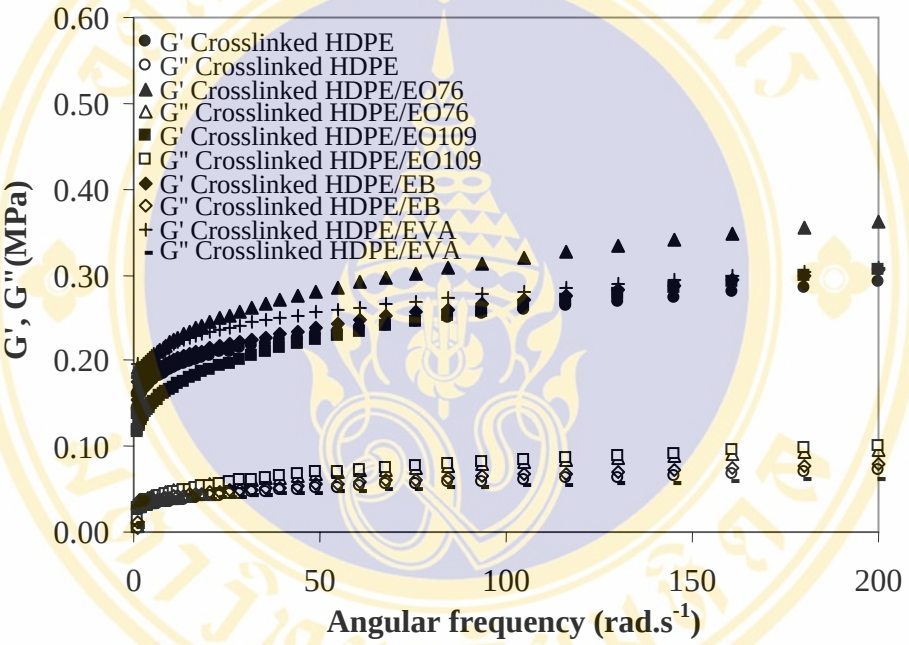

Figure 5.35 Storage and loss modulus of crosslinked HDPE and its blends

Copyright by Mahidol University

The effects of silane grafting and crosslinking on G′ of HDPE, HDPE/EO76, HDPE/EO109, HDPE/EB and HDPE/EVA are shown in Figure 5.36-5.40, respectively. Grafting of silane onto polymer results in a more difficulty in polymer chain movement due to an increasing in entangle chains inside the grafted sample. As a result, the G′ values of all grafted HDPE blends are higher than those of ungrafted systems.

In the case of crosslink system, the G′ values of crosslinked HDPE increase with an increase in the crosslinking time at low frequency ($f < 20$ rad.s^{-1}). The G′ values of all crosslinked HDPE become less dependent on angular frequency as increasing the crosslinking time. For the crosslinked HDPE/EO76, HDPE/EO109, HDPE/EB and HDPE/EVA blends, the results show an increase in G′ values with increasing the crosslinking time throughout the frequency range, indicating the higher density of crosslink network in the materials [16]. The increasing of G′ values are also dependent on angular frequency.

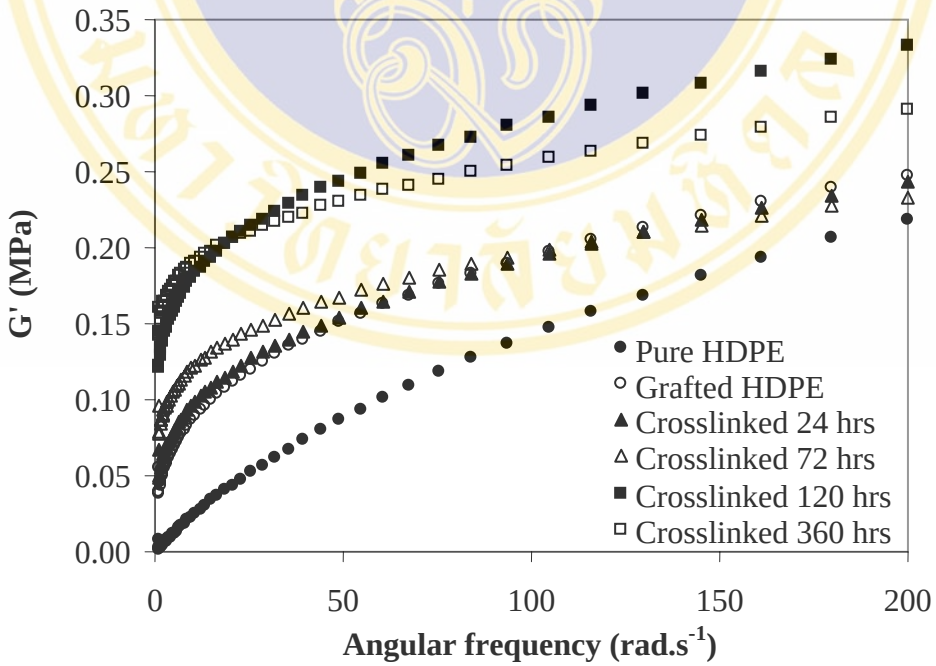

Figure 5.36 Storage modulus of pure, grafted and crosslinked HDPE

Copyright by Mahidol University

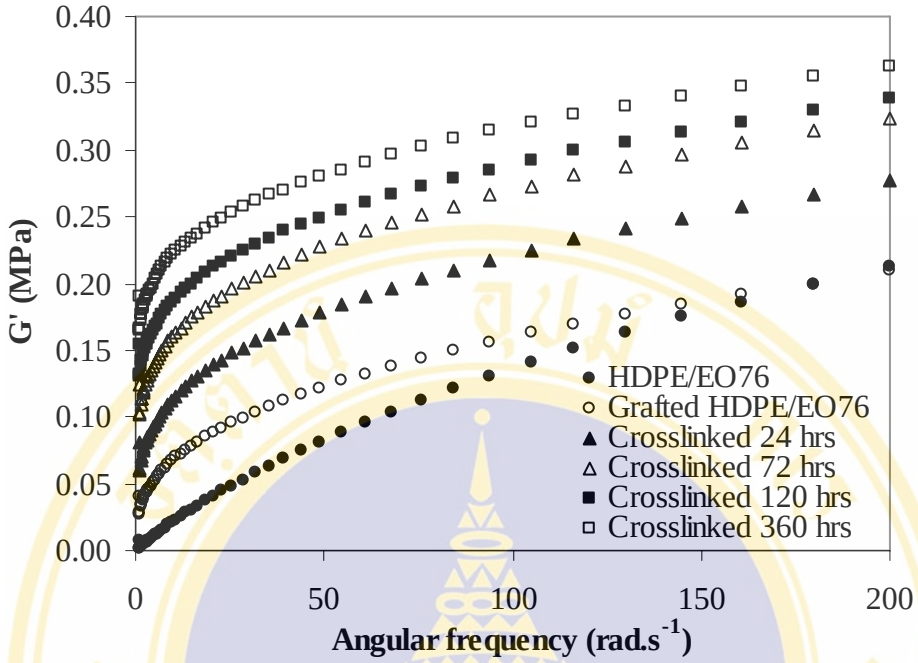

Figure 5.37 Storage modulus of unmodified, grafted and crosslinked HDPE/EO76 blend

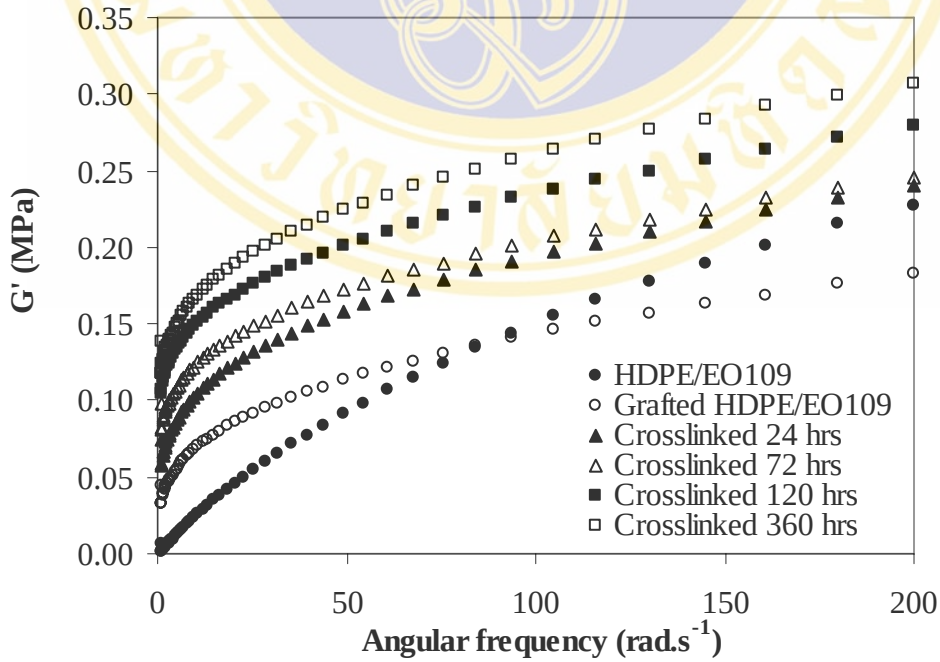

Figure 5.38 Storage modulus of unmodified, grafted and crosslinked HDPE/EO109 blend

Copyright by Mahidol University

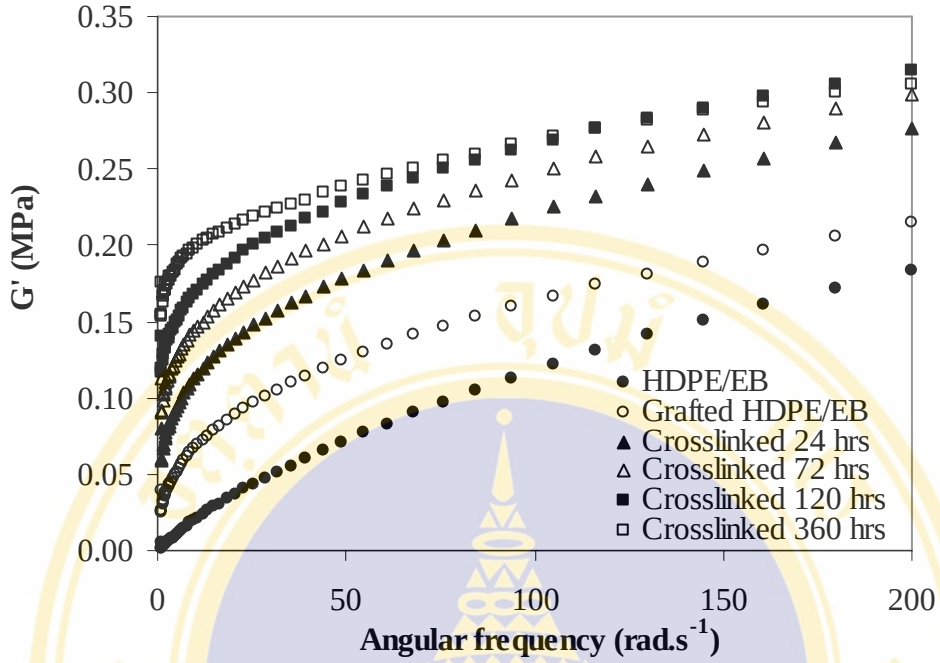

Figure 5.39 Storage modulus of unmodified, grafted and crosslinked HDPE/EB blend

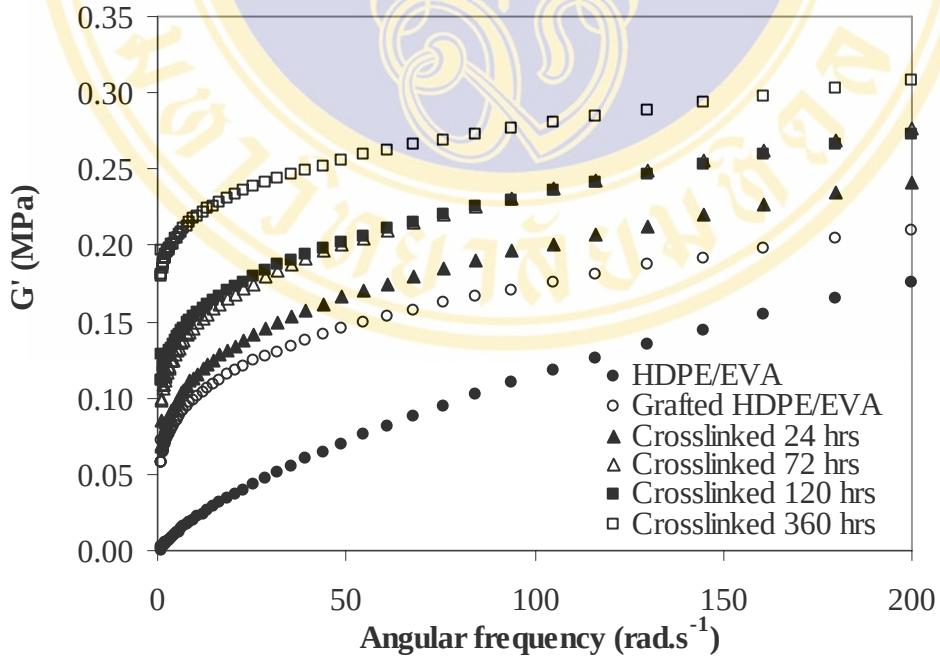

Figure 5.40 Storage modulus of unmodified, grafted and crosslinked HDPE/EVA blend

Copyright by Mahidol University

5.3.4 Mechanical properties

The effects of ethylene copolymers on mechanical properties of HDPE are investigated. The tensile strength at break, elongation at break, Young′s modulus and yield stress of individual polymers and HDPE blends are reported in Table 5.13. The rule of mixture was applied to calculate the tensile values of polymer blends as shown in equation 5.3.

$$P_b = f_1P_1 + f_2P_2 \quad (5.3)$$

where P is the tensile properties, f is volume fractions, b is the blend, and subscripts 1 and 2 refer to component 1 (HDPE) and component 2 (ethylene copolymers), respectively.

Pure HDPE clearly displays a much higher tensile yield stress, compared to its blends. From Table 5.13, the pure HDPE shows much higher tensile strength at break and modulus with a yielding characteristic compared to their four copolymers. By addition of these copolymers to the system, a reduction in tensile stress at yield and at break, also modulus is resulted. While the elongation at break is slightly increased.

The experimental tensile strength at break, elongation at break and modulus values compared to the values calculated from the rule of mixture (equation 5.3) are shown in Figures 5.41-5.43, respectively.

Copyright by Mahidol University

Table 5.13 Tensile data of HDPE, various copolymers and HDPE blends

Samples	Tensile strength at break (MPa)	Elongation at break (%)	Modulus (MPa)	Yield stress (MPa)
HDPE	36.55 (1.19)	657.67 (39.09)	518.22 (18.83)	23.70 (0.40)
EO76	19.19 (1.96)	884.65 (25.44)	33.27 (0.56)	-
EO109	14.99 (1.36)	890.43 (36.30)	20.68 (0.41)	-
EB	16.04 (0.69)	914.47 (31.95)	26.42 (0.92)	-
EVA	20.71 (0.29)	927.54 (17.98)	44.19 (1.18)	-
HDPE/EO76	33.84 (1.73)	706.15 (33.14)	337.68 (8.44)	18.18 (0.20)
HDPE/EO109	32.97 (1.35)	681.26 (37.22)	329.34 (7.59)	17.29 (0.19)
HDPE/EB	31.19 (1.48)	780.40 (38.23)	321.03 (11.58)	18.07 (0.21)
HDPE/EVA	32.64 (1.03)	795.83 (29.55)	344.18 (14.67)	19.01 (0.27)

Copyright by Mahidol University

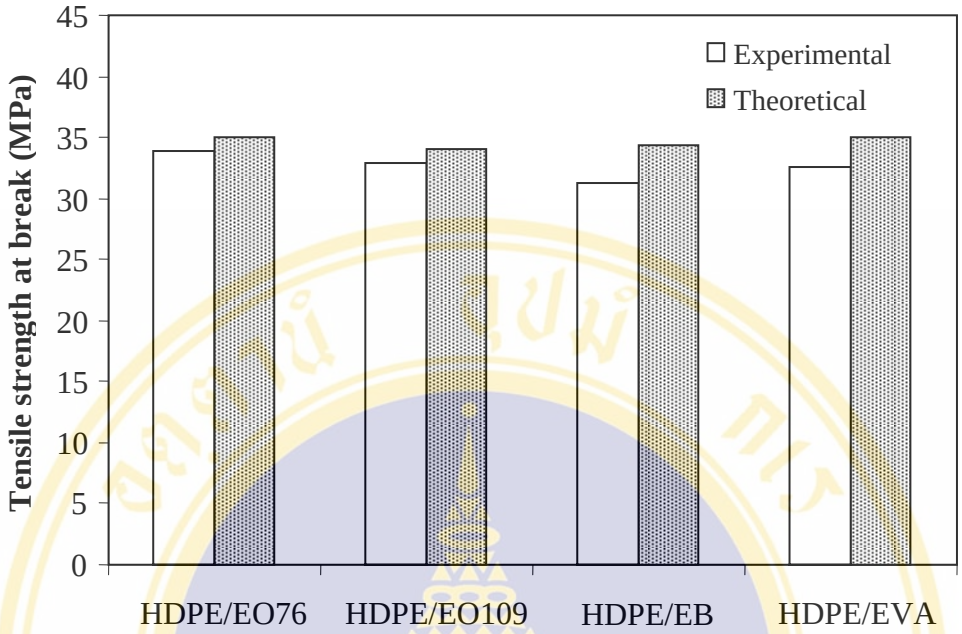

Figure 5.41 Experimental and theoretical tensile strength at break values of HDPE blends

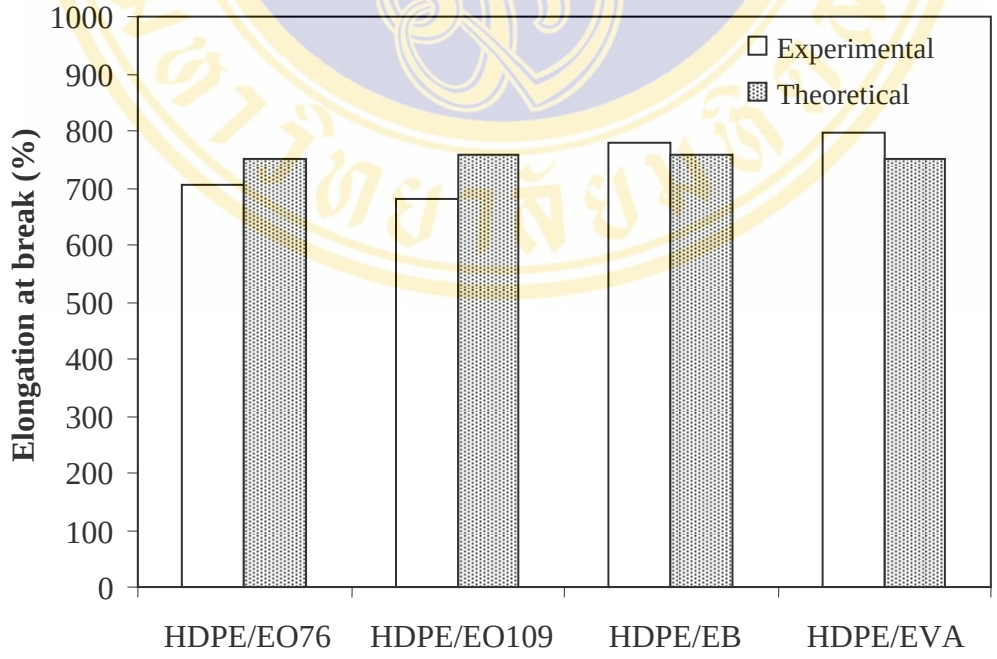

Figure 5.42 Experimental and theoretical elongation at break values of HDPE blends

Copyright by Mahidol University

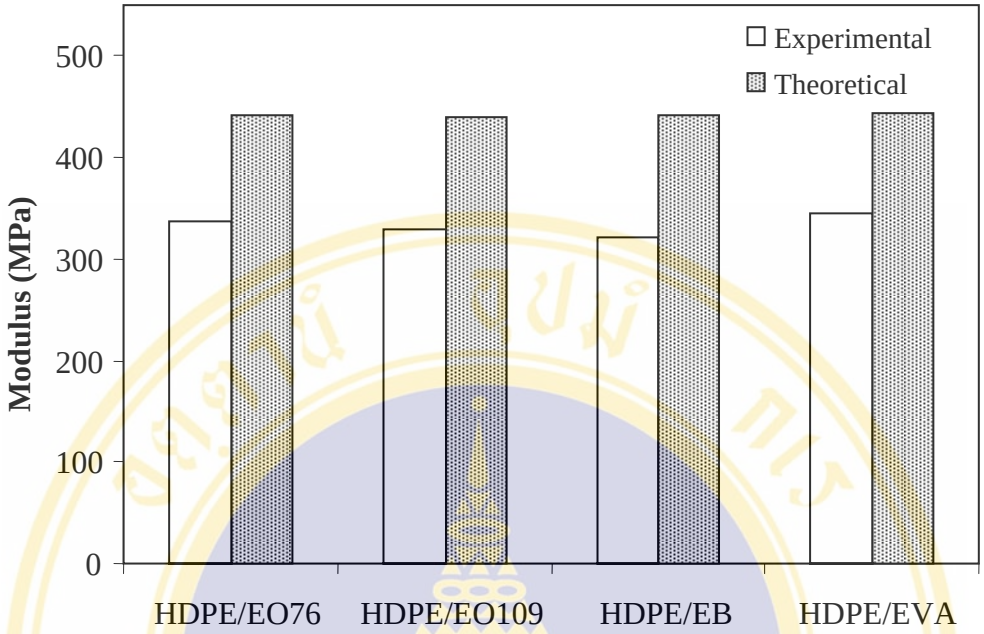

Figure 5.43 Experimental and theoretical modulus values of HDPE blends

The effects of grafting and crosslinking on the tensile properties of HDPE and its blends are investigated. The tensile strength at break, elongation at break, Young′s modulus and yield stress of various samples are shown in Figures 5.44-5.47, respectively. Tensile data of grafted and crosslinked HDPE and its blends are displayed in Table 5.14. In this study, the samples crosslinked for 360 hrs were selected as representatives of the crosslinked materials having ~80% gel.

The introduction of silane to the polymer chains causes a further reduction in tensile stress at yield and at break. The elongation at break also decreases while the modulus seems to be unaffected by the grafting process. Kawko [40] reported that a drastic drop in the elongation at break was observed in the silane-grafted PP. This might be due to the fact that the silane-grafted PP did not show necking behaviour, resulting in low extensibility. Compared to the ungrafted PP composites, the silane-grafted PP composites showed higher tensile stress and modulus.

Copyright by Mahidol University

For the crosslink system, the effect of crosslink seems to be significant for the properties at breaking point, i.e., tensile strength and elongation at break. Both properties show a drastic reduction after the materials have been crosslinked. The loss in polymer drawability prior to failure is partly due to the presence of crosslink network which forms chemical bonding between the polymer chains. In contrast to the failure properties, the tensile yield stress and modulus increase slightly by crosslinking. The four copolymers investigated show similar effect on HDPE properties in either grafting or crosslinking systems.

It had been reported by Krupa and Luyt [1], that the tensile strength at break of crosslinked LLDPE was reduced after radiation crosslinking since crosslinking reduced its drawability. Chimdist [19] reported an improvement in modulus of silane-crosslinked EO/LDPE blends after silane crosslinking. The opposite effect was found for elongation and tensile strength at break. An increase in modulus and a decrease in elongation at break of peroxide-crosslinked LDPE was also observed by Isac and George [88].

Copyright by Mahidol University

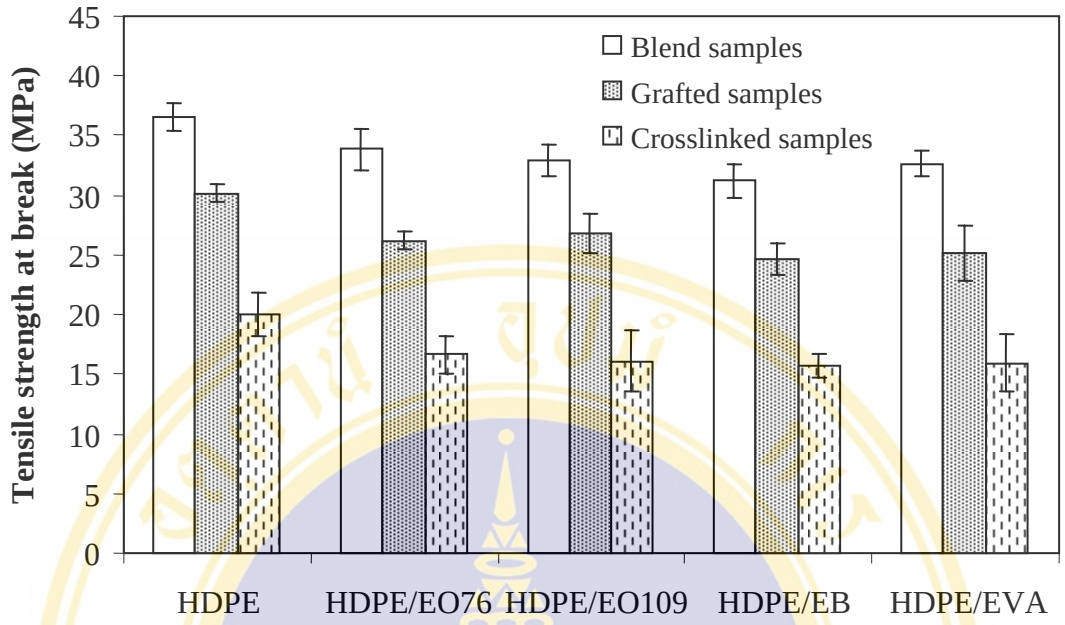

Figure 5.44 Tensile strength at break of various HDPE and its blends

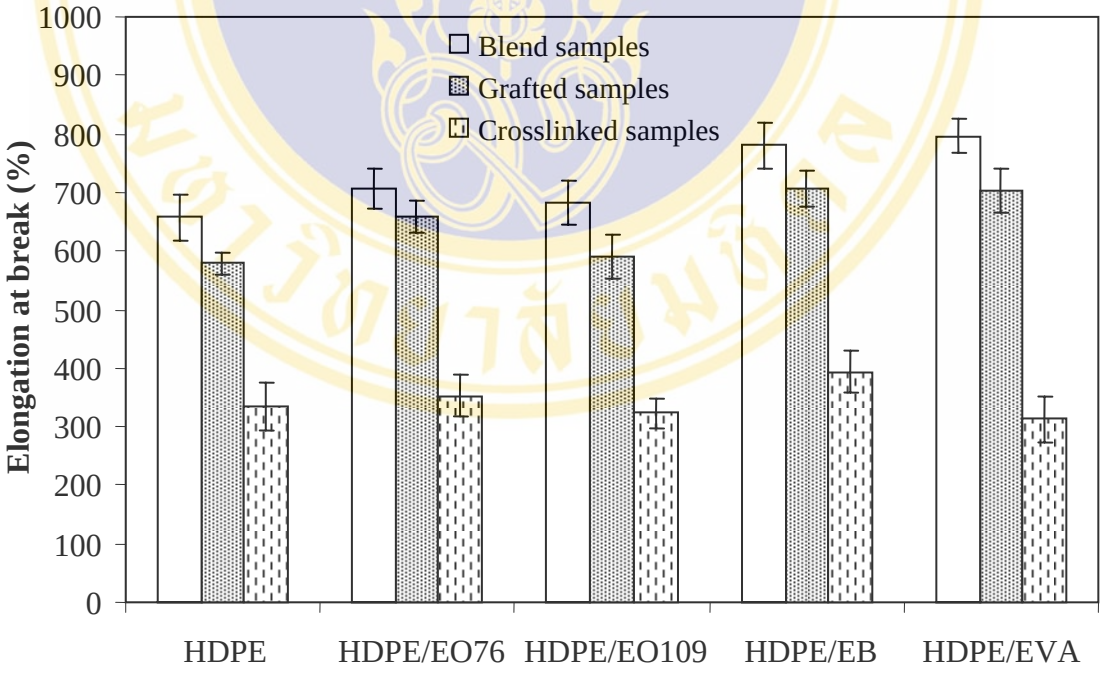

Figure 5.45 Elongation at break of various HDPE and its blends

Copyright by Mahidol University

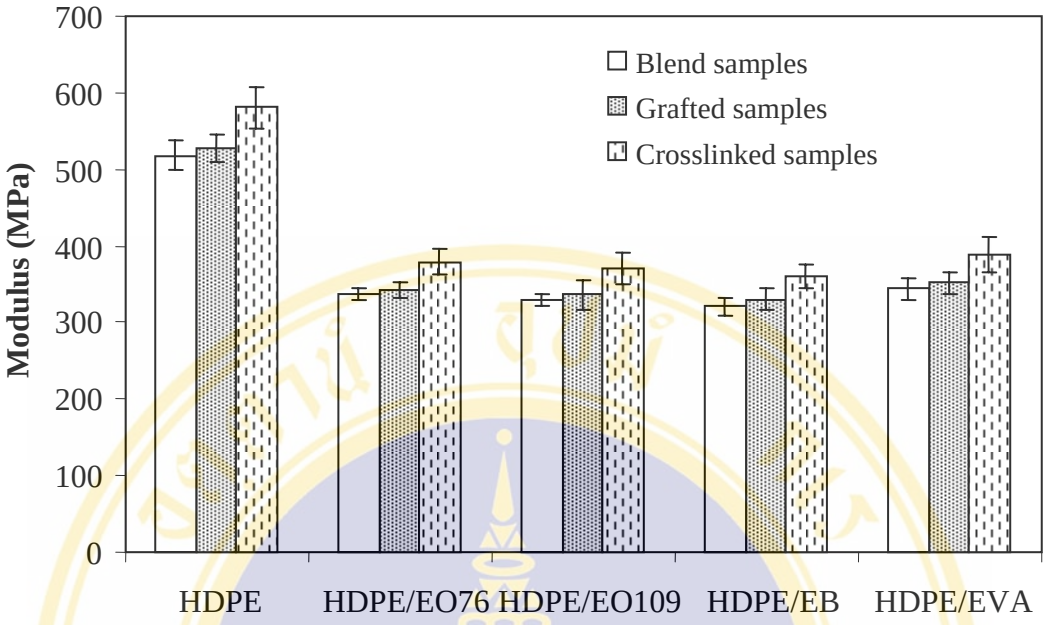

Figure 5.46 Modulus of various HDPE and its blends

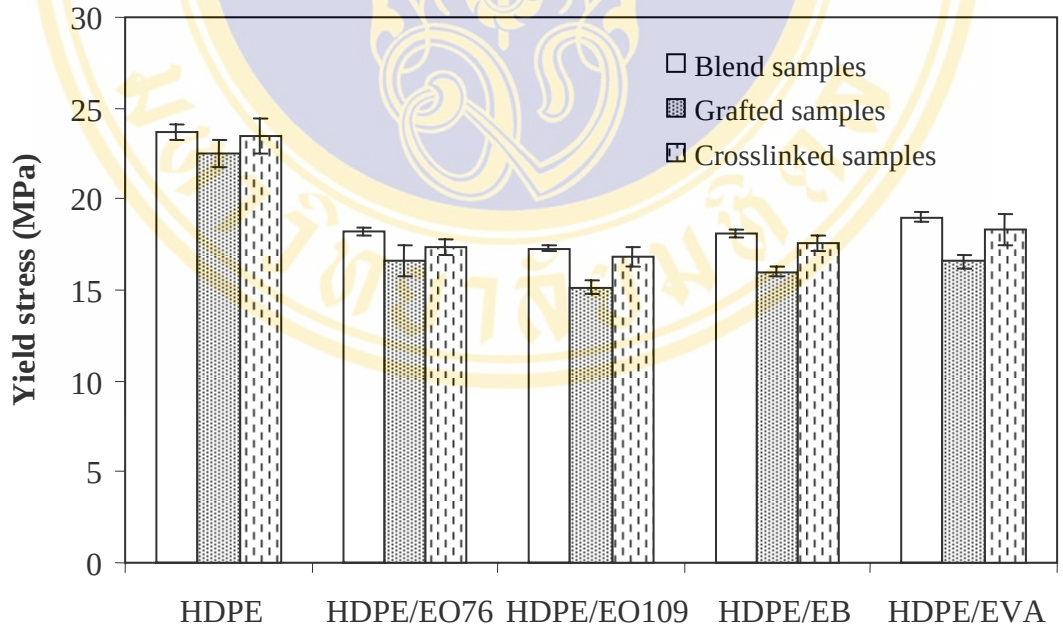

Figure 5.47 Yield stress of various HDPE and its blends

Copyright by Mahidol University

Table 5.14 Tensile data of grafted and crosslinked HDPE and its blends

System	Samples	Tensile strength at break (MPa)	Elongation at break (%)	Modulus (MPa)	Yield stress (MPa)
Grafted samples	HDPE	30.19 (0.78)	578.71 (17.31)	526.60 (18.02)	22.49 (0.73)
	HDPE/EO76	26.21 (0.70)	658.02 (28.32)	341.90 (11.18)	16.58 (0.84)
	HDPE/EO109	26.80 (1.61)	590.37 (37.02)	336.70 (18.91)	15.15 (0.39)
	HDPE/EB	24.65 (1.31)	704.95 (30.61)	329.65 (14.01)	16.00 (0.24)
	HDPE/EVA	25.16 (2.27)	702.22 (37.54)	351.42 (15.01)	16.56 (0.35)
Crosslinked samples	HDPE	20.02 (1.87)	335.30 (41.10)	580.83 (27.65)	23.47 (1.00)
	HDPE/EO76	16.65 (1.54)	352.74 (34.97)	379.53 (16.11)	17.34 (0.43)
	HDPE/EO109	16.13 (2.50)	322.70 (24.73)	371.01 (20.19)	16.82 (0.57)
	HDPE/EB	15.76 (1.03)	393.71 (35.40)	360.29 (15.09)	17.54 (0.42)
	HDPE/EVA	15.01 (2.41)	313.47 (39.12)	388.81 (23.47)	18.33 (0.86)

Copyright by Mahidol University

5.3.5 Heat deflection temperature

The heat deflection temperature (HDT) results of individual polymers and HDPE blends are presented in Table 5.15. A HDT value of pure HDPE is 66.0 °C. The HDT values of the HDPE slightly decreases with the addition of ethylene copolymers. The results show that a HDT values of the HDPE/EVA, HDPE/EO76, HDPE/EB and HDPE/EO109 blends decreases by 4.1, 5.3, 6.8 and 8.6%, respectively compared to pure HDPE. This decrease in HDT values of HDPE blends after the incorporation of ethylene copolymers is due to the presence of copolymers having lower HDT values.

Table 5.15 Heat deflection temperatures of HDPE, various copolymers and HDPE blends

Samples	Heat deflection temperature (°C)
HDPE	66.0
EO76	58.2
EO109	56.0
EB	57.2
EVA	60.2
HDPE/EO76	62.5
HDPE/EO109	60.3
HDPE/EB	61.5
HDPE/EVA	63.3

Copyright by Mahidol University

Figure 5.48 shows the effects of silane grafting and crosslinking on HDT values of HDPE and its blends and Table 5.16 summarises the HDT results of the grafted and crosslinked HDPE and its blends. The silane-grafted HDPE exhibits a higher HDT value than pure HDPE. An increase in HDT of grafted HDPE by 12.9% is observed. This may be due to the fact that the silane molecules are formed onto the polymer chains resulting in an increasing in polymer chain rigidity [40]. All grafted HDPE blends also show higher HDT values, compared to the ungrafted blends.

The samples crosslinked for 360 hrs were selected as representatives of the crosslinked materials having ~80% gel. The silane-crosslinked HDPE exhibits a higher HDT values than the pure HDPE since chemical bonding exists between the polymer chains of crosslinked materials [41]. A HDT value of crosslinked HDPE shows a significant increase from 66.0 to 93.0 °C (an increase by 40.9%), compared to pure HDPE. All crosslinked HDPE blends show similar HDT results where an increase in HDT values about 40% is observed.

Kawko [40] reported that an improvement of HDT was 3.8% and 51.7% for silane-grafted and silane-crosslinked PP, respectively. A dramatic increase in HDT value can be observed in the crosslinked systems. Kuan et al. [35] studied heat deflection properties of silane crosslinked HDPE. They found that the HDT values of crosslinked HDPE were increased with increasing crosslinking time. After being crosslinked for 6 hrs, the HDT was increased from 78.1 to 101.2 °C

Copyright by Mahidol University

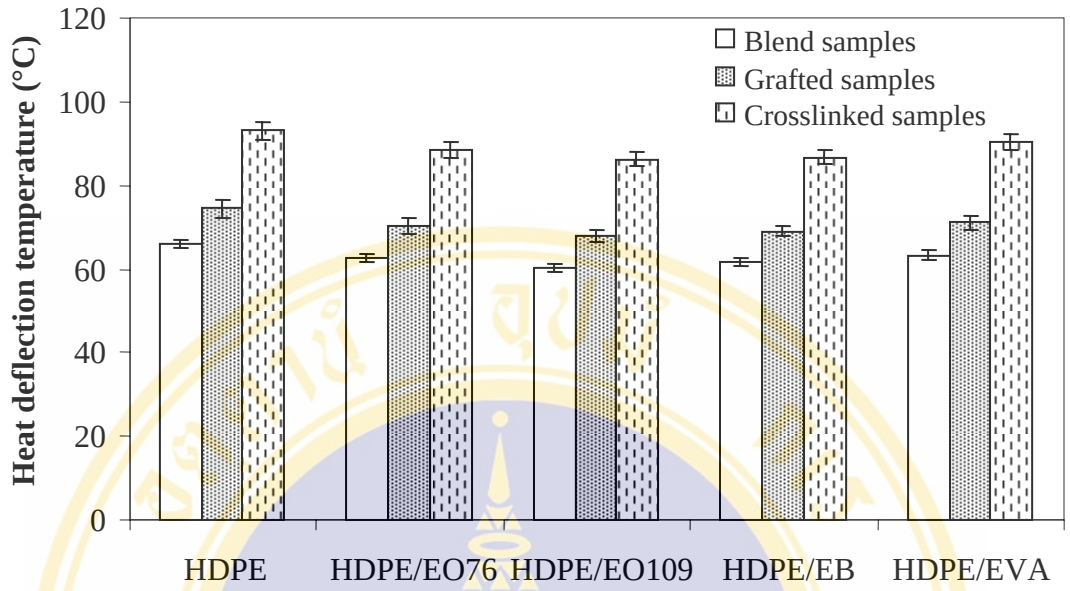

Figure 5.48 Heat deflection temperatures of various HDPE and its blends

Table 5.16 Heat deflection temperatures of grafted and crosslinked HDPE and its blends

System	Samples	Heat deflection temperature (°C)
Grafted samples	HDPE	74.5
	HDPE/EO76	70.2
	HDPE/EO109	67.8
	HDPE/EB	69.0
	HDPE/EVA	71.0
Crosslinked samples	HDPE	93.0
	HDPE/EO76	88.5
	HDPE/EO109	86.2
	HDPE/EB	86.7
	HDPE/EVA	90.3

Copyright by Mahidol University

CHAPTER 6
CONCLUSIONS

Silane grafting and water crosslinking of high-density polyethylene (HDPE) and its blends with various ethylene copolymers were carried out. The ethylene copolymers used in this study were ethylene-octene copolymer (EO), ethylene-butene copolymer (EB) and ethylene-vinyl acetate copolymer (EVA). The effects of chemical structure and polarity of the copolymers on the silane grafting and water crosslinking of HDPE were investigated. Their effects on thermal, rheological and mechanical properties of crosslinked products were also analysed. The following conclusions can be drawn.

1. The grafting of vinyl trimethoxysilane (VTMS) onto the HDPE blends was clearly revealed by the FTIR analysis. The incorporation of ethylene copolymers, although, increased silane absorption in the blends, it did not help improving the efficiency of silane grafting. The results showed that the ability of silane absorption depends strongly on polymer polarity and to a lesser extent on crystallinity while the extent of grafting depends mainly on the steric hindrance of the copolymers in performing reaction in the melt state.

2. The structure of ethylene copolymers played a significant role in silane crosslinking process. The degree of crosslinking in terms of gel as well as its rate increased with the incorporation of ethylene copolymers. The gel content of 80% was observed in all blends after a long crosslinking time. However, the FTIR and rheological results revealed a difference in crosslink density among those samples.

3. The presence of crosslink network in the blends had only slight effect on crystallisation. Silane crosslinking is believed to occur mainly in the amorphous region of the blends. An increase in activation energy and temperature of thermal decomposition as well as heat deflection temperature was observed after crosslinking. The difference in crosslink density observed among various blends showed no significant difference in those properties. Furthermore, an improvement in storage

Copyright by Mahidol University

modulus, tensile yield stress and modulus together with a reduction in tensile strength and elongation at break were obtained by silane crosslinking.

Copyright by Mahidol University

REFERENCES

1. Krupa I, Luyt AS. Thermal and mechanical properties of LLDPE cross-linked with gamma radiation. Polym Degrad Stab 2001; 71: 361-366.
2. Smedberg A, Hjertberg T. Crosslinking reactions in an unsaturated low density polyethylene. Polymer 1997; 38: 4127-4138.
3. Woods RJ, Pikaev AK. Applied radiation chemistry (radiation processing). New York: John Wiley & Sons; 1994.
4. Gheysari Dj, Behjat A, Haji-Saeid M. The effect of high-energy electron beam on mechanical and thermal properties of LDPE and HDPE. Eur Polym J 2001; 37: 295-302.
5. Gheysari Dj, Behjat A. Radiation crosslinking of LDPE and HDPE with 5 and 10 MeV electron beams. Eur Polym J 2001; 37: 2011-2016.
6. Forsythe JS, Hill DJT, Logothetis AL, Seguchi T, Whittaker AK. Thermal and mechanical properties of radiation crosslinked poly(tetrafluoroethylene-co-perfluoromethyl vinyl ether). Radiat Phys Chem 1998; 53: 657-667.
7. Kubo J, Otsuhata K, Iheda S, Seguchi T. Electron-Induced Crosslinking of Polypropylene with the Addition of Hydrogen-Donating Hydrocarbons. J Appl Polym Sci 1997; 64: 311-319.
8. AnBarasan R, Babot O, Maillard B. Crosslinking of high-density polyethylene in the presence of organic peroxides**.** J Appl Polym Sci 2004; 93: 75-81.
9. Khonakdar HA, Morshedian J, Wagenknecht U, Jafari SH. An investigation of chemical crosslinking effect on properties of high-density polyethylene. Polymer 2003; 44: 4301-4309.
10. Yu Q, Zhu S. Peroxide crosslinking of isotactic and syndiotactic polypropylene. Polymer 1999; 40: 2961-2968.
11. Romani F, Corrieri R, Braga V, Ciardelli F. Monitoring the chemical crosslinking of propylene polymers through rheology. Polymer 2002; 43: 1115-1131.

Copyright by Mahidol University

12. Bacci D, Marchini R, Scrivani MT. Peroxide crosslinking of Ziegler-Natta thermoplastic polyolefins. Polym Eng Sci 2004; 44: 131-140.
13. Shieh YT, Hsiao KI. Thermal properties of silane-grafted water-crosslinked polyethylene. J Appl Polym Sci 1998; 70: 1075-1082.
14. Sirisinha K, Kawko K. Properties and characterisation of filled poly(propylene) composites crosslinked through siloxane linkage. Macromol Mater Eng 2005; 290: 128-135.
15. Cartasegna S. Silane-grafted/moisture-curable ethylene-propylene elastomers for the cable industry. Rubber Chem Technol 1986; 59: 722-739.
16. Sirisinha K, Meksawat D. Changes in properties of silane-water crosslinked metaalocene ethylene-octene copolymer after prolonged crosslinking time. J App Polym Sci 2004; 93: 901-906.
17. Shieh YT, Liau JS, Chen TK. An investigation of water crosslinking reactions of silane-grafted LDPE. J Appl Polym Sci 2001; 81: 186-196.
18. Sirisinha K, Chimdist S. Comparison of techniques for determining crosslinking in silane-water crosslinked materials. Polym Testing 2006; 25: 518-526.
19. Chimdist S. A study on silane-grafting and water-crosslinking of ethylene-octene copolymer and low-density polyethylene (EOR/LDPE) blends. [M.Sc. Thesis in Polymer Science and Technology]. Bangkok: Faculty of Graduate Studies, Mahidol University; 2005.
20. Kamphunthong W. A study on ethylene-octene copolymer composites crosslinked through siloxane linkage. [M.Sc. Thesis in Polymer Science and Technology]. Bangkok: Faculty of Graduate Studies, Mahidol University; 2006.
21. Huang H, Lu HH, Liu NC. Influence of grafting formulations and extrusion conditions on properties of silane-grafted polypropylene. J Appl Polym Sci 2000; 78: 1233-1238.
22. Jiao C, Wang Z, Gui Z, Hu Y. Silane grafting and crosslinking of ethylene-octene copolymer. Eur Polym J 2005; 41: 1204-1211.
23. Nachtigall SMB, Stedile FC, Felix AHO, Mouler RS. Polypropylene functionalisation with vinyltriethoxysilane. J Appl Polym Sci 1999; 72: 1313-1319.

Copyright by Mahidol University

24. Shieh YT, Liu CM. Silane grafting reactions of LDPE, HDPE, and LLDPE. J Appl Polym Sci 1999; 74: 3404-3411.
25. Wang Z, Hu Y, Gui Z, Zong R. Halogen-free flame retardation and silane crosslinking of polyethylenes. Polym Testing 2003; 22: 533-538.
26. Meksawat D. An investigation on crosslinked ethylene-octene copolymer prepared by different crosslinking techniques [M.Sc. Thesis in Polymer Science and Technology]. Bangkok: Faculty of Graduate Studies, Mahidol University; 2003.
27. Liu NC, Yao GP, Huang H. Influences of grafting formulations and processing conditions on properties of silane grafted moisture crosslinked polypropylenes. Polymer 2000; 41: 4537-4542.
28. Sen AK, Mukherjee B, Bhattacharyya AS, De PP. Kinetics of silane grafting and moisture crosslinking of PE and ethylene propylene rubber. J Appl Polym Sci 1992; 44: 1153-1164.
29. Parent JS, Geramita K, Ranganathan S, Whitney RA. Silane-modified poly(ethylene-co-vinyl acetate): influence of comonomers on peroxide-initiated vinylsilane grafting. J Appl Polym Sci 2000; 76: 1308-1314.
30. Celina M, George GA. Characterisation and degradation studies of peroxide and silane crosslinked polyethylene. Polym Degrad Stab 1995; 48: 297-312.
31. Narkis M, Tzur A, Vaxman A, Fritz HG. Some properties of silane-grafted moisture-crosslinked polyethylene. Polym Eng Sci 1985, 25; 13: 857-862.
32. Hjertberg T, Palmlof M, Sultan BA. Chemical reactions in crosslinking of copolymers of ethylene and vinyltrimethoxy silane. J Appl Polym Sci 1991; 42: 1185-1192.
33. Sirisinha K, Meksawat D. Comparison in processability and mechanical and thermal properties of ethylene-octent copolymer crosslinkined by different techniques. J App Polym Sci 2004; 93: 1179-1185.
34. Palmlof M, Hjertberg T. Catalysis of the crosslinking reactions of ethylene vinyl silane copolymers using carboxylic acid and DBTDL. J Appl Polym Sci 1999; 72: 521-528.

Copyright by Mahidol University

35. Kuan HC, Kuan JF, Ma CCM, Huang JM. Thermal and Mechanical Properties of Silane-Grafted Water Crosslinked Polyethylene. J Appl Polym Sci 2005; 96: 2383-2391.
36. Shieh YT, Tsai TH. Silane grafting reactions of low-density polyethylene. J Appl Polym Sci 1998; 69: 255-261.
37. Beltran M, Mijangos C. Silane grafting and moisture crosslinking of polypropylene. Polym Eng Sci 2000; 40: 1534-1541.
38. Shah GB, Fuzail M, Anwar J. Aspects of the crosslinking of polyethylene with vinyl silane. J Appl Polym Sci 2004; 92: 3796-3803.
39. McCormick JA, Royer JR, Hwang RC, Khan SA. Tailored rheology of a metallocene polyolefin through silane grafting and subsequent silane crosslinking. J Polym Sci, Part B: Polym Phys 2000; 38: 2468-2479.
40. Kawko K. A study on silane grafting and water crosslinking of polypropylene and its filled composites [M.Sc. Thesis in Polymer Science and Technology]. Bangkok: Faculty of Graduate Studies, Mahidol University; 2004.
41. Kuan CF, Kuan HC, Ma CCM, Huang CM. Mechanical, thermal and morphological properties of water-crosslinked wood flour reinforced linear low-density polyethylene composites. Composites: Part A 2006; 37: 1696-1707.
42. Feldman D, Barbalata A. Synthetic Polymers. London: Chapman and Hall; 1996.
43. Brydson JA. Plastics Materials. Oxford: Butterworth-Heinemann; 1999.
44. Simanke AG, Galland GB, Freitas L, da Jornada JAH, Quijada R, Mauler RS. Influence of the comonomer content on the thermal and dynamic mechanical properties of metallocene ethylene/1-octene copolymers. Polymer 1999; 40: 5489-5495.
45. Defoor F, Groeninckx G, Schouterden P, Van der Heiden A. Molecular, thermal and morphological characterization of narrowly branched fractions of 1-octene linear low-density polyethylene: 1. Molecular and thermal characterization. Polymer 1992; 33: 3878-3883.
46. Vanden ES, Mathot VBF, Höhne GWH, Schawe JWK, Reynaers H. Thermal behaviour of homogeneous ethylene-1-octene copolymers and linear polyethylene at high pressures. Polymer 2000; 41: 3411-3423.

Copyright by Mahidol University

47. Utracki LA. Multiphase Polymers: Blends and Ionomers. Washington DC: American Chemical Society; 1989.
48. Choi P. Molecular dynamics studies of the thermodynamics of HDPE/butene-based LLDPE blends. Polymer 2000; 41: 8741-8747.
49. Zhao LY, Choi P. Study of the effect of branch content of octene-based linear low-density polyethylene on its melt miscibility with high-density polyethylene by inverse gas chromatography. J Appl Polym Sci 2004; 91: 1927-1931.
50. Alamo RG, Londono JD, Mandelkern L, Stehling FC, Wignall GD. Phase behavior of blends of linear and branched polyethylenes in the molten and solid states by small-angle neutron scattering. Macromolecules 1994; 27: 411-417.
51. Ree J, Crist B. Thermodynamics and phase separation in melt blends of polyethylene and model copolymers. Macromolecules 1991; 24: 5663-5669.
52. Alamo RG, Glaser RH, Mandelkern L. The cocrystallization of polymers: Polyethylene and its copolymers. J Polym Sci Part B: Polym Phys 1988; 26: 2169-2195.
53. Galante MJ, Mandelkern L, Alamo RG. The crystallization of blends of different types of polyethylene: The role of crystallization conditions. Polymer 1998; 39: 5105-5119.
54. Nicholson JC, Finerman TM, Crist B. Thermodynamics of polyolefin blends: small-angle neutron scattering studies with partially deuterated chains. Polymer 1990; 31: 2287-2293.
55. Hu SR, Kyu T, Stein RS. Characterization and properties of polyethylene blends I. Linear low-density polyethylene with high-density polyethylene. J Poly Sci Polym 1987; 25: 71-87.
56. Stein RS, Satkowski M, Noda I. Polymer Blends, Solutions and Interfaces. New York: Elsevier; 1992.
57. Stafford BB. Application of differential thermal analysis to polyethylene blends. J Appl Polym Sci 1965; 9: 729-737.
58. Clampitt BH. Differential thermal analysis of the cocrystal peak in linear-high pressure polyethylene blends. J Appl Polym Sci 1965; 3: 671-679.
59. Robertson RE, Paul DR. Stress-strain behavior of polyolefin blends. J Appl Polym Sci 1973; 17: 2579-2595.

Copyright by Mahidol University

60. Rueda DR, Malers L, Viksne A, Balta-Calleja FJ. Study of blends based on recycled polyethylene wastes. J Mater Sci 1996; 31: 3915-3920.
61. Hussein IA. Melt miscibility and mechanical properties of metallocene linear low-density polyethylene blends with high-density polyethylene: influence of comonomer type. Polymer International 2005; 54: 1330-1336.
62. Garcia-Rejon A, Alvarez C. Mechanical and flow properties of high-density polyethylene/low-density polyethylene blends. Polym Eng Sci 1987; 27: 640-646.
63. Cho K, Lee BH, Hwang KM, Lee H, Choe S. Rheological and mechanical properties in polyethylene blends. Polym Eng Sci 1998; 38: 1969-1975.
64. Viksne A, Malers L, Bledzki AK. Mechanical properties-structure relationships of crosslinked blends based on LDPE/HDPE waste. Angew Makromol Chem 1997; 249: 47-57.
65. Gupta AK, Rana SK, Deopura BL. Mechanical properties and morphology of high-density polyethylene/linear low-density polyethylene blend. J Appl Polym Sci 1992; 46: 99-108.
66. Gupta AK, Rana SK, Deopura BL. Flexural and impact properties of high-density polyethylene/linear low-density polyethylene blend. J Appl Polym Sci 1992; 49: 477-485.
67. Sarkhel G, Banerjee A, Bhattacharya P. Rheological and Mechanical Properties of LDPE/HDPE Blends. Polymer-Plastics Technology and Engineering 2006; 45: 713-718.
68. Elias HG. Macromolecules Structure and Properties, 2nd ed. New York: Plenum Press; 1983.
69. Saunders KJ. Organic polymer chemistry, 2nd ed. New York: Chapman and Hall; 1973.
70. Brandrup J, Immergut EH. Polymer Handbook, 3rd ed. New York: Wiley; 1989.
71. Morrison RT, Boyd RN. Organic Chemistry, 6th ed. NJ: Prentice Hall: Englewood Cliffs; 1992.
72. Rojas B, Marquez L, Manosalva JL, Lopez J, Ruiz V, and Muller AJ. Experimental analysis of the grafting products of diethyl maleate onto linear and branched polyethylenes. Polymer 2002; 43: 2151-2159.

Copyright by Mahidol University

73. Xanthos M. Reactive extrusion: Principles and practice. Munich: Hanser; 1992.
74. Dadbin S, Frounchi M, Saeid MH, Gangi F. Molecular structure and physical properties of E-beam crosslinked low-density polyethylene for wire and cable insulation applications. J Appl Polym Sci 2002; 86: 1959-1969.
75. Mandelkern L. Crystallization of polymer. New York: McGraw-Hill; 1964.
76. Kissinger HE. Reaction Kinetics in Differential Thermal Analysis. Anal Chem 1957; 29: 1702-1706.
77. Socrates G. Infrared Characteristic Group Frequencies. New York: Wiley-Interscience; 1980.
78. Chattopadhyay S, Chaki TK, Bhowmick AK. Structural characterization of electron-beam crosslinked thermoplastic elastomeric films from blends of polyethylene and ethylene-vinyl acetate copolymers. J Appl Polym Sci 2001; 81: 1936-1950.
79. Ringrose BJ, Kronfli E. Preirradiation grafting of ethylene vinyl acetate copolymer resins. Radiat Phys Chem 1999; 55: 451-460.
80. Cho YS, Shim MJ, Kim SW. Thermal degradation kinetics of PE by the Kissinger equation. Mater Chem Phys 1998; 52: 94-97.
81. Marcilla A, Gomez-Siurana A, Menargues S, Ruiz-Femenia R, Garcia-Quesada JC. Oxidative degradation of EVA copolymers in the presence of MCM-41. J Anal Appl Pyrolysis 2006; 76: 138-143.
82. Saunders KJ. Organic polymer chemistry. London: Chapman and Hall; 1973.
83. Kim S, Eun-Suk Jang ES, Shin DH, Lee KH. Using peak properties of a DTG curve to estimate the kinetic parameters of the pyrolysis reaction: application to high density polyethylene. Polym Degrad Stab 2004; 85: 799-805.
84. Park JW, Oh SC, Lee HP, Kim HT, Yoo KO. A kinetic analysis of thermal degradation of polymers using a dynamic method. Polym Degrad Stab 2000; 67: 535-540.
85. Chan JH, Balke ST. The thermal degradation kinetics of polypropylene: Part III. Thermogravimetric analyses. Polym Degrad Stab 1997; 57: 135-149.
86. Raghavan SR, Chen LA, McDowell C, Khan SA. Rheological study of crosslinking and gelation in chlorobutyl elastomer systems. Polymer 1996; 37: 5869-5875.

Copyright by Mahidol University

87. Chiou BS, Khan SA. Real-time FTIR and in situ rheological studies on the UV Curing kinetics of thiol-ene polymers. Macromolecules 1997; 30: 7322-7328.
88. Isac SK, George KE. Reactive processing of polyethylenes on a single screw extruder. J Appl Polym Sci 2001; 81: 2545-2549.

Copyright by Mahidol University

APPENDIX

Copyright by Mahidol University

Appendix A: Characteristic of crosslinked samples

Table A1 Effect of immersing time on gel content of HDPE and its blends with various copolymers (crosslinking at 70 °C)

Immersing time (hrs)	Gel content[a] (%)				
	HDPE	HDPE/EO76	HDPE/EO109	HDPE/EB	HDPE/EVA
0	0.02 ± 0.01	0.03 ± 0.02	0.06 ± 0.02	0.03 ± 0.01	0.07 ± 0.03
3	12.93 ± 1.92	16.45 ± 0.49	22.04 ± 1.33	12.42 ± 1.09	32.80 ± 1.03
6	16.66 ± 1.73	20.79 ± 2.90	28.83 ± 1.74	12.96 ± 0.94	39.89 ± 1.11
9	19.64 ± 3.20	26.19 ± 0.40	36.91 ± 1.64	20.10 ± 1.45	46.79 ± 0.47
12	23.27 ± 0.64	28.56 ± 1.61	38.21 ± 1.77	20.96 ± 0.71	48.44 ± 2.38
24	31.78 ± 0.66	40.25 ± 1.53	49.56 ± 2.09	27.27 ± 3.13	55.37 ± 3.29
48	45.69 ± 0.48	58.65 ± 2.35	62.55 ± 2.24	47.63 ± 2.99	67.20 ± 0.52
72	55.95 ± 1.40	70.10 ± 2.47	68.53 ± 2.20	60.62 ± 0.99	71.80 ± 1.42
96	64.50 ± 1.33	76.11 ± 2.99	73.20 ± 2.24	68.24 ± 0.79	74.93 ± 0.88
120	67.16 ± 0.12	81.20 ± 0.92	79.58 ± 0.94	76.83 ± 1.40	74.79 ± 1.78
360	79.10 ± 1.08	80.87 ± 1.01	81.66 ± 1.55	80.83 ± 1.87	80.33 ± 0.63
600	80.03 ± 1.24	81.27 ± 1.06	82.00 ± 0.67	81.22 ± 0.85	83.35 ± 0.67

[a] average gel content values from 3 experiments

Copyright by Mahidol University

Table A2 Effect of immersing time on swollen factor of HDPE and its blends with various copolymers (crosslinking at 70 °C)

Immersing time (hrs)	Swollen factor [a]				
	HDPE	HDPE/EO76	HDPE/EO109	HDPE/EB	HDPE/EVA
0	0.00	0.00	0.00	0.00	0.00
3	3.31 ± 0.02	3.78 ± 0.13	4.27 ± 0.28	3.29 ± 0.38	4.73 ± 0.18
6	3.42 ± 0.33	4.35 ± 0.68	4.94 ± 0.32	3.27 ± 0.30	4.67 ± 0.04
9	4.02 ± 0.06	4.44 ± 0.03	4.99 ± 0.12	4.19 ± 0.07	4.76 ± 0.06
12	4.39 ± 0.20	4.68 ± 0.21	5.03 ± 0.25	4.31 ± 0.22	4.81 ± 0.02
24	4.55 ± 0.59	5.33 ± 0.17	5.25 ± 0.25	4.48 ± 0.16	5.11 ± 0.27
48	5.01 ± 0.32	5.42 ± 0.09	5.71 ± 0.42	5.28 ± 0.69	5.40 ± 0.12
72	5.59 ± 0.39	5.57 ± 0.49	5.52 ± 0.42	5.71 ± 0.19	5.15 ± 0.23
96	5.35 ± 0.23	5.29 ± 0.07	5.22 ± 0.21	5.61 ± 0.06	4.88 ± 0.03
120	5.27 ± 0.12	5.41 ± 0.35	5.40 ± 0.06	5.69 ± 0.10	4.85 ± 0.06
360	5.41 ± 0.27	5.36 ± 0.06	5.22 ± 0.16	5.30 ± 0.22	5.16 ± 0.21
600	5.35 ± 0.04	4.94 ± 0.19	5.10 ± 0.34	5.12 ± 0.27	4.96 ± 0.13

[a] average swollen factor values from 3 experiments

Copyright by Mahidol University

Table A3 Effect of immersing time on solvent uptake factor HDPE and its blends with various copolymers (crosslinking at 70 °C)

Immersing time (hrs)	Solvent uptake factor[a]				
	HDPE	HDPE/EO76	HDPE/EO109	HDPE/EB	HDPE/EVA
0	0.00	0.00	0.00	0.00	0.00
3	25.94 ± 3.72	22.99 ± 1.45	19.38 ± 0.17	26.47 ± 1.38	14.43 ± 0.31
6	20.73 ± 3.36	21.03 ± 2.62	17.16 ± 0.86	25.24 ± 1.07	11.71 ± 0.41
9	20.84 ± 3.53	16.96 ± 0.29	13.56 ± 0.93	20.90 ± 1.29	10.18 ± 0.12
12	18.85 ± 0.43	16.41 ± 0.48	13.20 ± 1.18	20.62 ± 1.74	9.94 ± 0.47
24	14.35 ± 2.14	13.24 ± 0.17	10.60 ± 0.08	16.56 ± 2.03	9.23 ± 0.38
48	10.97 ± 0.76	9.25 ± 0.23	9.11 ± 0.33	11.05 ± 0.75	8.03 ± 0.11
72	9.98 ± 0.50	7.95 ± 0.54	8.05 ± 0.35	9.41 ± 0.22	7.17 ± 0.19
96	8.30 ± 0.29	6.95 ± 0.26	7.13 ± 0.09	8.22 ± 0.04	6.52 ± 0.04
120	7.85 ± 0.18	6.66 ± 0.36	6.79 ± 0.05	7.41± 0.25	6.49 ± 0.15
360	6.84 ± 0.43	6.63 ± 0.09	6.40 ± 0.31	6.56 ± 0.29	6.43 ± 0.22
600	6.68 ± 0.13	6.08 ± 0.32	6.22 ± 0.36	6.30 ± 0.36	5.96 ± 0.17

[a] average solvent uptake factor values from 3 experiments

Copyright by Mahidol University

Table A4 Effect of immersing time on absorption index at 1092 cm^{-1} of HDPE and its blends with various copolymers (crosslinking at 70 °C)

Immersing time (hrs)	Absorption index[a] at 1092 cm^{-1}				
	HDPE	HDPE/EO76	HDPE/EO109	HDPE/EB	HDPE/EVA
0	1.94 ± 0.04	1.58 ± 0.05	1.14 ± 0.02	1.74 ± 0.06	0.73 ± 0.04
3	1.73 ± 0.03	1.38 ± 0.04	1.16 ± 0.02	1.69 ± 0.05	0.69 ± 0.02
6	1.48 ± 0.02	1.38 ± 0.02	1.10 ± 0.01	1.67 ± 0.07	0.68 ± 0.02
9	1.53 ± 0.02	1.33 ± 0.03	1.05 ± 0.04	1.56 ± 0.05	0.70 ± 0.01
12	1.47 ± 0.03	1.27 ± 0.07	1.04 ± 0.02	1.54 ± 0.03	0.66 ± 0.02
24	1.45 ± 0.07	1.27 ± 0.02	0.99 ± 0.04	1.52 ± 0.06	0.63 ± 0.01
48	1.20 ± 0.04	1.15 ± 0.04	0.92 ± 0.03	1.27 ± 0.03	0.59 ± 0.00
72	1.26 ± 0.03	1.07 ± 0.03	0.89 ± 0.03	1.18 ± 0.08	0.57 ± 0.01
96	1.17 ± 0.04	0.93 ± 0.05	0.79 ± 0.01	1.00 ± 0.02	0.55 ± 0.00
120	1.17 ± 0.02	0.98 ± 0.04	0.80 ± 0.02	1.02 ± 0.06	0.43 ± 0.02
360	0.88 ± 0.03	0.68 ± 0.04	0.50 ± 0.03	0.75 ± 0.03	0.40 ± 0.03
600	0.89 ± 0.02	0.57 ± 0.01	0.28 ± 0.02	0.60 ± 0.01	0.38 ± 0.02

[a] average absorption index values from 5 experiments

Copyright by Mahidol University

Table A5 Effect of immersing time on complex modulus at 10 rad.s^{-1} of HDPE and its blends with various copolymers (crosslinking at 70 °C)

Immersing time (hrs)	Complex modulus at 10 rad.s^{-1} (kPa)				
	HDPE	HDPE/EO76	HDPE/EO109	HDPE/EB	HDPE/EVA
0	10.9	16.8	21.8	11.8	10.8
24	107	126	129	126	132
72	128	171	178	155	184
120	190	195	197	177	199
360	195	229	235	205	240
600	212	238	237	217	246

Table A6 Effect of immersing time on crosslink density of HDPE and its blends with various copolymers

Immersing time (hrs)	Crosslink density (mol.L^{-1})				
	HDPE	HDPE/EO76	HDPE/EO109	HDPE/EB	HDPE/EVA
0	0.003	0.004	0.006	0.003	0.003
24	0.027	0.032	0.033	0.032	0.034
72	0.033	0.043	0.045	0.039	0.047
120	0.048	0.050	0.050	0.045	0.051
360	0.050	0.058	0.060	0.052	0.061
600	0.054	0.061	0.060	0.055	0.063

Copyright by Mahidol University

Appendix B: Properties of various samples

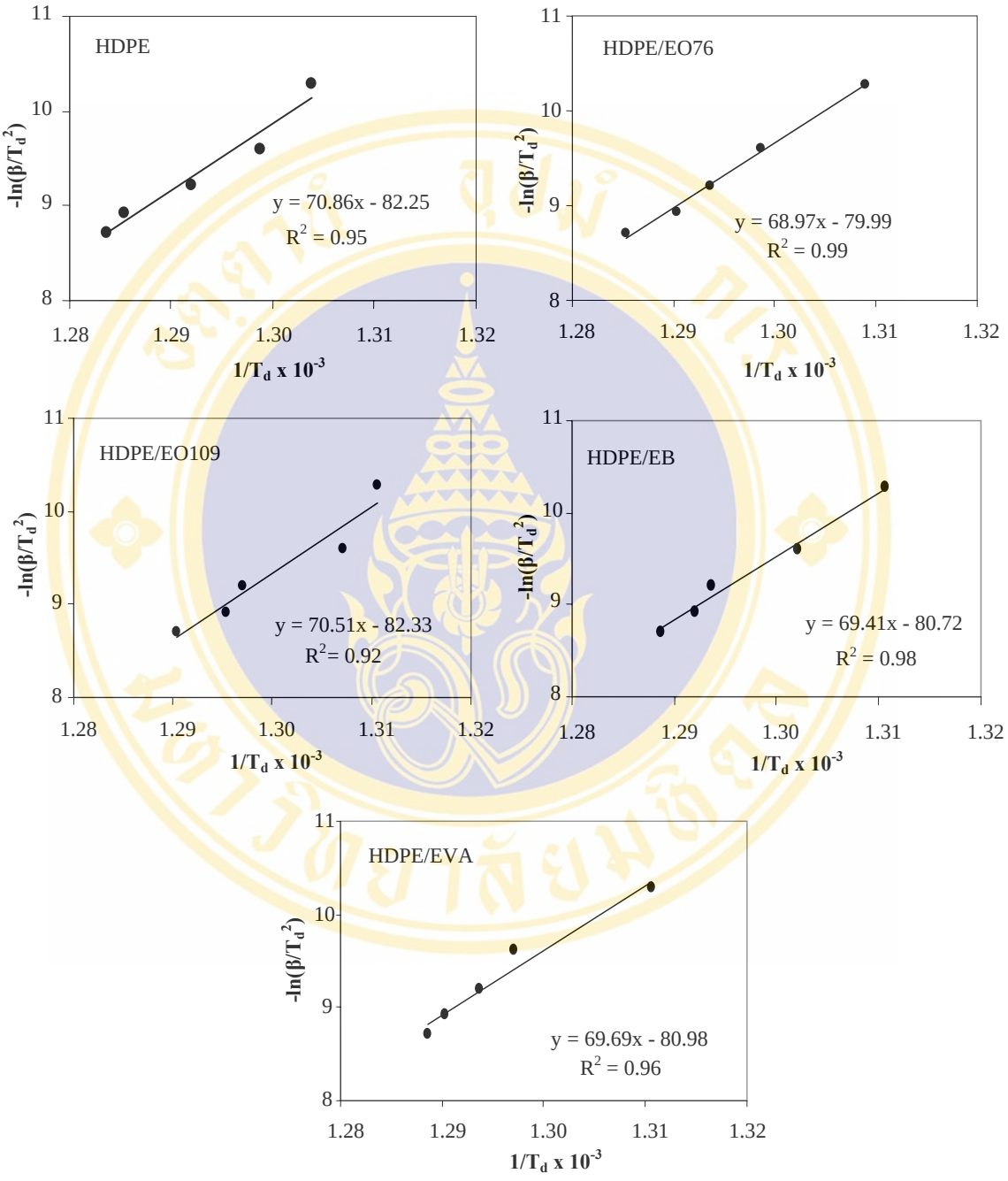

Figure B1 Plot of $-\ln(\beta/T_d^2)$ versus $1/T_d \times 10^{-3}$ for HDPE and its blends with various copolymers

Copyright by Mahidol University

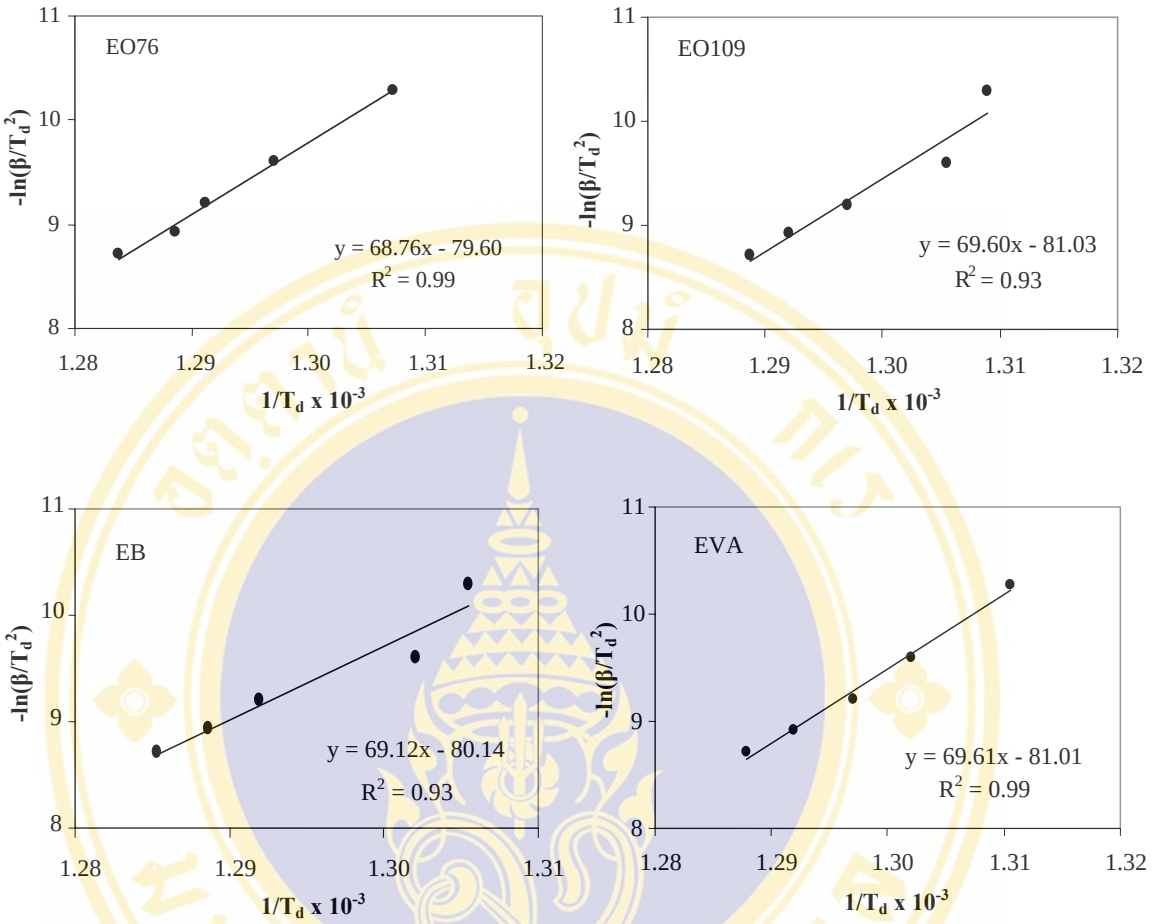

Figure B2 Plot of $-\ln(\beta/T_d^2)$ versus $1/T_d \times 10^{-3}$ for various ethylene copolymers

Copyright by Mahidol University

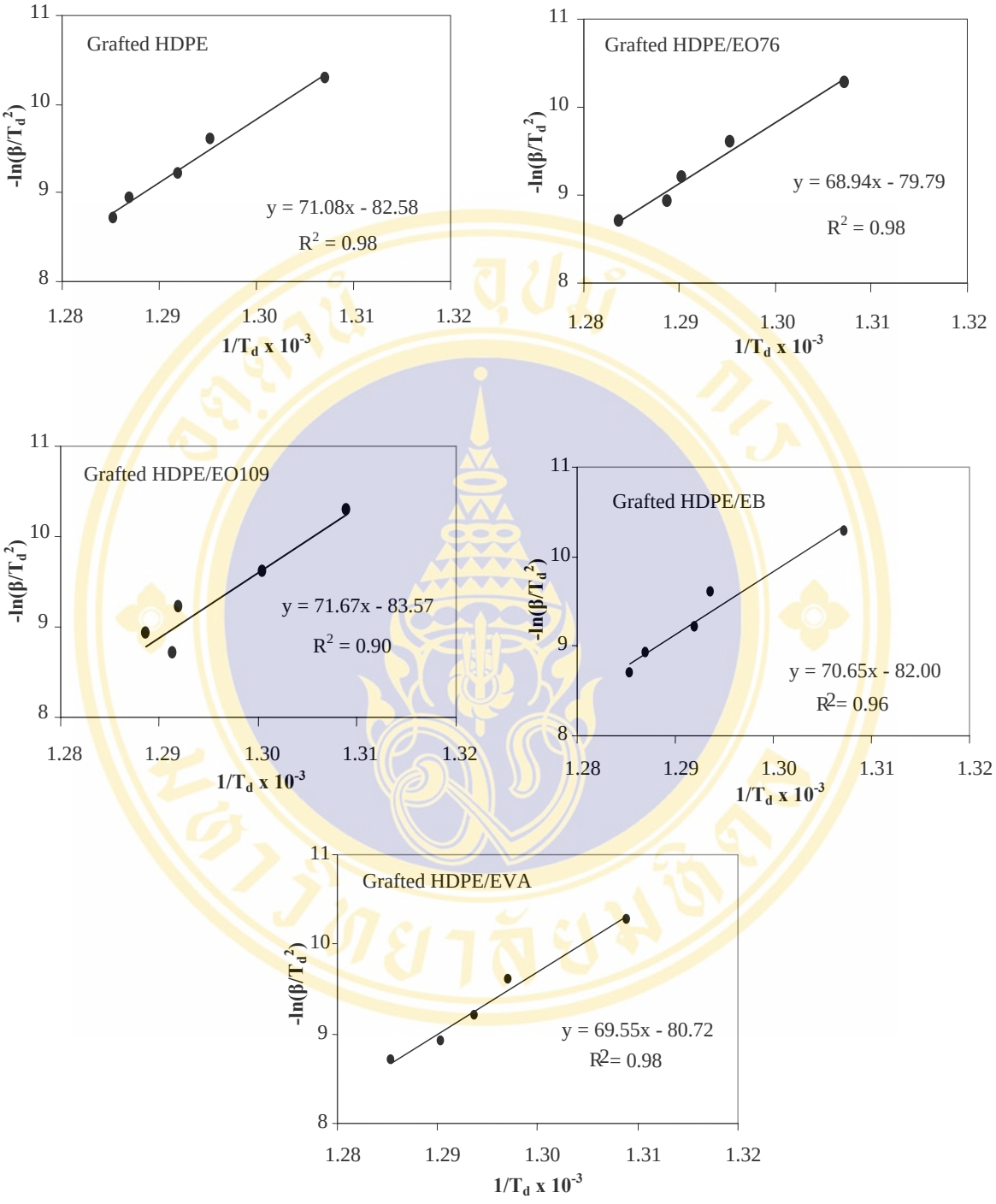

Figure B3 Plot of $-\ln(\beta/T_d^2)$ versus $1/T_d \times 10^{-3}$ for silane-grafted HDPE and its blends with various copolymers

Copyright by Mahidol University

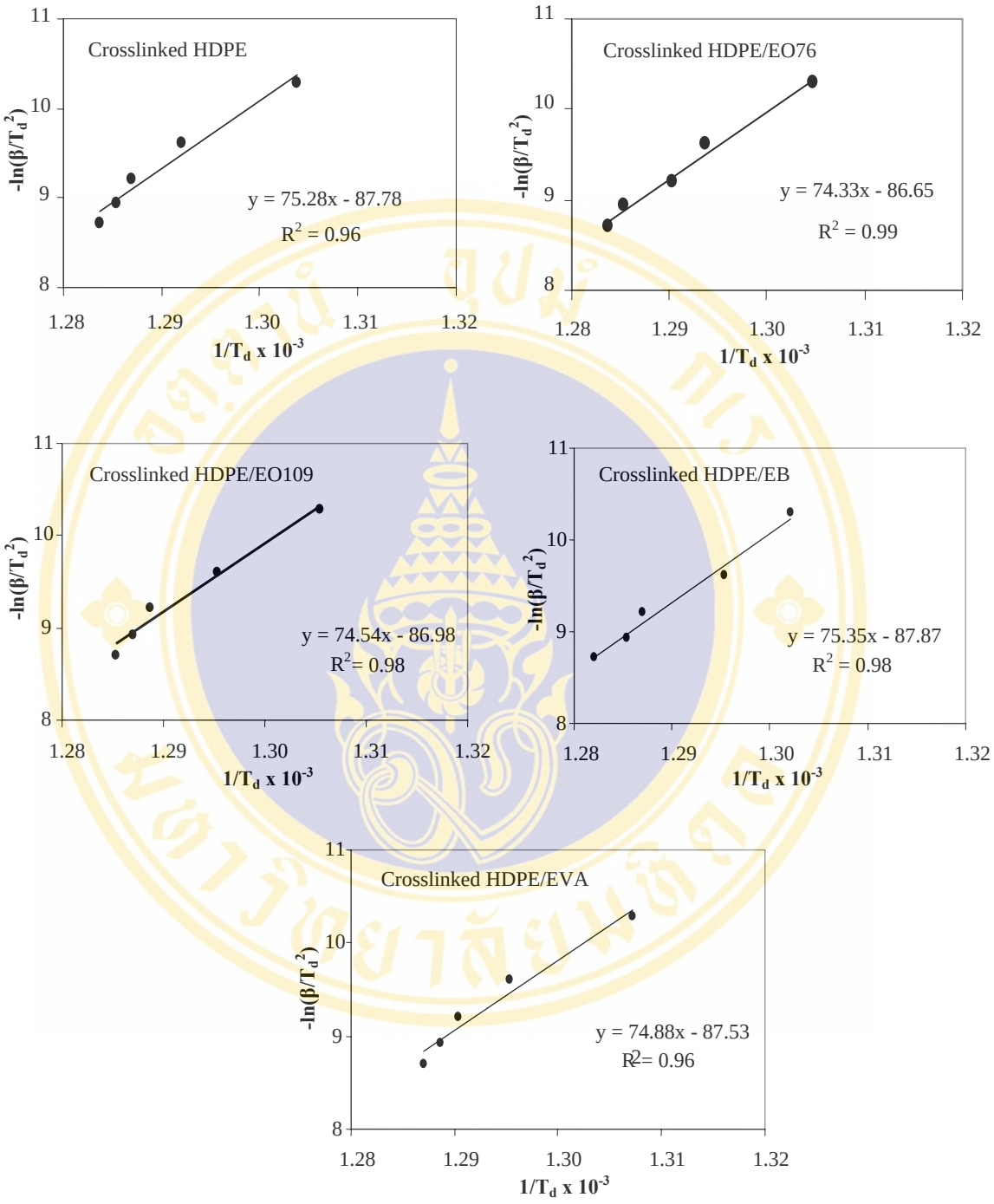

Figure B4 Plot of $-\ln(\beta/T_d^2)$ versus $1/T_d \times 10^{-3}$ for silane-crosslinked HDPE and its blends with various copolymers

Copyright by Mahidol University

BIOGRAPHY

NAME	Miss Soontaree Kositchaiyong
DATE OF BIRTH	June 23, 1981
PLACE OF BIRTH	Nakhon Pathom, Thailand
INSTITUTIONS ATTENDED	Silpakorn University, 1999-2002: Bachelor of Science (Chemistry) Mahidol University, 2004-2007: Master of Science (Polymer Science and Technology)
EXPERIENCE	Mahidol University, 2005-2007: Teaching assistance
POSTER PRESENTATION	The 1st Polymer Graduate Conference of Thailand, May 10-11, 2007. Mahidol University, Salaya, Nakhon Pathom, Thailand.
HOME-ADDRESS	36/2 M.7 Setwithi Rd., T. Bo Phlap, A. Muang, Nakhon Pathom 73000, Thailand

Copyright by Mahidol University